In Vivo Characterization of *Mycobacterium marinum* Virulence Genes with Unknown Functions and Larval Activation of Mycobacterial Virulence in the Medaka Infection Model

A Dissertation

Presented to the

Graduate Faculty of the

University of Louisiana at Lafayette

In Partial Fulfillment of the

Requirements for the Degree

Doctor of Philosophy

Amrita Mallick

Summer 2014

ProQuest LLC.
789 East Eisenhower Parkway
P.O. Box 1346
Ann Arbor, MI 48106 - 1346

In Vivo Characterization of *Mycobacterium marinum* Virulence Genes with Unknown Functions and Larval Activation of Mycobacterial Virulence in the Medaka Infection Model

Amrita Mallick

APPROVED:

Don G. Ennis, Chair
Associate Professor of Biology

Andrei Chistoserdov
Associate Professor of Biology

Lewis Deaton
Associate Professor of Biology

Glen M. Watson
Professor of Biology

Lynn Harrison
Professor of Molecular and
Cellular Biology
Louisiana State University
Health Sciences Center, Shreveport

Mary Farmer-Kaiser
Interim Dean of the Graduate School

ACKNOWLEDGMENTS

I would like to acknowledge my advisor and mentor Dr. Don Ennis, who gave me the opportunity to work under his fantastic supervision. You are a great scientist and professor, even greater human being. This would be impossible without your unwavering support throughout. I would rejoice all the good times we have spent learning science. I sincerely thank you for your infinite contributions towards my life.

I would also like to extend my thanks to my Committee, Dr. Lynn Harrison, Dr. Glen M. Watson, Dr. Andrei Chistoserdov, and Dr. Lewis Deaton for being so helpful.

I once again thank Dr. Lewis Deaton and Dr. Jeffery Spring for being incredibly supportive of my teaching duties.

I am grateful to Miss Gigi, In-charge of University Family Housing, for being extremely considerate and providing me a peaceful accommodation for all this time.

I thank my past and present lab mates Dr. Greggory Broussard, Lynsey Wilcox, Dr. Nadine Mutoji, Kate Root, Kalyn Schreiffer, Martin Cheremie and Jarrett Woock for being invaluable friends; I would always treasure your love and friendship.

I extend my gratitude to my undergraduates; Meagan Bahlinger, Katherine Palmer, Dane Phelan, Juan Rodrigues, Brooke Richards, Jesse Soileau, Dustin Todero and Serena Murphy. Your support and dedication has always motivated me.

To my wonderful parents; Shikha and Asok Sarkar, for your endless sacrifices and unconditional love. Your pursuit for excellence has brought me here.

I thank my husband, Avishek Mallick for his insights and help with the statistical analysis, for always being there for me. I admire your love and your optimism towards life has inspired me. I could not have done this without you

This project would be incomplete without acknowledging the enormous contribution of a tiny person, my baby girl, Anvi. Last year has been awesome with you in my life; your smile has brightened my days.

Table of Contents

LIST OF TABLES

LIST OF FIGURES

CHAPTER ONE: Introduction

1.1 Global Burden of Human Tuberculosis – Present Scenario in the World

Tuberculosis (TB) is an infectious disease caused by the bacillus *Mycobacterium tuberculosis*. The global burden of TB is enormous and most recently this scenario has been severely threatened by the emergence of multi drug resistance (MDR) strains as well as coinfection with Human Immunodeficiency Virus (HIV). Worldwide, TB ranks as the leading cause of death from a single infectious agent. Even among HIV associated deaths that are attributed to other pathogens, *M. tuberculosis* is the leading one (WHO 2012). In the year 2011, an estimated 9 million new cases of TB have emerged, of which 13% are coinfected with HIV. Anually, 2 million people succumb to TB (approximately million deaths have occurred among HIV-negative people and 430,000 have been HIV-associated TB deaths each year) (WHO 2012). The likelihood of developing symptomatic TB is 5% to 10% among the infected individual, but with HIV coinfection or other factors such as malaria, malnutrition, diabetes, or tobacco use, the risk of developing clinical manifestation of the disease is substantially elevated (Harries et al. 2006; WHO 2012). TB has taken a huge toll on people in the most economically productive age group, resulting a total socio-economic setback in nations affected with TB endemic in developing countries. It is one of the top killers in women, with the estimated number of TB deaths among women at 0.5 million in 2011. The burden of TB in children is also high, with an estimation of 490,000 cases and 64,000 deaths in 2011 in children below 15 years. Not only does TB have a huge impact on children's health directly, but parental deaths from TB have created around 10 million orphans in 2009 (WHO 2012). Geographical distribution (as shown in Figure 1.1) of the disease indicates

that the incidence of new TB cases is highest in Asia and Africa. Africa is known to have the highest rates of new cases and per capita deaths. Southeast Asia and the Western Pacific region (Cambodia, China, Philippines and Indonesia) account for 60% of world's TB cases. India and China together account for approximately 40% of the TB cases worldwide (WHO 2012). It is highly likely that these report statistics are underestimated, due to gaps in surveillance systems in the developing nations, but nonetheless, the fact remains that the global epidemic of TB is huge.

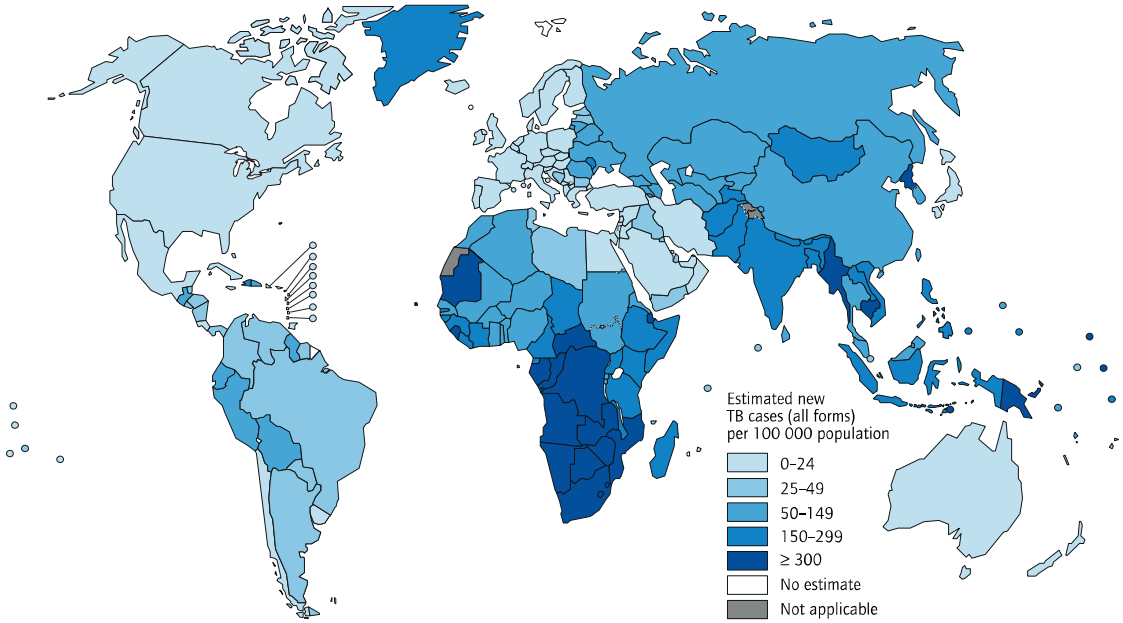

Figure 1.1 **Estimated new TB cases, 2011**
(WHO 2012)

1.2 History of the Tuberculosis

TB is considered to be one of the top killers throughout human history. It is predicted that the genus mycobacteria may have originated 150 million years ago before the southern land mass broke up to form the present day continents. The *Mycobacterium ulcerans* strain isolated from different continents likely has a similar long-standing human burden, although *M. ulcerans* infections are endemic in nature (Heyman 1984). A progenitor specie of *M. tuberculosis* clonal group has been estimated to have evolved approximately 3 million years ago suggesting that hominid ancestors of human residing in East Africa may have also suffered from tuberculosis (Gutierrez et al. 2005). In addition, the low level of genetic variation of *M. tuberculosis* indicates that the modern members of *M. tuberculosis* complex have evolved following a clonal expansion around 35,000 years ago (Gutierrez et al. 2005). Global population of *M. tuberculosis* has been categorized into six different lineages that have highly geographically structured and all these lineages were initially represented in Africa (Gagneux 2006). TB description has been documented in India as early as 3,300 years ago and in China 2,300 years ago (Daniel 2006). Archeological evidence, literature, art and human remains have indicated presence of TB in ancient Egypt. Microscopic examination of mummies dated back to 1550 BC has indicated the presence of tubercle bacilli in vertebral bone and fresh blood in trachea and lungs. Presence of *M. tuberculosis* DNA in samples from mummified tissues has been further affirmed by molecular technology as well (for example, PCR amplification of *M. tuberculosis* DNA using specific primers) (Nerlich et al. 1997; Zimmerman 1997). *M. tuberculosis* DNA has also been recovered from at least a 1,000 year old lung lesion of a Peruvian mummy (Salo et al. 1993). During the middle ages in Europe, although TB was clearly present, written documentation about it remained sparse. New

knowledge about the diseases emerged at the time of renaissance, and so did the TB epidemic, with exceptionally high death rates ranging from eight hundred to thousand per hundred thousand population per year in Europe (Daniel 2006). At the time, TB was believed to be both a heritable and infectious disease. In 1865, Jean-Antoine Villemin, a French millitary scientist convincingly demonstrated the infectious nature of TB by inoculating a rabbit with "puruent liquid from tuberculous cavity" (Daniel 2006). The history of TB entered a new era in 1882, when Robert Koch convincingly demonstrated the "tubercle bacillus" as the causative agent for TB at Berlin Physiological Society and proposed the famous Koch–Henly postulates to establish the infectious etiology of a disease, that holds true until today. For Koch's phenomenal achievement in discovery of the cause of TB, he was awarded the Nobel Prize in 1905. Despite his many contributions in understanding TB, he failed to treat the disease with Tuberculin (antigen of tubercle bacilli); however, it became useful in the diagnosis of sero-positive TB patients (Daniel 2006). By the beginning and middle of the twentieth century, the TB death rates began to decline with the advancement in knowledge of the disease. The probable reason for this is attributed to improved social and living conditions, improved nutrition, increases in birth rates and natural selection of genetically resistant populations. During this time, Europe and America turned to quarantining infectious TB patients in sanitaria (an isolated facility for TB patients) not only for the protection of the general population but also for comfort and relief of the TB patients due to lack of any effective treatment to block the spread of the disease (Daniel 2006). An important milestone in controlling TB was development of the of BCG vaccine, an attenuated strain of *M. bovis* by Albert Calmette and Camille Guerin in 1921. This vaccine was widely accepted and more than 100,000 children were immunized over the next few years (Daniel 2006). The trend of

declining TB prevalence was disrupted at the time of World War I, when TB deaths peaked all over the world (Drolet 1945; Daniel 2006). It is estimated that in 1917, in the US alone, eighteen to twenty thousand people died of TB. Armed forces were greatly affected, with thirty six thousand living veterans infected with TB out of approximately five million soldiers who fought in the war. A Similar pattern of elevation in death rate was seen in all the European countries (Drolet 1945). In United Kingdom, the pre war death rate in 1913 was 135 per 100,000 people, which rose to 169 in 1918. World war II also had a major impact on TB scenario, with escalation of mortality and incidence rates, needless to say the socio–economic destruction and disruption it caused world wide (Daniels 1949). By the end of World War II, to control TB, Unicef sponsored a campaign where people were subjected to tuberculin testing and BCG vaccination was administered to the nonreacters. Effective treatment and cure for TB were non-existent until the availability of chemotherapeutic agents, PAS (para amino salicylic acid) and thiosemicarbazine in1943 and 1945 respectively; both were bacteriostatic and did not prove very effective against TB. The first bactericidal agent to be used against *M. tuberculosis* was the antibiotic Streptomycin, but had some variable efficacy in TB treatment. However, the discovery of Isoniazid (in 1952) and Rifamycin (in 1957), the first oral mycobactericidal drug, still used today, signified a major victory in modern medicine and in the history of TB treatment and cure (Daniel 2006). Since 1974, WHO promoted sputum microscopy to screen for 'active', or infectious patients in both symptomatic people and those at risk of TB. WHO also advocated mass BCG vaccination of individuals less than 15-20 years of age and recommended against hospitalization of TB patients (Daniel 2006). Unfortunately, even today, the battle against TB is far from being won, owing to many potential challenges, such as its vast reservoir, with nearly one in three people infected, a

situation further worsened by the coinfection with HIV as well as the emergence of drug resistant strains and the lack of an effective vaccine.

1.3 *Mycobacterium tuberculosis* Complex

Mycobacterium tuberculosis complex (MTBC) consists of six members: *M. tuberculosis, M. africanum, M. microti, M. bovis, M. bovis* BCG and *M. canetti* (Cole 2002). Based on spectrophotometric analysis of DNA/DNA hybridization, these members are considered single species with identical 16S rRNA sequences and over 99.9% nucleotide identity (Imeada 1985). It is thought that MTBC has originated in Africa, and their association with humans is at least 70,000 years old (Comas et al. 2013). There is a strong correlation in tree topology and phylogeoraphic structuring indicate that MTBC infected the early human population and has co-evolved with its host. An analysis of whole genome of a number of MTBC pathovars have completely refuted the idea of zoonotic transfer of MTBC to human hosts; instead MTBC has successfully expanded due to the demographic explosion of the human population (Brosch et al. 2002; Writh et al. 2008; Comas et al. 2013). In other words, there is a historic association and adaptation between humans and one of their pathogens, MTBC.

MTBC is limited in its DNA sequence variation, but has a marked difference in the host range they infect, immune response they induce, and over all pathogenesis of the disease they cause. The host range of MTBC is charted below. *M. africanum*, prevalent in Western Africa, where it causes half of all TB cases, has been endemic. Although transmission rates and susceptibility to regular anti TB drugs are comparable, a lower progression to disease is observed in *M. africanum* relative to *M. tuberculosis* (Jong et al. 2010). *M. bovis* accounts for a small percentage of the reported cases of TB in human but in TB endemic areas the exact

proportion of human disease due to *M. bovis* is largely unknown (Mostowy et al. 2005). However, it is of major socio economic importance as it causes zoonotic disease affecting cattle all over the world. Human health risk has been controlled by pasteurization of dairy products and descending rates of *M. bovis* infection in cattle (Cousins 2001; LoBue et al. 2010). This pathogen is the primary cause of TB in cattle and other ruminant like water buffaloes in Africa and India. Pigs and goats are susceptible too, with the level of infection in pigs are similar to that of cattle but infection in goats are a serious problem mostly in Mediterranean region. Incidents of infections in camels where they were closely associated with cattle have been reported as well, but it is an uncommon infection in horse and sheep (Cousins 2001). Dogs are equally susceptible to *M. tuberculosis* and *M. bovis*, but cats are more susceptible to *M. bovis* than *M. tuberculosis* (Cousins 2001). *M. canettii* is characterized by smooth morphology (due to presence of a type specific phenolic glycolipid) unlike any other member of MTBC. It seems to preferentially infect children and is geographically restricted to Horn of Africa (Koeck et al. 2010). *M. microti* typically infects voles, wood mice and shrews; human infections are rare and limited to immunocompromised patients.

Mycobacterium tuberculosis Complex (adapted from Cole 2002)

Species	**Host range**
M. africanum	Human (Sub Saharan Africa)
M. bovis	Badger, cattle, deer, elephant, goat, human, lion, seal, etc
M. bovis BCG	
M. canettii	Human
M. microti	Vole

M. tuberculosis Human

A significant comparative genomics study by Mostowy et al. (2005), revealed the phylogenetic stratification of MTBC. This study based on deletion-based phylogeny suggested that *M. tuberculosis* and *M. canettii* were likely the progenitors and with around four deletions, gave rise to *M. afficanum* and *M. microti*. *M. bovis* emerged by reductive evolution, acquiring five additional deletions. This contrasts with the popularly-held assumptions by some biologists, and indicates that in fact humans likely gave TB to cattle with their domestication and not otherwise.

M. tuberculosis is a rod-shaped bacteria, 2-4 micrometers in length and 0.2–0.5 micrometers in width. It is a non-motile, obligate aerobe, and has a generation time of 15–20 hours.

Mycobacterial cell envelope consists of a cell membrane, a cell wall and a complex outer layer (Saier 2008). The cell membrane is composed of phospholipid and protein. Exterior to the cell membrane is the peptidoglycan cell wall, the arabinogalactan/arabinomannan polysaccharide layer and then the outer membrane (Saier 2008). Peptidoglycan are covalently linked to arabinogalactans, which in turn is attached to mycolic acids with their long meromycolate and short α-chains (Brennan 2003). The outermost layer in the outer membrane is made up of longer and shorter fatty acids complementing shorter alpha chains and longer chains respectively. The cell wall proteins, the phosphotidylinositol mannosides, the pthiocerol containing lipids, lipomannan and lipoarabinomannan are interspread in this layer (Brennan 2003). The presence of waxy mycolic acid in the cell walls makes *M. tuberculosis* acid fast. In this differential staining technique, carbolfuchsin, a lipid soluble

phenolic compound is used as the primary stain that penetrates the waxy cell wall. The stain resists acid alcohol wash, addition of methylene blue counter stain and the cells appear reddish purple in color. *M. tuberculosis* genome contains 4,411,529 base pairs, containing about 4,000 genes, and has a high G+C content of 65.6%.

1.4 Pathogenesis and Immunity of Tuberculosis

Mycobacterium tuberculosis has been identified as the causative agent of TB more than a century ago and a substantial progress in terms of understanding the bacterial pathogenesis and host immunity has been made since then. Still, enormous amount of basic important facts about the disease remain elusive. Successful inoculation of *M. tuberculosis* and deposition in the lungs leads to one of four possible outcomes (Riley 2013):

- Immediate clearance of the organism
- Latent infection
- Immediate onset of active disease (primary disease)
- Onset of active disease many years following exposure (reactivation disease)

A majority of *M. tuberculosis* infections are latent and asymptomatic, the only indication of the infection is the existence of immune response against mycobacterial antigens. In this state, the bacterial replication and transmission is believed to be restricted. The active disease with a clinical state of high bacterial burden eventuates in only a small fraction (5-10%) of infected individuals (Philips et al. 2012). Most interestingly, how this alignment steers towards the benefit of the pathogen developing active disease is not completely understood. *M. tuberculosis* initially gains entry into the distal alveoli via aerosol droplets and encounters and infects resting alveolar macrophages. Additional phagocytic cells are then recruited at the site of initial infection are neutrophils, monocyte derived macrophages and dendritic cells

(DC) (Philips et al. 2012). Phagocytosis is normally an important factor for controlling bacterial invasion by the host. In the course of events, phagosome combines with several endosomes before finally fusing with lysosome forming phagolysosome. Lysosome harbors highly reactive enzymes like proteases and lysozymes along with defensins (that leak out bacterial cytoplasmic components) and myeloperonidases (that produce reactive form of oxygen) ultimately leading to oxidative burst of the pathogen. However, mycobacteria exploit this destruction strategy by surviving and replicating inside the phagocytic cells in order to spread and expand successfully within the host. *M. tuberculosis* is recognized by a number of phagocytic cell surface receptors (listed in table) that significantly determines the initiation and coordination of host response. The mechanism of uptake of the bacteria is complex, perhaps co-engaging diverse receptors, ultimately leading to the delivery of bacteria into phagosomes (Jo 2008; Philips et al. 2012). The multiple receptors involved in binding and internalization include C-type lectin receptors (CLRs), scavenger receptors and complement receptors (CRs). Macrophage mannose receptor (MMR), DC specific intracellular adhesion molecule 3-grabbing nonintegrin (DC-SIGN) and Dectin–1 are the key CLRs implicated in recognition, binding, phagocytosis, phagosome maturation and intracellular signaling. An integral (lipoglycan) component of mycobacterial cell wall, mannose capped liparabinomannan (ManLAM) is recognized by MMR and DC-SIGN (Philips et al. 2012).

Upon entry, as recent studies have suggested, *M. tuberculosis* adapts more than one intracellular niches mostly depending upon the host cell type (as shown in Figure 1.2). Mycobacterial phagosome is far from being static instead; *M. tuberculosis* allows early fusion of endosomes early on but arrests phagosome maturation or phagosome-lysososme

fusion. They undergo incomplete luminal acidification, absence of mature lysosomal hydrolases are evident, and is inefficient in antigen processing ability (Vergne et al. 2005; Deretic et al. 2006). *M. tuberculosis* modulates multiple lipid and protein effectors to control phagolysosome biogenesis block. These include small GTP binding proteins Rab5 (present in abundance in early endosomes) and Rab7 (associated with late endosome) that direct endosomal sorting and membrane trafficking. Rab5 participates in receptor mediated endocytosis, formation of clatheren coated vesicles carrying the endocytosed cargo and fusion with early endosomes. Rab5 is normally replaced by Rab7, a late endosome marker that assist in phagosome maturation via few fusion-fusion events ultimately leading to the formation of phagolysosome (Vergne et al. 2005; Deretic et al. 2006). Although Rab5 is detected in mycobacterial phagosome, Rab7 is absent at the times expected for its recruitment and strongly indicates a plausible reason for phagosomal maturation block. At present only little is known about signaling and molecular machinery that dictates Rab conversions, but role of two secreted *M. tuberculosis* effectors, PtpA and NdkA have been implicated. PptA is a tyrosine phosphatase that dephosphorylates Vps33b, a component of the homotypic fusion and protein-sorting complex that converts Rab7 to its GTP bound active form (Philips et al. 2012). NdkA is a guanosine triphosphatase activating protein that probably catalyzes conversion of Rab7 GTP (active) to Rab7 GDP (inactive) (Philips et al. 2012). A well investigated lipid effector; phosphatidylinosotol-3-phosphate (PI3P) generated by host cell enzyme hVPS34 is critical for phagosome formation and its maturation. PI3P is associated with proper membrane trafficking, endosomal sorting and formation of late endosomal multivesicular bodies. Two essential products synthesized by *M. tuberculosis* target to resist PI3P action and block phagosome maturation. These are mycobacterial cell

wall component ManLAM (lipidoarabinomannin) and a secreted enzyme PI3P phosphatase, Sap M. LAM inhibits phosphoitidyl inositol phosphorylation into PI3P that is a glycosylated phospotidylinositol and Sap M breaks down whatever PI3P is generated escaping LAM block (Vergne et al. 2005; Deretic et al. 2006; Philips et al. 2012). LAM also inhibits Ca^{2+} fluxes, increased concentration of cytosolic Ca^{2+} enhances fusion; Ca^{2+} and calmodulin influence recruitment of PI3 kinase (I) on the membrane as well (Deretic et al. 2006). Recent investigations suggest that mycobacteria also orchestrate phagosomal membrane damage, escape and survive in the cytosol. Esx-1 system and its two secreted effectors Exs-A/ESAT-6 and Esx-B/CFP-10 mediated cell membrane damage is one of the aspect being considered (Philips et al. 2012). In addition to intracellular survival and replication Mycobacteria also expands its niche by spreading on to adjacent host cells that are being recruited at the site of infection (Philips et al. 2012).

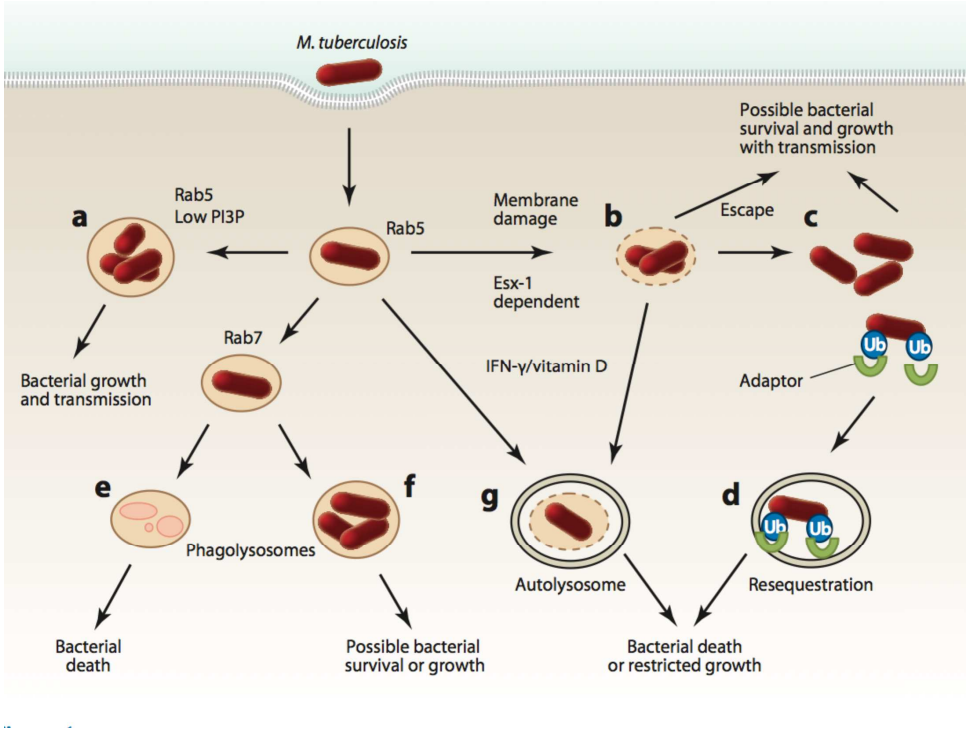

Figure 1.2 **Possible fates of *M. tuberculosis* following phagocytosis.**
(Figure adapted as is from Philip et al. 2012)

1.5 Tuberculine Granuloma

Granuloma is the classical histopathological leision, which is considered hallmark structure of tuberculosis. It is an organized aggregation of immune system cells with a distinct morphology, initiated at the site of infection, and is presently believed to be beneficial to both host and the pathogen (Ramakrishnan 2012; Philips et al. 2012). Mature macrophages are the primary constituents of granuloma and present multiple phenotypes including increased cytoplasmic size, larger number of organelles, ruffled cell membranes that are thought to contribute in their increased mircobicidal activity (Ramakrishnan 2012). Multiple macrophages fuse to form multinucleated giant cells that differentiates into foamy macrophages containing large amount of lipids (mycolic acids). It has been observed that

only virulent mycobacteria stimulate formation of these multinucleated giant foamy cells, but not less virulent mutants (Philips et al. 2012). Additionally, a number of other immune system cells like dendritic cells, B cells, T cells and natural killer cells are also housed in granuloma. Dendritic cells are similar to macrophages but are quite mobile, travelling from peripheral lung tissues to lymph nodes, are also antigens presenting cells, interacting with T lymphocytes and activate initial adaptive response (Wolf et al. 2008). During the initial acute phase of granuloma formation, macrophage and neutrophils are predominant, however with progression towards chronic phase, T cells and macrophage become the major players. T cells, either present as a distinct band towards the periphery of granulomas or infiltrated overall, have now been documented to traffic throughout the granuloma structure (Tsai et al. 2006; Philips et al. 2012). T cells are critical in releasing specific cytokines like interferon γ (INF-γ), which shows significant anti-mycobacterial effects by activating nitric oxide synthase and reactive nitrogen intermediate production within several professional phagocytes. INF-γ also activates macrophages, plays a role in phagosome maturation, limits bacterial access to cellular iron and carbon among its many other plausible roles (Philips et al. 2012). Tumor necrosis factor (TNF) and vitamin D influence intracellular killing of *M. tuberculosis*. TNF also contributes in activating macrophages and controlling apoptosis of infected cells, but high amounts of TNF causes collateral damage to the surrounding host cells by leakage of nitric oxide and other toxic chemicals. B-lymphocytes also populate granuloma in form of a well organized aggregates surrounded by T cells and few macrophages are postulated to have an immunoregulatory function (Tsai et al. 2006). Early events in granuloma formation have been studied in *Mycobacterium marinum*, a close relative of *M. tuberculosis* (Davis et al. 2002, Davis et al. 2009). Intravital studies in the *M.*

marinum-zebrafish hatchling model have shown that bacteria are involved in actively recruiting the macrophages to the site of infection, further infected macrophage relocate to distal places and initiate secondary granuloma formation. Mycobacteria replicate inside the macrophages and once these macrophages undergo apoptosis, these bacteria inside 'blebs' are phagocytosed by newly arriving macrophages, thereby the number of infected macrophage escalate (Davis et al. 2002, Davis et al. 2009). A number of known key virulent factors of mycobacteria contribute to the granuloma formation process by communicating with the host. For example, ESAT6 (early secreted antigenic target-6), a 6-kd secreted protein encoded within the chromosomal interval called *RD1* (region of difference -1), an interval that includes virulence genes that promote granuloma formation by inducing matrix metalloproteinase-9 (MMP9) expression in adjacent host epithelial cells (Volkman et al. 2010). MMP9 induction enhances granuloma formation and maturation, recruits macrophages to the vicinity and thus expanding bacterial niche. Bacterial growth and granuloma formation were attenuated by disruption of MMP9 function (Volkman et al. 2010). Mycobacterial ManLAM (Manosylated lipidoarabinomannin) and AraLAM (arabinan LAM) promote aggregation of mononuclear cells during initial phases of granuloma formation (Philips et al. 2012). Thus, granulomas once thought to be a physical barrier by the host to restrict mycobacteria is now thought to be manipulated by the bacteria likely for its benefit. It is possible that the vast aggregate of immune cells (macrophages, DCs, B and T cells, natural killer cells, fibroblasts and the epithelial cells) that concentrated the granuloma should or do prohibit the spread of infection but definitely is not sufficient to eradicate the bacteria completely. However, many important aspects in to the granuloma is yet to understood

completely, like the factors driving expansion or dissemination of granuloma or the physiological state of bacteria residing in these granuloma.

1.6 Treatment of Tuberculosis

Medical treatment of TB is complicated due to a variety of reasons. TB is highly contagious and there is an enormous global burden of TB that makes treatment of TB in naïve as well as the successfully treated people challenging among many other factors. A major risk of contracting *M. tuberculosis* is that only small number of bacteria (10-100) as an aerosol is believed to be sufficient for causing the disease. Once inside the host, *M. tuberculosis* has a fair number of ways to successfully evade the immune system and establish a niche, where they are hypothesized to prevail in heterogeneous physiological state including actively growing bacteria, persistent and perhaps slowly replicating bacteria. During the intensive phase of TB treatment, actively dividing bacteria are rapidly killed by antibiotics; thereby tackling the clinical symptoms. This is followed by an essential as well as challenging continuation phase of treatment that aims to completely eradicate the 'persisters' the slow growing or possibly latent mycobacteria bacteria (Laurenzi et al. 2007; Sarkar et al. 2011; Jain et al. 2008). The current standard short course anti-TB therapy consists of administration of four front line drugs; rifampin, isoniazid, pyrazinamide and ethambutol for the first two months (intensive phase) pursued by four months of treatment with rifampin and isoniazid (continuation phase) (Jain et al. 2008).

Isoniazid

The mechanism of action of isoniazid was not clear for a long time until recently, isoniazid seems to be non-toxic to the bacterial cell, it is a pro drug which is activated by bacterial enzyme KatG (Timmins et al. 2006). KatG is multifunctional in nature, has activities like

catalase-peroxidase, peroxinitritase, NADH oxidase etc., and is protective against host phagocytic damage (Timmins et al. 2006). KatG catalyzes peroxidation of isoniazid to produce damaging species including acyl, acylperoxo, pyridyl radical adducts of phenylbutylnitrone and nitric oxide radical (NO) that affects a variety of cellular components such as lipids, protein and nucleic acids. In addition, activated isoniazid disrupts synthesis of both mycolic acids and nucleic acids oxidation, by formation of covalent INH-NAD and INH-NAPD adducts. INH-NADH adducts inhibit an enoyl acyl carrier protein reductase encoded by *inhA* that is important in mycolic acid synthesis for the cell wall formation (Timmins et al. 2006; Da silva et al. 2011). Thus, inhibition of cell wall lipid synthesis, depletion of nucleic acid pools and metabolic depression are the important effects of this drug against mycobacteria. Two main causes of isoniazid resistance are mutations in *katG* and *inhA* particularly in their promoter region (Da silva et al. 2011).

Rifampin

Rifampin has a high level of anti bacterial activity; it binds to the bacterial DNA dependent RNA polymerase forming a stable complex and inhibits initiation phase of bacterial transcription (Wherli 1983). RNA polymerase enzyme consists of $\alpha_2 \beta \beta' \sigma$ subunit structure. Rifampin specifically binds to a site located at the β subunit (specifically within the main DNA-RNA channel) encoded by *rpoB* gene (Floss et al. 2005). Due to binding of rifampin to the RNA polymerase, extension of the nascent RNA chain is blocked sterically; so once the enzyme passes the initiation and elongation step and carries a longer RNA chain, it is not sensitive to inhibition by the drug anymore (Floss et al. 2005). Resistance to rifampin is an 'all or nothing' phenomena and happens in bacteria predominantly due to genetic modification of the drug target, *rpoB*, by point mutation. Rifampin resistance has been

extensively studied in *E. coli* where mutations in *rpoB* gene have been mapped (Floss et al. 2005). These Rif^R mutants have also been studied in *T. aquaticus*, all but one of the twelve amino acids involved in interaction with the bound rifampin are susceptible to mutation resulting rifampin resistance (Floss et al. 2005). Additional reasons of rifampin resistance are decreased sensitivity due to covalent modification of rifampin (for example, ribosylation) of by the bacteria (Floss et al. 2005).

Pyrazinamide

Unlike most of the anti TB antibiotics that actively kill growing bacteria, Pyrazinamide is more effective against non-dividing or possibly 'latent' bacteria. Although under normal culture conditions, at neutral pH pyrazinamide is not effective against *M. tuberculosis*, but it effectively wipes out semi-dormant bacilli in acidic environment (Zhang et al. 2003). This plays an important role in reduction of duration in TB treatment. Despite being such unique drug, understanding its mode of action has been elusive. Pyrazinamide is also a pro drug that needs conversion by bacterial enzyme nicotinamidase/pyrazinamidase into pyranoic acid (the active form) (Zhang et al. 2003). Pyranoic acid efflux mechanism is uniquely deficient in *M. tuberculosis* unlike many other bacteria. Studies have shown that Pyranoic acid decouples the membrane potential of bacteria and interrupts the membrane transport function at acidid pH. Pyrazinamide resistance mainly occurs due to mutation in *pncA* gene encoding a pyrazinamidase enzyme and presence of an active acid efflux mechanism that pumps out pyranoic acid out of the cell rapidly (Zhang et al. 2003).

Ethambutol

Ethambutol is bacteriostatic, it inhibits biosynthesis of arabinogalactan, a core polymer component of mycobacterial cell wall. Arabinogalactan linked to peptidoglycan and mycolic

acid forms the major structure of the cell wall (Takayama et al. 1989). In addition, the antibiotic also inhibits the formation of lipoarabinomannon, an important immunogenic surface molecule by disrupting synthesis of arabinan (Goude et al. 2009). The mechanism of resistance has been linked to *emb* locus that codes for three arabinosyltransferases; EmbA, EmbB and EmbC along with a regulator EmbR located elsewhere in the chromosome (Goude et al. 2009). Since EmbB is the primary (although not the only one) target of the drug, mutations in *embB* gene are implicated in resistance, although a lot is not yet known about the precise resistance mechanism (Goude et al. 2009).

1.7 Challenges Associated with TB Treatment

While the anti-TB antibiotics are very successful in eradication of the infection by sensitive strains of *M. tuberculosis*, compliance to the prolonged and complex antibiotics treatment regimen has been difficult to achieve and this has significantly contributed to the emergence of multiple drug resistance *M. tuberculosis* (MDR TB) strains (Laurenzi et al. 2007). MDR TB strains are usually resistant to two frontline potent antibiotics, isoniazid and rifampin, most commonly used in the treatment. Treatment of MDR TB involves a combination of second-line drugs, which include streptomycin, capreomycin, kanamycin, amikacin, ethionamide, para-aminosalicylic acid, cycloserine, ciprofloxacin, ofloxacin, levofloxacin, moxifloxacin, gatifloxacin and clofazimine. This is economically challenging as the currently MDR TB requires 20 months of antibiotic treatment as per WHO's recommendation, also these drugs are not optimum with serious side effects and less efficacy (Mukherjee et al. 2004; Laurenzi et al. 2007; Jain et al. 2008; WHO 2012). In the past, resource-intensive programs such as DOTS (directly observed treatment-Short course) that involves consumption of drugs by the TB patient in the direct presence of a health care personnel has

been promoted by WHO, to ensure proper implementation of anti-TB regimens in terms of continuation of treatment, dosage and quality of drugs (Raviglione 2002; Laurenzi et al. 2007). Inadequacy of any sort in the treatment process leads into selection of drug resistant strains and emergence of additional drug resistance over time is a severe challenge for both public health and TB control. In 2006, Centers for Disease Control and Prevention (CDC) and WHO have jointly reported emergence of Extremely Drug resistance (XDR) in TB (CDC 2006). According to this report, of all the 17,690 TB isolates from 2000- 2004, 20% were MDR and 2% were XDR. The fact that XDR TB is present worldwide set an immediate concern of virtually untreatable future TB epidemic (CDC 2006). XDR TB strains are not only resistant to isoniazid and rifampicin (MDR-TB) but also to at least three of the six of second-line antiTB drugs (aminoglyco-sides, polypeptides, fluoroquinolones, thioamides, cycloserine and para aminosalycilic acid) (CDC 2006). In 2012, as per WHO estimation, 3.7% of new and 20% of previously treated TB cases were MDR-TB and 9.0% of the average proportion of MDR-TB cases were reported to be XDR-TB. Incidents of XDR-TB are spread across at least 84 countries included in the study; eastern Europe and central Asia were stated to have highest proportions of MDR-TB patients (WHO 2012). A key factor responsible for therapeutic challenge in TB is the subpopulation called ‘persisters’, bacteria that prolongs and complicates the antibiotic treatment process. As noted above, the persisters are subpopulations of bacteria, although they are genetically drug sensitive, under the influence of perhaps altered physiological environments are refractory to lethal actions of antibiotics and requires the lengthy therapy (continuation phase). If antibiotic treatment is halted leaving behind persisters, a few ‘stem’ persisters from these heterogenous subpopulations have the capacity to spread and reinitiate the disease or possibly reactivate

other mycobacteria (Zhang et al. 2012). We have limited knowledge about the anatomical location for persisters, but are believed to persist both intracellularly and extracellularly in different locations and cell types including macrophages (Zhang et al. 2012). Persisters are believed to be in a non replicating or slowly growing metabolic state with an underlying diverse growth state due to residing in different microenvironmental conditions like high oxygen (in lung cavities) or low oxygen (in host macrophages or in granulomatous lesions) content, nutrient starvation, oxidative stress, acidic pH etc. Such conditions determine the respective physiological conditions for the bacteria and induce heterogeneous bacterial populations with different capacities for persister formation and therefore, various susceptibilities to anti-TB drugs (Zhang et al. 2012). An additional barrier in the TB treatment is the confluence of this disease with the HIV epidemic, as TB is the leading cause of death in HIV infected people. HIV infection has exacerbated TB cases globally but the scenario in sub Saharan African region is the most severe which accounts for 79% of the total HIV positive TB cases (WHO 2012). The risk of progression from latent TB infection to active disease escalates with HIV coinfection and two billion individuals estimated with latent TB worldwide. TB/HIV crisis deserves combined and coordinated efforts globally for addressing the different health and social component of these diseases. WHO recommends HIV/TB collaborative activities to prevent, diagnose and treat TB patients living with HIV, including screening of TB patients for HIV, then administering co-trimoxazole preventive therapy (CPT) and antiretroviral therapy (ART) to those who test positive for HIV; in addition provide isoniazid preventive therapy to HIV affected people who do not have active TB (WHO 2012). In 2011, WHO estimated that 40 % of TB patients had a documented HIV test results and the collaborative measures ensured 79% of TB patients known to be HIV-

positive, were provided with CPT, and 48% were started on ART. Similarly, 3.2 million people enrolled in HIV care were reported to have been screened for TB and 0.45 million of those without active TB disease were administered IPT (WHO 2012).

At present, a number of national and global programs are employed and encouraged to aim for a TB free world. “The Stop TB Strategy” of WHO advocates for a number of policies for TB control including expansion and enhancement of high-quality DOTS, better addressing the needs of poor and vulnerable populations specially for TB/HIV, MDR-TB and emphasizing as well as promoting research for better diagnosis and treatment of TB. During the past decade considerable progress has been made towards TB diagnostics and treatment, and for the first time in 40 years, 11 new anti-TB drugs have entered clinical trials. Hopefully, the new drugs would be effective in treating the persisters, achieve the goal of eradicating them and potentially shorten the TB therapy.

1.8 Vaccination Against Tuberculosis

With the huge global burden of the disease, its severe immunopathology, complicated drug therapy and emergence of drug resistant strains, quest for better preventive measures such as vaccination has become critical. Unfortunately the only vaccine available since the last century against TB is BCG, isolated by and named after Calmette and Guerin in 1920s. BCG is a multiple attenuated mutant *M. bovis* strain that was derived from a virulent strain of *M. bovis* after more than 13 years of continuous in vitro passage on bile soaked potato medium. The use of BCG started with the vaccination of children in Europe at the end of Second World War, and then by early 1950s WHO campaigned for its use worldwide, especially in TB endemic areas (Anderson et al. 2005; Ottenhoff et al. 2012). Since then, a single intradermal dose of BCG (as recommended by WHO) is routinely administered to infants

soon after birth in all countries with a high risk of TB infection. Although BCG provides significant protection against acute TB in children, its efficacy against adult pulmonary TB, which represents the transmissible form of this disease, is inconsistent and incomplete (Anderson et al. 2005; Ottenhoff et al. 2012). The level of protection has been found to be lowest in countries with the highest incidence of TB. The reason for the protective effect of neonatal BCG vaccination often beginning to wane in early adolescence is not known. It is possibly due to the loss of immune memory, there is an indication that environmental factor such as co-infections (with helminthes parasites or viruses that compromise host immunity like HIV or super infection with non tuberculosis mycobacteria), co-morbidity, nutrition, genetics and TB exposure intensity also play a role. There is a concern of developing disseminated BCG-osis in infants with HIV, which is why WHO Global Advisory Committee on Vaccine Safety, recommends that BCG should not be used in HIV- positive children (Anderson et al. 2005; Ottenhoff et al. 2012). Despite these limitations, BCG remains one of the most widely administered vaccines worldwide, having been given over 4 billion times and the truth remains obvious that its efficacy is disappointing in controlling TB worldwide. Reasons to continue to employ BCG are that it is an old vaccine and there is not a clearly preferred vaccine. Consequently there is a dire need to develop more effective vaccines that can either repair or replace BCG. Due to the fact that BCG confers reliable protection against disseminated disease in childhood, there is more inclination towards development of vaccine that would boost BCG's initial priming and protective effects. The newer vaccine candidates being considered could be broadly categorized into: live mycobacterial vaccines and subunit vaccines (Anderson et al. 2005). Live vaccines could either contain a genetically attenuated strain of *M. tuberculosis* or a genetically augmented

BCG. Since BCG strain has been weakened by the accumulation of spontaneous mutation, including deletions, the BCG live vaccine could improve upon continued attenuation and gene loss, it could be restored either by introducing immunodominant *M. tuberculosis*-specific antigens that are absent from BCG, such as RD1 locus-encoded antigens (ESAT6, CFP10), or by over-expressing antigens that BCG already expresses by itself (for example, the Ag85 complex). Attenuated *M. tuberculosis* vaccine strains are being developed by inducing auxotrophy, or by deleting essential virulence genes like RD1 virulence gene cluster. In either option, the ultimate aim is to achieve a vaccine that is safe, more immunogenic inducing longer lasting protective immunity in adults as well as children (Ottenhoff et al. 2012). Subunit vaccines, on the other hand are non-living components of bacteria like proteins, or in the case of viral vectors, non-replicating vaccines, which can be safely administered to human host regardless of immunocompetence (Ottenhoff et al. 2012). An example of subunit vaccine under trial is a fusion molecule composed of two immunodominant, secreted proteins from *M. tuberculosis* (ESAT-6 and Ag85B). Subunit vaccines are anticipated to serve as booster vaccines in addition to BCG, augmented BCG, or attenuated *M. tuberculosis* priming vaccines for strong, long-lived immune responses (Ottenhoff et al. 2012). At present, more than a dozen TB vaccine candidates are in clinical trials, and many more are in the pre-clinical pipeline to be considered for testing and well over 20 next-generation candidates are in the discovery pipeline giving us hope for an effective vaccination strategy against adult pulmonary TB in the near future (Anderson et al. 2005; Ottenhoff et al. 2012).

1.9 Studying Human Tuberculosis with a Surrogate Mycobacteria - *Mycobacterium marinum*

Due to the fact that *Mycobacterium tuberculosis* is an extremely slow growing pathogen and

requires strenuous safety precautions to prevent the threat of exposure to researchers, other mycobacterial species have been considered as surrogate models to study tuberculosis, including *Mycobacterium marinum*, *Mycobacterium bovis* and *Mycobacterium smegmatis*. Another important issue to be considered is that, experimental infections of *M. tuberculosis* to mammalian animal models (used successfully to study other diseases) are not authentic hosts, do not mimic human infection per se, even if they do to some extent, there are other drawbacks associated with these systems.

M. bovis has been a favorable model for studying TB and vaccine discovery owing to these facts:

- The genome sequence is >99.95% identical to that of *M. tuberculosis,* shows colinearity and no evidence of extensive translocations, duplications or inversions; has 11 deletions that led to a reduced genome size (Garnier et al. 2003).
- It is the progenitor of the only current vaccine against tuberculosis, BCG, a strain that was attenuated by accumulation of mutation from serial passage of *M. bovis* for over 13 years (Garnier et al. 2003). Comparative studies with BCG and *M. tuberculosis* strains have contributed to the discovery of the mutant genes that attenuates this pathogen.
- *M. bovis* naturally causes tuberculosis like disease in cattle as well as in other mammalian host models like swine, rabbits, guinea pigs and mice, it has also been considered a surrogate for human TB study (Bolin et al. 1997; Dannenberg 1994; . Converse et al. 1996; Mc Murray 1994).

M. smegmatis serves as the most tractable model to study mycobacterial genetics.

It is a fast growing, saprophytic species and allows expression of genes from other mycobacterial species.

1.10 *Mycobacterium marinum* as a Surrogate for *M. tuberculosis*

M. marinum is one of the closest related specie to the *M. tuberculosis* complex, based on 16S rRNA gene sequence analysis (99.4% identity), fatty acid profiling, DNA-DNA hybridization (>85% nucleotide identity) and genome wide comparisons. *M. marinum* shares over 3000 orthologs with an amino acid identity of 85% or greater (Stinear et al. 2008). *M. marinum* has comparable genomic organization and pathogenesis along with sharing virulence determinants with *M. tuberculosis*, all of these attributes make it a good choice as a surrogate model to study human tuberculosis (Tobin et al. 2008). *M. marinum* grows at a considerably faster rate, with an optimal generation time of 4 hours, opposed to about 20 hours for *M. tuberculosis* (Clark et al. 1963). This means *M. marinum* colonies appear on plates in about 1 week compared to 3-4 weeks in case of *M. tuberculosis*, enhancing the pace of research. In addition, *M. marinum* can be more safely studied in biosafety level 2 (BSL-2) facility as opposed to the stringent BSL-3 conditions with respirators that are needed to work with *M. tuberculosis*. The lower risk contributes to decrease in research costs and makes manipulation of this pathogen less cumbersome. Among the distinct physiological attributes of *M. marinum*, its optimal growth temperature is 27°C - 30°C when grown in Middlebrook 7H9 medium. Unlike *M. tuberculosis*, *M. marinum* grows poorly at 37°C, does not reduce nitrate and is photochromogenic. It synthesizes characteristic bright yellow carotenoid pigments when exposed to light; these pigments have been suggested to offer protection from oxidative damage or from UV damage in incident sunlight by reducing singlet oxygen species (Clark et al. 1963; Stinear et al. 2008). It is a facultative anaerobe, adapted to persist

in both free-living and intracellular life style unlike *M. tuberculosis,* which is thought to be specialized pathogen and has no known environmental reservoirs. *M. marinum* thrives in various aquatic systems, forms biofilms and replicate within protozoan (such as Dictyostelium discoidieum), fish and occasionally in mammalian hosts (Leoni et al. 1999; Solomon et al. 2003; Bardouniotis et al. 2003; Hagedorn et al. 2007; Stinear et al. 2008). The *M. marinum* genome consists of 6,636,827 bp in a single circular chromosome and one large plasmid with an average G/C content of 62.5%, whereas *M.tuberculosis* genome is 4,411,529 bp and similar G/C content. It is speculated that the extra *M. marinum* genome encodes determinants for environmental survival while with downsizing and lateral gene transfer *M. tuberculosis* became a specialized intracellular pathogen (Ramakrishan 2004; Stinear et al. 2008).

1.11 *Mycobacterium marinum* as a Pathogen

M. marinum causes systemic TB like disease principally in poikilotherms but also in some warm-blooded animals. In mammals, it typically mounts superficial infection, restricted to cooler extremities of the body (Stinear et al. 2008). It was first isolated in 1926 by Joseph D. Aronson from tubercles observed predominantly in the spleen and liver of diseased fish that had died in the Philadelphia Aquarium. *M. marinum* has been reported to infect over 160 different fish species all over the world in both cultured and natural populations of freshwater, estuarine, and saltwater environments. Its host range is extensive including some of the most economically and recreationally important species such as striped bass (*Morone saxatilis*), sea bass (*Dicentrarchus labrax*), and tilapia (*Oreochromis mossambicus*) (Chinabut 1999; Kaattari et al. 2006). A recent incident of an ongoing epizootic crisis is in Chesapeake Bay, this outbreak brought attention to mycobacteriosis in wild fish populations. Over 60% of

striped bass sampled in the Maryland portion of the Bay to be infected with mycobacteriosis, causing a huge economical loss of approximately 200 million dollars per year. A number of other fish in the Bay have also tested positive including blueback herring (*Alosa aestivalis)*, winter flounder (*Pleuronectes americanus)*, striped killifish (*Fundulus majalis),* largemouth bass (*Micropterus salmoides)*, and weakfish (*Cynoscion regalis*) (Ottinger et al. 2006). In addition, other poikilothermic species, including the leopard frog (*Rana pipiens*), the American alligator (*Alligator mississippiensis*), the green anole (*Anolis carolinensis carolinensis*), and the common snapping turtle (*Chelydra serpentine*) may have also been shown to be susceptible (Clark et al. 1963; Bouley et al. 2001).

As in human TB, the diagnosis of mycobacterial fish disease can also be difficult, since many of the infected fish in a population develop chronic infections and thus, do not present any outward symptoms of the disease. Often histopathology of sacrificed, but healthy-looking animals may be the first evidence to reveal a mycobacterial infection, such as granulomas with acid-fast rods in tissues, the hallmark lesions in human *M. tuberculosis* infections. Given the major economic set back associated with the disease, unfortunately, thus far, there is no known effective method of curing such outbreaks but to eradicate the infected population.

M. marinum occasionally infects human causing superficial lesions called fish tank granuloma, aquarium finger or swimmer's granulomas as these infections are usually result from aquatic activities associated including swimming, fishing, boating, and keeping tropical fish tanks. The lesions which are clinically and pathologically identical to the dermal *M. tuberculosis* lesions in terms of being non-tender, warty inflammations, or ulcerated granulomatous, are typically restricted to extremities like elbows, knees, feet, fingers, and

hands, consistent with the lower growth temperature optimum of *M. marinum*. If *M. marinum* skin lesions are accurately diagnosed, they are readily treated by short regimens of front-line anti-TB drugs (e g. rifampin and isoniazid). In rare incidents, infections have been reported to penetrate into deeper tissues such as tendons, bones and joints, particularly in cases of compromised immunity. However, dissemination to organs rarely occurs, even in severely immunocompromised patients. In addition, person-to-person *M. marinum* transmission by aerosol infection or otherwise have not been documented (Collins et al. 1985; Ramakrishan 2004).

1.12 Mycobacteriosis Caused by *Mycobacterium marinum*

M. marinum produces a systemic granulomatous TB like disease with pathology similar to its relative *M. tuberculosis*, experimental infection of *M. marinum* to its naturally susceptible ectothermic hosts have helped us gain deeper insights into this disease and thus better understanding the dynamics of human TB. Also, *M. marinum* and *M. tuberculosis* share orthologous virulence determinants, and it has been seen in several cases that mutation in *M. marinum* genes can be complemented by *M. tuberculosis* virulence genes demonstrating conserved function (Cosma et al. 2003, 2006; Gao et al. 2004; Mehta et al. 2006; Volkman et al. 2004, 2010)

Ramakrishnan et al. (1997) have shown that Leopard frogs (*Rana pipiens*) also develop lifelong asymptomatic infections (as in case of majority of human TB infections), with formation of highly organized non-caseating granulomas in infected organs like liver, kidney and other target organs. Experimental infections with *M. marinum* in other hosts like goldfish (*Carassius auratus*), zebrafish (*Danio rerio*) produced necrotizing granulomas that are reminiscent of active or acute human TB that is ultimately lethal while studies with medaka

(*Oryzias latipes*) exhibit that both chronic or acute infections are inducible in this model in a dose dependent manner. (Broussard et al. 2007; Talaat et al. 1998; Swaim et al. 2006; Prouty et al. 2003).

Virulence of *M. marinum* (like *M. tuberculosis*, discussed above) is greatly enhanced by its ability to thrive within host macrophages; to an extent by arresting phagosome maturation prior to phagolysosome fusion. As indicated above, the classic hallmark structure of TB in human, 'granuloma' are also evident in fish and frog organs infected with *M. marinum*; although these granulomas have very few lymphocytes compared to *M. tuberculosis* and *M. marinum*-induced granulomas in mammals. *M. marinum* granulomas have the basic core of epithelioid cells in all infected species and like *M. tuberculosis*, *M. marinum* can also produce caseating or noncaseating granulomas depending on the infected host (Tobin et al. 2008). Real-time imaging of transparent zebrafish hatchlings infected with *M. marinum* have detected role of bacterial virulence determinants in exploiting macrophages for their dissemination through several modes, bacteria were transmitted from one macrophage to another by membrane tethers. Dead infected macrophages were also phagocytosed by uninfected macrophages resulting infected phagocytes without requiring the bacteria to be exposed to an extracellular environment. Moreover macrophages were observed migrating-in from distant sites in tissues and new infected macrophages aggregate into tissues to initiate granuloma formation (Volkman et al. 2004). These observations from zebra fish collectively suggest that early granuloma promotes bacterial proliferation. Granulomas have long been considered host protective structure made up of aggregates of immune system cells to restrict or eradicate infection, but studies like those performed by Volkman et al. (2010) using zebrafish-*M. marinum* model provided novel understanding into the mechanisms and

consequences of granuloma formation, which suggest otherwise. Mycobacterial important virulence chromosomal region called *RD1* encodes ESAT6, which signals rapid macrophage migration to the granuloma and move randomly within the structure. On the other hand, a deletion of *RD1* region was associated with poor granuloma formation and attenuated infection suggesting granuloma formation might actually aid bacterial proliferation. Mycobacterial virulence protein ESAT6 induces host matrix metalloproteinase 9 (MMP9) by neighboring epithelial cells that surrounds the growing granuloma that results in recruitment of new macrophages to the granuloma (Ramakrishnan 2012).

1.13 Study of mutants in *Mycobacterium marinum*

Described below are the *M. marinum* mutants employed in the studies described in this dissertation**.**

1.13.1 *RD1* Mutant of *Mycobacterium marinum*

The *RD1* interval is perhaps the most famous or widely researched gene complex in mycobacteria. *RD1* (or region of difference-1) has been identified as one of the several regions of the chromosome that are missing from various BCG substrains but present in all virulent strains of *M. tuberculosis*, *M. bovis* and *M. marinum*. *RD1* locus in *M. tuberculosis* has 9 predicted open-reading frames (from *Rv3871–Rv3879c*) within a 9.5-kb region and codes for prominent antigens like ESAT-6 and CFP-10 along with their specialized secretion system (Volkman et al. 2004). Studies with human and murine macrophages have demonstrated that *RD1* mutants are strikingly less virulent than *M. tuberculosis* (Lewis et al. 2003). Similarly, *M. marinum RD1* mutant is also attenuated for growth in cultured human and murine macrophages as well as in infection models using zebrafish and adult frogs. The RD1 regions in *M. tuberculosis* and *M. marinum* share functional homology and synteny

(Volkman et al. 2004). *M. marinum RD1* mutants were attenuated in infection of zebrafish embryos; showing reduced macrophage aggregation, intercellular bacterial spread and thus poor granuloma formation. On the contrary, virulent mycobacteria could rapidly recruit macrophage to the nascent granuloma and enhance infection within them; supporting the notion that mycobacteria, equipped with an intact *RD1* locus encoding all virulence factors probably dictates and exploits the granuloma formation process (Volkman et al. 2004; Ramakrishnan 2012). Gao et al. (2004) had screened for mutants with transposon insertions in *M. marinum* genes homologous to *M. tuberculosis RD1* and surrounding genes, a gene cluster (*Mh3866–Mh3881c*) that has been referred to as extended *RD1* (*extRD1*) (as shown in Figure 1.3). These mutants lacked haemolytic activity, showed reduced cytolysis and cytotoxicity to macrophages, also exhibited decreased intracellular growth at later stags of infection. These defects were complemented in *M. marinum* by expression of homologous genes from *M. tuberculosis*, indicating *extRD1* genes are conserved between *M. marinum* and *M. tuberculosis* in terms of both structure and function. Gao et al. (2004) showed that *extRD1* genes are required for secretion of ESAT-6 and CFP-10 effector proteins. In the zebrafish acute infection model, wild-type strains showed enhanced pathogenicity with severe symptoms like extensive necrosis in tissues, high bacterial burden and high mortality but infrequent mature granuloma formation; where as, fish infected by extRD1mutants like *Mh3868::Tn* showed no significant tissue damage, granulomas containing few mycobacteria. *Mh3868::Tn* is of special interest as it has been used in studies described here. Additionally, *extRD1* genes were shown to be required for *M. marinum* spreading in cell culture, again the defects were fully complemented by corresponding *M. tuberculosis* or *M. marinum* genes (Gao et al. 2004). A related and significant study by Volkman et al. (2010) have implicated

the role of ESAT-6 secretion system–1 (ESX-1) in inducing MMP9 secretion in epithelial cell and there by enhancing apoptosis of infected macrophages, recruitment of new macrophages at the site of nascent granulomas and aid in its expansion and bacterial dissemination.

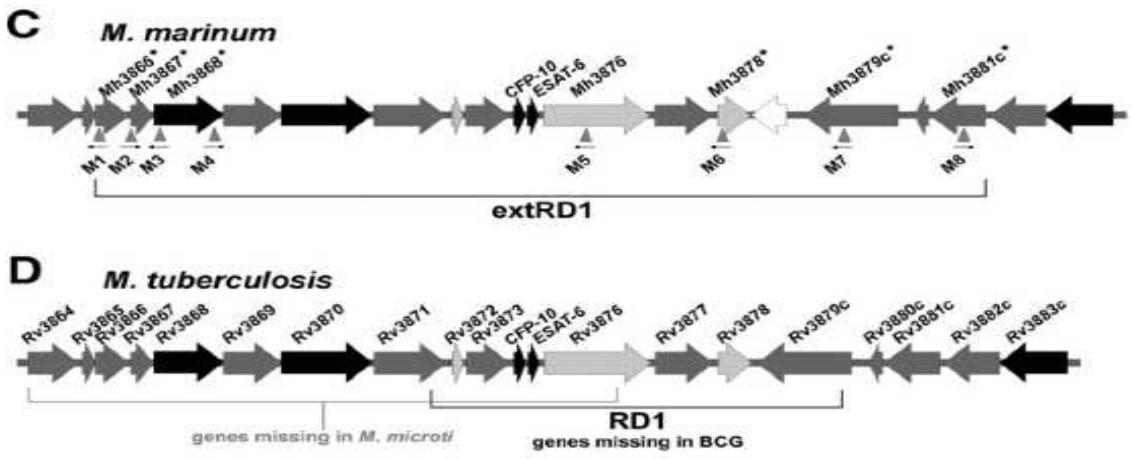

Figure 1.3 **The extended RD1 Locus in *M. tuberculosis* and *M. marinum***.
(Adapted from Gao et al. 2004)

1.13.2 *iipA* Mutant of *Mycobacterium marinum*

Gao et al. (2006) identified *M. marinum* mutants that were defective for invasion and intracellular persistence (*iip*) in murine macrophages. In particular, mutant (*iipA::kan*) was created by inserting a kanamycin resistance gene cassette, at the 5′ region of the Rv1477 gene homologue (of *M. tuberculosis*) by homologous recombination. *iipA* mutant is highly attenuated at an early step for entry as well as for intracellular survival (or persistence) in macrophages, a defect that is fully complemented expression of highly conserved *Rv1477* gene of *M. tuberculosis*. Zebrafish infection showed that *M. marinum iipA* gene is essential for virulence; the bacterial burden in organs and mortality of wild-type *M. marinum* infected

fish were significantly lower in the *iipA* mutant, however, the virulence of the mutant was fully restored when complemented by *M. tuberculosis Rv1477*.

1.13.3 *Mycobacterium marinum* Mim mutants

Virulence of *M. marinum* is dependent on its ability to survive and replicate within macrophages during the infection cycle, but the comprehensive understanding of the molecular mechanisms or the genes involved in this process is yet to be resolved. A set of mutants were isolated by Mehta et al. (2006) identified following random transposon mutagenesis of *M. marinum* chromosome, that were defective in macrophage infection, growth in association with macrophages or both. Here we describe the *in vivo* characterization for three of these Mim (macrophage infection mutants) mutants, they include; *mimI*, *mimD* and *mimH*. Studies with murine macrophages showed that *mimH* is significantly defective in cell association or binding to macrophage, but once entered (in low numbers compared to the wild-type), the bacteria efficiently survives inside the macrophage to the level comparable to the wild-type. On the other hand, *mimD* can bind to the macrophages as efficiently as the wild-type, but its capacity to survive inside the hostile environment of macrophage is greatly diminished. Both attachment to the macrophage and survival inside is substantially compromised for the *mimI* mutant. *M. tuberculosis* homolog of *mimI*, *Rv1502* (with an average of more than 70% amino acid similarity) successfully complemented the defect indicating conserved structure and function between the two. Prior to this study, there is no *in vivo* documentation of virulence of these Mim mutants.

1.14 *Mycobacterium marinum*-Medaka Model

In order to better understand the disease of TB, studying different aspects of host-pathogen interaction is essential. To be able to study controlled experimental infections and not

retrospective speculations, involving outbreaks of the pathogen is invaluable. A fish TB model has been developed in our lab, using *M. marinum* as the pathogen and Japanese medaka (*Oryzias latipes*) as the host for chronic mycobacteriosis that closely resembles the human TB infections (Broussard et al. 2007).

Japanese medaka is a small freshwater teleost fish native to Japan, Korea, and Eastern China, has a preferred habitat of small still bodies of water, and since the domestication of rice, are abundant in rice paddies. They are small, approximately three to four centimeters in length, and are able to tolerate a wide range of salinities and temperatures extending from 10 to 40 degree Celsius. It rapidly reaches sexual maturity, requiring only two to three months. Eggs are fertilized and spawned externally with as many as 3,000 eggs produced during a mating season (Wittbrodt et al. 2002). Eggs are transparent throughout development and hatch around 10 days post-fertilization. In nature, the medaka is omnivorous, feeding on small invertebrates, but mostly on zooplankton and phytoplankton and algae. Synthetic diets and brine shrimp (*Artemia*) are typically given two-three times per day in laboratory settings. The lifespan of the medaka averages approximately one year under temperature controlled laboratory conditions of 27 degrees Celsius; however, can extend as long as two-three years in other conditions. Disease prevalence in this fish is relatively low. Since 1850, it has served as a model for physiology, embryology and genetics. Recently, the genome has been sequenced and annotated; also there are various genomic libraries, cloned genes, microarrays and other genetic resources available for medaka research.

1.15 Antibiotic Treatment in fish

Although there is a substantial amount of documentation about different types of antibiotics usage in aquaculture for prophylaxis in ‘mediated food’ and in treatment, the method of

administration of the drugs is rather crude in both natural and cultured settings. Most of the information implies that the drugs were incorporated into the fish food but none have carefully followed an effective protocol for treatment and their efficacy of bacterial clearance (Benbrook 2002). There is information about the estimated quantity of drugs used in aquaculture mostly, but it is obvious that the treatment practices are far from being regulated or standardized. Given that there is a big threat of emergence of drug resistance, many are linked to overuse of drugs particularly in aquatic settings. Public health emphasis is mainly on controlling the excessive use of antimicrobials in aquaculture that also negatively impacts animal and human health as well as the aquatic environment (Alderman et al. 1998; Benbrook 2002; Cabello et al. 2013).

Treatment of *M. marinum* in zebrafish larvae model using antibiotics (isoniazid) has been described in a study by Adams et al. (2011), which claimed reduction in bacterial burden. In this case, infected animals were immersed into water supplemented with antibiotics renewed daily; with concentrations much higher than *M. marinuum* MIC. However, many fundamental issues like how or at what dose are drugs being absorbed by the fish have not been addressed. Moreover, similar efforts in our lab to treat *M. marinum* in adult medaka by immersion in isoniazid suggested that it not effective (Broussard and Ennis, unpublished observation).

As mentioned before, rifampin and isoniazid are the two frontline antibiotics used effectively for the treatment of both *M. tuberculosis* and *M. marinum* human infections; additionally these drugs have also been employed to study different aspects of TB therapy in many experimentally infected mammalian hosts (Zhang et al. 2011; Rosenthal et al. 2012). *In vitro* tests have confirmed the susceptibility of many clinical strains of *M. marinum* to these

antibiotics, with an average MIC_{50} of 0.25 μg/mL and 4 μg/mL for rifampin and isoniazid, respectively (Aubry et al. 2000). This suggests that both rifampin and isoniazid could be potentially used to cure *M. marinum* infections in various poikilothermic hosts like fish.

1.16 Transmission of *Mycobacterium marinum*

Reported modes of transmission of *M. marinum* are largely based on retrospective speculations that follow fish outbreaks in nature as well as in aquatic and in research fish colonies. Three of the major proposed transmission models include; one, vertical transmission between an infected mother to offspring, two, infection by ingestion of *M. marinum* -laced foods, and three, horizontal transmission by shedding bacteria (e g., released in feces) into water and then infecting other fish (Mutoji 2011; Ackleh et al. 2014). Unfortunately, little experimental research has been conducted to support one or more of these postulated transmission models. Significant efforts in our lab failed to obtain any positive evidence for vertical transmission. Oral route, in which fish were fed *M. marinum* – infected tissues proved an effective portal of *M. marinum* infection, such as, fish fed with infected tissues became infected by *M. marinum* presumably carrying sufficient loads in their organs and a large proportion some individuals developed acute mycobacteriosis (70%) and died. In contrast, feeding fish feeding fish food lace with culture grown *M. marinum*, rarely produced infections (Broussard 2007; Mutoji 2011; Ackleh et al. 2014). These results reiterated other similar studies lead to the conclusion that *M. marinum* retrieved from infected tissues becomes considerably more infectious, likely because these bacteria reside in host macrophages of the target organs (Cirillo et al. 1997; Peterson et al. 2013). Intermediate hosts and vector organisms have become increasingly important for transmission studies of mycobacteria. Free-living amoebae are commonly found in nature, also in fish culture

aquaria and experimental studies have shown that protozoa may serve as environmental reservoirs (Cirillo et al. 1997; Harriff et al. 2007). Bacteria, in particular are water-borne NTMs, like *M. marinum* and *M. ulcerans* along with algae, plankton etc accumulates in the gut of mosquito larvae (Merritt et al. 2010). Medaka in the wild principally consume algae, plankton, much smaller aquatic animals, like mosquito larvae and occasionally ingests tissues from dead fish carcasses. It was postulated that ingested *M. marinum* carried in mosquito larvae might serve as a natural vector for mycobacteriosis in fish (Mutoji 2011; Ackleh et al. 2014).

1.17 The Yellow fever mosquito, *Aedes aegypti* as a Mycobacterial Vector

The adult yellow fever or 'house' mosquito, *Aedes aegypti*, is the main insect vector for the transmission of yellow fever, chikungunya and dengue fever in humans inhabiting tropical countries (Gusmão et al. 2007). Recently, the potential role of adult *A. aegypti* mosquitoes to serve as vectors or as environmental reservoirs for the causative agent for Buruli ulcer, *M. ulcerans,* have been investigated. This hypothesis was based on a previous study that found that mosquitoes belonging to the same genus (*Aedes camptorhynchus, Aedes notoscriptus*) were positive for *M. ulcerans* through a PCR diagnostic test (Merritt et al. 2010; Wallace et al. 2010). The Larval mosquitoes feed by filtering particles from the water and biofilms using labral head fans and their food sources may include bacteria and algae. By way of this feeding method, the study by Wallace et al. (2010) showed that the mosquito larvae can readily ingest mycobacteria such as *M. ulcerans* and *M. marinum* and remain infected throughout larval stage but these bacteria are not retained into the pupae or adult mosquitoes. These results indicate an unlikely role for adult mosquitoes as biological vectors although they may serve to maintain in an aquatic food web for *M. ulcerans*. Additionally, the passage

of *M. ulcerans* through three trophic levels was demonstrated, indicating the potential for bioaccumulation of mycobacteria in the environment (Merritt et al. 2010; Wallace et al. 2010).

The hemocoel of the larvae contains principally and cellular components of immune response involved in recognizing foreign agents. These cellular defense mechanisms include, phagocytosis and encapsulation by professional phagocytes as well as, triggering the release of peptides involved in antimicrobial and antifungal activities (Biron et al. 2005). Three types of immune cells, or hemocytes, are found within the hemolymph of *A. aegyti* larvae: granulocytes, oenocytoids, and prohemocytes. Granulocytes like the vertebrate neutrophils compose the majority of immune cell types, while oenocytoids and prohemocytes together comprise less than 10% of the population. Oenocytoids provide a source of phenoloxidases, lysing following an immune challenge, whereas prohemocytes are thought to function as putative stem cells. Granulocytes are the professional phagocytes of the insect immune system and have been observed to internalize bacteria (Castillo et al. 2006). These cells may be especially important in mycobacterial infections, due to their phagocytic nature.

An additional consideration, relevant to mycobacterial transmission via a mosquito larval vector, is the maintenance of suitable environmental conditions within the gut of the insect. The pH of the mosquito larvae gut can be as high as twelve and is necessary for nutritional digestion by alkaline hydrolysis and normal development (Boudko et al. 2001). The development of *Aedes aegypti* progresses through four larval stages, termed instars, leading up to the pupal and adult life stages (Corena et al. 2002), providing a significant period of time for microbial harboring within the larval digestive tract. Without a doubt, the mosquito larvae gut is a highly caustic and degradative environment, harboring digestive enzymes and

proteases; bacterial pathogens must not only survive but may be important in pre-conditioning mycobacteria to mount infection by *M. marinum* (Zieler et al. 2000).

1.18 Preconditioning Mycobacteria

Mycobacteria retrieved from infected tissues become considerably more infectious, likely because these bacteria reside in host macrophages of the target organs as compared to bacteria grown in culture (Broussard et al. 2007; Mutoji 2011; Ackleh et al. 2014)**.** Similarly, increased virulence has been described for bacteria engulfed in macrophages and other phagocytes like protozoans (Peterson et al. 2013; Cirillo et al. 1997; Mutoji 2011). This activation of virulence is believed to result from the induction of a metabolic state primed for infection, where specific virulence gene sets are induced in the caustic environments within phagocytic vacuoles (Ackleh et al. 2014; Tenant et al. 2006). It was observed that cultured Pacific salmon fed with mycobacterial infected fish carcasses escalated the incidence of mycobacterial infections in hatcheries, reiterates the same idea (Jacobs et al. 2009). A significant study by Cirillo et al. (1997) showed that *M. avium* survives and replicate within amoeba (*A. castellanii*) by usual inhibition of phagosome-lysosome fusion and passing through this hostile environment enhances *M. avium* virulence in the macrophage and mouse models of infection. Further research involving *M. avium*-amoeba infection model, showed that genes are commonly upregulated during and these genes were found to encode a variety of functions, including sigma factors and gene expression profiles, metabolic pathways and macromolecule degradation; interestingly, many of the upregulated genes were same as those upregulated upon human macrophage infection (Tenant et al. 2006). Harriff et al. (2007) showed that zebrafish (*Danio rerio*) were more likely to become infected by *M. marinum* and *M. peregrinum* obtained from phagocytes compared to grown in culture. Interestingly,

passage of the bacteria through amoebae (*Acanthamoeba castellanii*) resulted in increased virulence and enhanced bacterial growth within the fish. Consistent with this general impression, we have also we observed similar results when zebrafish fed with paramecia that ingested *M. marinum* were infected at a higher rate than fish fed on culture mycobacterial controls (Peterson et al. 2013).

1.19 Research Statement

The goal of this study was to experimentally investigate established and novel *Mycobacterium marinum* mutants in the chronic *in vivo* medaka model and characterize them in terms of their ability to colonize the target organs as compared to the wild-type strain following two different routes of infection, IP injections and oral ingestions. Activation of virulence in *Mycobacterium marinum* was also investigated upon incubation with mosquito larvae extracts and then inoculating medaka with IP injections. Additionally we also investigated into development of an antibiotic regimen against mycobacteriosis in fish.

CHAPTER TWO: Materials and Methods

Materials and methods pertaining to all result chapters.

2.1. Bacterial Strains and Cultures

Experimental infections listed here have used strains of *Mycobacterium marinum* derived from either the original type strain, a fish outbreak isolate (Aronson, 1926) (Trudeau Mycobacterial Collection 1218R, American Type Culture Collection ATCC927) provided by Lucia Barker (University of Minnesota Medical Center), or derived from a human isolate, called the M strain, obtained from Lian-Yong Gao (University of Maryland) or Lalita Ramakrishnan (University of Washington) (ATCC; BAA535). All the strains employed were derived from these above two parental strains, were constructed using standard laboratory conditions like introduction of mycobacteriophage L5 integration plasmid, pMH94, (a gift from Graham Hatfull, University of Pittsburgh), carrying kanamycin or a hygromycin resistance marker; and the red shifted, mutant fluorescent reporter genes, *rfp* or *gfp* driven by an intermediate strength promoter called *msp12P* derived from pMSP12 plasmid. This promoter was shown to be up-regulated in granulomas (a gift from Lalita Ramakrishnan, University of Washington; Cosma et al. 2004). These plasmids were integrated into the L5 *attB* site of the *M. marinum* chromosome. The mutant strains, carrying *mimD*, *mimH* and *mimI* mutations used in the competition studies described here were received from Jeffery Cirillo (Texas A&M University Health Sciences Center). These random transposon insertion mutants of the *M. marinum* (M strain) were shown to be defective in macrophage infection, growth in association with macrophages or both (Mehta et al. 2006). Other *M. marinum* M strain mutants investigated here were obtained from Gao et al. (2004; 2006). These strains were built by transposon insertion, equipped with a kanamycin resistance marker; within the

RD1 virulence gene cluster of the chromosome (homologous to Rv3868 in *Mycobacterium tuberculosis*) shown to be important for secretion of virulence factor ESAT-6 and showed decreased virulence in a zebrafish model. Also obtained from Gao, another transposon inserted mutation within an operon *iipA* (homologous to Rv1477 of *M. tuberculosis*), was demonstrated to be inefficient in macrophage invasion and intracellular persistence. Another mutant strain, also studied here *ΔRD1-6* was provided by Lalita Ramakrishnan (University of Washington).

All the strains were frozen and stored at -80^{o}C in 50% glycerol until needed. *Mycobacterium marinum* strains were cultured either in Middlebrook 7H9 (M7H9) liquid media supplemented with 10% albumin dextrose salt (ADS), 100 μg/mL cycloheximide, 0.2% tween 80, and 0.5% glycerol at 28°C with shaking for a week or on Middlebrook 7H10 agar (M7H10) plates supplemented with 10% albumin dextrose salt (ADS), cycloheximide (100 μg/mL) and 0.5% glycerol and incubated at 30°C for 7-10 days. The strains used in all the experiments described here are listed in Table 1.

2.2. Medaka Aquaculture

Fish used in most of the experiments presented here is from a transgenic line of Japanese medaka (*Oryzias latipes*) carrying multiple copies of a λ bacteriophage vector that was developed by Dr. Richard Winn (University of Georgia; Winn et al. 2000). The see-through (ST) line of fish was obtained from Dr. Yuko Wakamatsu (Nagoya University, Nagoya, Japan). These fish have been used to study temporal progression of infections by fluorescent bacteria in a live translucent host (Broussard et al. 2007; Broussard 2007). All the fish were propagated in the laboratory at the University of Louisiana. A maximum density of 30-40 adult fish were cultivated per 10-gallon tank with a recirculating filtration and held at 28°C.

All animal facilities were maintained with a photoperiod of 16 hours light and 8 hours dark cycle. Twice monthly, 20 % of water was replaced in each of the tanks. Fish were fed three times a day with different combination of Otohime, brine shrimp, or Aquatic Ecosystems high protein flakes as required.

For a standard infection experiment, 3-5 month old fish were transferred to a Biosafety Level 2 (BSL-2) laboratory at least two days prior to the *M. marinum* infection and were maintained in that facility for the entire duration of the experiment. A constant temperature of 28°C was maintained in the infection lab as well. Infected fish were either kept individually in the smaller 640 mL containers or in a group of ten in 3.7 liter containers. Water was changed once a week by transferring the fish to cleaned containers filled with carbon filtered water that was allowed to acclimate to room temperature for at least 24 hours. Weekly water changes prevented ammonia, nitrite, and other waste products from accumulating in these containers. All procedures were conducted as prescribed by the National Institutes of Health-Biosafety in Microbiological and Biomedical Laboratories (NIH-BMBL) guidelines and were approved by the Institutional Biosafety Committee and the Institutional Animal Care and Use Committee (IACUC).

2.3. Preparation of Infective Doses

Infective doses of *M. marinum* for fish inoculation were prepared largely by the method previously described (Broussard 2007; Broussard et al. 2007; Broussard et al. 2009). Strains were prepared following inoculation of liquid or solid from frozen stocks stored at -80°C in 29% glycerol or from previously prepared concentrated stock. Bacterial cells were cultured in volume of 5 mL grown in test tubes, or 100 mL grown in 250 mL bottles with Middlebrook 7H9 broth depending upon the experimental need. Liquid media was

supplemented with 10% albumin dextrose salt (ADS), 100 µg/mL cycloheximide, 0.5% glycerol, and 0.2% tween 80. The selective antibiotics, kanamycin (20 µg/mL) or hygromycin (50 µg/mL), were added to the broth as required by the particular strain that was used. Cultures were allowed to grow at 28°C with continuous aeration by shaking, *M. marinum* were collected when the culture reached an optical density at 600 nm ($O.D._{600}$) of .6 to 1.0. The cells were then washed twice with phosphate buffer saline solution (PBS; pH 7.4), and the concentration was adjusted to the appropriate infective dose by resuspending the bacteria in pertinent volumes of PBS. As suggested by the previous studies, a correlation between $O.D._{600}$, equal to 0.6, and viable bacterial counts, of 10^8 colony forming units (CFU) per mL, was sustained for all infection. In the experimental doses, *M. marinum* viable cells were directly documented by serially diluting the cultures in PBS with the addition of 0.01% sodium dodecyl sulfate (SDS) at times to reduce bacterial clumping, and then plating the appropriate dilutions on Middlebrook 7H10 agar plates. Duplicate or triplicate plates of the chosen dilutions were incubated at 30°C for seven to ten days. Upon removal from the incubator, plates were left in the light for 24 to 48 hours to allow yellow pigment development as a diagnostic trait for *M. marinum*.

Viable bacteria from each inoculum were calculated by the average CFU seen on the plates. During infection with mixed cultures in competition studies, consisting of two bacterial strains, each strain was grown separately as previously described. As the $O.D._{600}$ of the cultures approached 0.6 - 1.0, the cells were obtained, washed and resuspended in suitable volumes of PBS, to obtain the same density, then mixed at an equal ratio of one to one, with an $O.D._{600}$ of 0.6 for each strain. As described earlier, for estimating the input dose, viable cells from each strain were counted from plates that were spread with appropriate dilutions of

the mixed culture. To confirm bacterial concentration, cultures were plated on permissive media, allowing both strains to grow, and at times on selective media, selecting only the resistant strain. Permissive media consisted of Middlebrook 7H10 supplemented with 10% ADS, 0.5% glycerol, and at times, 100 μg/mL cycloheximide; and kanamycin or hygromycin. Plates were incubated for up to 10 days, then colonies were counted using fluorescence microscopy or by patching colonies to both diagnostic selective plates.

2.4. Infecting Medaka with *Mycobacterium marinum* via Intraperitoneal (IP) Injection

An infective dose of 10^2 to 10^4 colony forming units (CFU) were targeted to be administered to each fish. Fish were anaesthetized in a solution of Tricaine Methanesulfonate (MS-222) at a concentration of 0.0175% (0.035 g/ 200 mL preceeding inoculation, then twenty microliter inoculations were delivered by intraperitoneal (IP) injections to the fish using 26 gauge needles and 1.25 mL syringes. For "sham infections," only sterile PBS was administered by IP injections in the same manner as infection-negative controls. Post injection, fish were transferred to a 3.7 liter container with fresh water to recover, and remained in the BSL-2 laboratory with weekly water changes for the duration of the experiment. During this period, fish were monitored for mortality and were eventually sacrificed typically ranging from 3-8 weeks post infection and target organs were dissected, homogenized and plated for detection of *M. marinum* colonies. In case of coinfection experiments, fish were IP injected as previously mentioned, with twenty microliter of mixed culture consisting of two *M. marinum* strains present in equal ratios.

2.5. Mosquito Larvae Aquaculture

Yellow fever mosquito (*Aedes aegypti*) eggs were supplied by Benzon Research (Carlisle, Pennsylvania) and hatched in the lab as per vendor instructions. Environments with low

oxygen levels facilitate and synchronize hatching of mosquito eggs, therefore they were cultured in water containing crushed fish flakes in order to boost bacterial growth, thereby, diminishing dissolved oxygen levels. The water was taken from an occupied fish tank placed into a 1-liter beaker and incubated at 27°C for 24 to 48 hours. The eggs were submerged in the water for up to three days to allow maximal hatching time. Newly emerged mosquito larvae were transferred to 3.7 liter containers and raised for seven to eleven days until they achieve maturation status likely of instar three or four in order to be used for experiments. Larvae were housed in a BSL-2 laboratory for the duration of their development and fed once daily with crushed Aquatic Ecosystems high protein flakes.

2.6. Infecting Medaka With *Mycobacterium marinum* Using Live Mosquito Larvae

Bacterial cultures were grown individually in 5 mL broths to an $O.D._{600}$ of approximately 1.0 and adjusted to a final $O.D._{600}$ of 0.6 with PBS. For coinfection, both the cultures were combined in equal volume to attain one to one ratio, with both cultures amended to $O.D._{600}$ of 0.6. The 5 ml cultures were transferred to 640 mL containers and approximately 60-100 mosquito larvae were immersed into the bacterial suspensions. Larvae were exposed to the culture for 24 hours prior to their use in experiments. Mosquito larvae were cleaned multiple times (4-5 times) with deoxygenated water and fed to the fish over a one week interval. Four meals of mosquito larvae (five larvae per meal) were given to each fish during this time period. Freshly prepared cultures and newly infected larvae were made separately for each meal. Mosquito larvae were surveyed randomly to determine the ingestion of fluorescent bacteria by inspection under a fluorescent dissection microscope for the presence of fluorescence in the gut. Insect larvae were washed up to four times in clean filtered water, then, briefly put into ice water, to reduce movement of the organisms during microscopy.

Larvae with extensive levels of bacterial load (i.e, heavy fluorescence) were used to feed the medaka.

2.7. Quantification of *Mycobacterium marinum* Ingested by Mosquito Larvae

Bacteria ingested by mature mosquito larvae were quantified for each meal administered to medaka. A sample of five larvae, equivalent to one meal, was visually inspected by microscopy to have ingested the appropriate strains of fluorescent bacteria as previously described. These larvae were then suspended in 500 µL PBS and homogenized with a small pestle in a microcentrifuge tube. Dilutions of the homogenate were plated in duplicate or triplicate on Middlebrook 7H10 plates containing 10% ADS, 0.5% glycerol, 100 µg/mL cycloheximide, 100 µg/mL ampicillin, and 20 µg/mL polymixyn B. Plates were incubated at 30°C for up to 10 days and colonies of fluorescent bacteria were enumerated. Average CFU between two meals of larvae were recorded for each feeding.

2.8. Plating for Viable Count of Fluorescent *Mycobacterium marinum* in Infected Organs

Fish were sacrificed 4-6 weeks post infection to determine the bacterial loads of *M. marinum* from infected organs by the established euthanasia method using a high concentration, an over dose of 0.5% (1 g/200 mL) solution of Tricaine Methanesulfonate (MS-222). In order to retrieve the organs from fish, a ventral excision was made with sterile scalpel to expose the viscera. Liver and kidney of each fish was removed aseptically with sterile forceps and homogenized in 400 µL of sterile PBS. When required, serial dilutions were prepared in PBS and plated on Middlebrook 7H10 plates in duplicate or triplicate. Media was supplemented with 10% ADS, 0.5% glycerol, 100 µg/mL cycloheximide, 100 µg/mL ampicillin, 20 µg/mL polymixyn B, and the selective antibiotic 20 µg/mL kanamycin or 50 µg/mL hygromycin, when necessary. Plates were incubated at 30°C for 10 to 12 days, then, left in the light for 24

to 48 hours to allow pigment development. Viable cells were determined for each organ by counting the colonies observed on the plates. For competition experiments, colonies were differentiated by fluorescence microscopy or by patching the colonies onto selective diagnostic plates.

2.9. Observation of Bacterial Colonies Using Fluorescent Microscopy

A NikonSMZ800 (Nikon, Tokyo, Japan) Stereoscopic Microscope furnished with X-Cite™ 120 for fluorescence illumination and filters for green fluorescent protein (Gfp) or red fluorescent protein (Rfp) detection were used for inspection of colonies on plates. Colonies were observed for fluorescence, differentiate between strains and to confirm appropriate protein expression. Microscopy was also used to view ingested fluorescent bacteria present in the gut of *Aedes aegypti* mosquito larvae.

2.10.Competitive Index (CI) Calculation

The competitive index (CI) ratios for colonies from each organ were calculated as previously described by Ruley et al. (2004) and by Mutoji (2011) using the equation: [(CFU mutant $_{output}$) / (CFU wild-type $_{output}$)] / [(CFU mutant $_{input}$) / (CFU wild-type $_{input}$)]. A CI value of one indicates equal colonization by each of the two strains in target organs, whereas values greater or less than one represents unequal colonization or relative difference in colonization between the two strains, reflective of the relative fitness of the mutant strain to wild-type to mount an infection. CI ratios have been used in experiments to reflect the fitness of wild-type strains and mutants, carrying different diagnostic fluorescent reporters resistance markers. However, in experiments investigating various treatment conditions using two wild-type strains, the strain, which received the treatment, was considered ‘mutant’; therefore, the ‘wild-type’ strain received no treatment conditions.

2.11.Genomic DNA Isolation from *Mycobacterium marinum*

The procedure used for *M. marinum* genomic DNA isolation was an adaptation from Larsen (2000) and Greg Broussard (2007). In this technique, glycine was added to the 100 mL *M. marinum* culture for a 1% final concentration using 10% stock, twenty four hours prior to harvesting DNA and the culture was returned to shaking at 30°C. Glycine 'weakens' *M. marinum* cell walls, which could lead to higher yield of DNA. Twenty four hours later, 10 mL of this culture was transferred into 15 mL conical tube and centrifuge at 2,000 x g for 20 min. After discarding the supernatant, the pellet of cells was resuspended in 1 mL of GTE Buffer (25 mM Tris-HCL, pH 8.0, 10 mM EDTA, 50 mM glucose) then transferred into a 1.5 mL microcentrifuge tube and centrifuge at 10,000 rpm for 10 min. The supernatant was again discarded and the pellet of cells resuspended in 450 µL of GTE Buffer. A 50 µL of a 10 mg/mL lysozyme solution was added into the tube with the cells, mixed gently and incubated at 37°C overnight. The next day 100 µL of 10% SDS was added into the overnight tube and mixed gently. 50 µL of 10 mg/mL proteinase K was added and mixed gently. They were incubated at 55°C for 20-40 min. 200 µL of 5 M NaCl was added and mixed gently (the NaCl blocks the binding of DNA to cetyltrimethylammonium bromide in later steps). The cetyltrimethylammonium bromide (CTAB) solution was pre-heated to 65°C. 160 µL of the CTAB solution was added to the DNA solution and mixed gently. This was incubated at 65°C for 10 min. The CTAB-DNA solution was divided into two 1.5 mL tubes and an equal volume of chloroform-isoamy alcohol (24:1) was added to each tube, and inverted 6 times gently to mix the two phases of liquid and centrifuge in an Eppendorf microcentrifuge at 13,000 rpm for 5 min. The aqueous phase was transferred to fresh 1.5 mL tubes and the above chloroform-isoamyl alcohol extraction was repeated. The aqueous phase was

transferred to clean 1.5 mL tubes, and 0.7 times the aqueous phase volume of room temperature isopropanol was added and mixed gently by inversion until the DNA has precipitated out of solution. This mixture was incubated at room temperature for 5 min followed by centrifugation at 13,000 rpm for 10 minutes. The supernatant was removed and 1 mL of 70% ethanol was added to wash the pellets and bring both pellets to one 1.5 mL tube. This was mixed gently by inversion and centrifuge again at 13,000 rpm for 5 min. The supernatant was removed and the DNA pellet air-dried for 15 minutes being careful not to over dry. The dried DNA pellet was covered with 50 µL of TE Buffer and store at 4°C and the pellet was allowed to dissolve overnight.

2.12. Preparation of Concentrated Stocks of *Mycobacterium marinum*

To achieve the desired growth phase and optical density of *M. marinum*, within a convenient time frame, to be used in experiments concentrated stocks of strains were prepared. Initially, 5mL cultures were inoculated with strains from freezer stocks and allowed to grow at 28°C with shaking for approximately 7-10 days. These cultures were then used to inoculate 100 mL of Middlebrook 7H9 broth in 250 mL bottles, augmented by 10% ADS, 100 µg/mL cycloheximide, 0.5% glycerol, 0.2% tween 80, occasionally 100 µg/mL ampicillin, and the selective antibiotics, kanamycin (20 µg/mL) or hygromycin (50 µg/mL), when necessary. The bottles were incubated, shaking in a 28°C water bath, until an $O.D._{600}$ of 0.6 to 1.0 was reached. Cells were pelleted for 10 minutes with centrifugation at 7,000 revolutions per minute and 4°C. The supernatant was discarded and replaced with 20 mL Middlebrook 7H9 supplemented with only 4 mL 87 % glycerol. After thoroughly vortexing the mixture, 200 µL aliquots were divided into 1.5 mL microcentrifuge tubes and stored at -80°C.

2.13. Preparation of Electrocompetent *Mycobacterium* cells

Transformation of mycobacterial cells was perfomed by electroporation as previously described (Broussard 2007). To prepare electrocompetant cells, a 5 mL culture ($O.D._{600}$ of 0.6) was used to inoculate a 100 mL of M7H9 supplemented with Tween 80 (0.2%), cycloheximide (100 µg/mL), 10% albumin dextrose salt (ADS), and 0.5% glycerol and selective antibiotics, kanamycin (20 µg/mL) or hygromycin (50 µg/mL), when necessary. The culture was incubated at 30°C, shaking at 250 rpm until density of 0.6 at $O.D._{600}$ reached. The culture was then transferred into two prechilled 50 mL conical tubes and incubated on ice for an hour. Tubes were then centrifuged at 5000 rpm for 10 minutes at 4°C, and the supernatant were discarded. The pellet was resuspended in 25 mL (1/2 volume) of cold 10% glycerol centrifuged as above. Centrifugation and washing of the cells were repeated a few times, and each time the pellet was resuspended in half the volume of 10% glycerol. Finally the pellet was resuspended in 1mL of cold 10% glycerol and 100 µL aliquots were put into 1.5 mL tubes. The cells were either used immediately or stored at -80°C for later use.

When using the frozen cells for electroporation, the cells were first thawed, resuspended in 900 µl of cold 10% glycerol, and centrifuged at 13,000 rpm for 1 minute. The supernant was discarded, and the pellet was resuspended in 1 mL for a repeat wash using the same conditions used above. After the second wash, the pellet was immediately resuspended in 100 µL of cold 10% glycerol to be used for electroporation. The two post-freezing washes with 10% glycerol, helped to remove salts, which may have been concentrated during the freezing process.

2.14. Electroporation of *Mycobacterium marinum* Electrocompetent cells

Electroporation procedures are modifications of those previously described by Larsen (2000) and Jacobs et al. (1991). DNA (0.1 μg DNA, 2 μL maximum volumes) was added to 100 μL prepared electrocompetent mycobacterial cells and was incubated on ice for about 10 minutes. Then the cells and DNA were transferred to pre-chilled 0.2 cm electrode-gap cuvettes. Care was taken to make sure the suspension of cells and DNA was at the bottom of the cuvette and that the suspension touched both electrodes. The voltage of the electoporator was set at 2,500 volts. The cuvette was wiped off and placed in the electroporator and electroporation was carried out making sure the time constant was between 4-6. Immediately following electroporation, 900 μL M7H9 broth (without Tween 80 or antibiotics) was immediately added to the electroporation cuvette to aid in protecting the cells by diluting any ion radicals produced during the electroporation process. The suspension of cells was then transferred to a 10 mL snap-cap tube and incubated at 30°C for 4 hours to allow for expression of antibiotic resistance genes carried on the transforming plasmid. Cells were then plated on M7H10 plates containing selective antibiotics for isolation of transformed cells carrying the desired plasmid.

2.15. Intra-Peritoneal (IP) Injection of Medaka with Microspheres

Polyanhydride nanoparticles composed of 20:80 copolymers of 1,6-bis-(p carboxyphenoxy) hexane (CPH) anhydride and sebacic anhydride (SA) carrying a cargo of fluorescene were obtained from Bryan Bellaire (Iowa State University). 2-3 Polyanhydride co-polymer microsphere particles were mixed with PBS to make a total volume of 10 μL was used to inject into See through medaka peritoneal cavity. Fish were then monitored for three weeks until their death.

2.16. Quantification of Rifampin Using Spectrophotometer

Rifampin was dissolved in 1:1 ratio of DMSO (Dimethyl sulfoxide) and water at a concentration of 10 mg/mL. This stock solution was serially diluted (in 1:1 DMSO:Water) to obtain desired lower dilution Rifampin solutions. The OD of rifampin solutions was measured at the diagnostic 475 nm using spectrophotometer (Thermo- Spectronis 20 Genesis).

2.17. Preparation and Administration of Rifampin Embedded Jell-O shot

A rifampin stock at a lower concentration of 10 mg/mL was prepared suspended only in water (DMSO was not pallatable for medaka). Rifampin embedded Jell-O shot were prepared by adding 1 mL of 13% warm liquefied gelatin (into a microcentrifuge tube), along with 0.1 g crushed otohime fish food, 50 µL fish oil and the required amount of rifampin solution. . All the contents were then mixed thoroughly by vortexing and stirring. Aliquots of 20 µL were placed on parafilm and immediately solidified in shape of beads called 'Jell-O shots' held in a biocontainment hood for 1 hour. Jell-O shots were formulated at two different concentrations of rifampin, first, to be administered to infected and control fish; second, for estimation of rifampin leached out into the water during delivery. 20 µL of 10 mg/mL rifampin stock was added to prepare Jell-O shots (each shot containing 4 µg of rifampin) for the purpose of feeding madaka, half of the 20 µL Jell-O shot (containing 2 µg of rifampin) was cut into four quarters with a razor blade and fed to each fish everyday during the entire treatment period. Since the average body weight of medaka is 0.2 gram, a 2µg rifampin/fish/day is comparable to the recommended human dose of 10 mg rifampin/kg body weight/day for TB treatment. Freshly prepared Jell-O shots were administered for each meal.

For rifampin estimation purpose, 120 µL of 10 mg/mL rifampin stock was added to prepare Jell-O shots, so each shot would contain 24 µg of rifampin.

2.18. Estimation of Rifampin Leaching from Jell-O shot

To estimate the amount of rifampin lost to the surrounding water due to leaching out of Jell-O shots, two randomly selected Jell-O shots were cut into four pieces and transferred into microfuge tubes containing 1 mL of water. The tubes were let to sit at room temperature for different time frames (1-5 hours). At each hour interval, a 10 µL aliquot taken out of the microfuge tube was used to measure rifampin concentration by OD at 475 nm. The known extinction coefficient (at 475 nm) of rifampin solution was employed to calculate concentrations in water.

2.19. Preparation of Mosquito Larvae Extracts

Mosquito larvae were intended to be raised to a mature larval stage (likely third or fourth instar) and then used to prepare the extracts. Approximately 60 larvae were collected and placed in a petri dish. Adherent water was removed from the larvae by blotting with Kimwipes. Dried larvae were transferred to a 1.5 mL microcentrifuge tube using a toothpick and macerated with a small sterile pestle. Fully homogenized insects were then centrifuged in the microcentrifuge tube at 13,000 revolutions per minute for three minutes at room temperature. The liquid supernatant was collected as the mosquito larvae extracts, leaving the pelleted particles and debris behind (Figure 2.1). For preconditioning of *M. marinum* culture, extracts in volumes of 100 µL were incubated with 500 µL cultures (adjusted to the appropriate concentrations), for one hour.

2.20 Statistical Analysis

Statistical analysis was used for comparing between the colonization of the mutant and wild-type bacteria in the competition experiments described (Chapter 3.3) in this dissertation. We have used boxplots and the paired t-test (performed with R statistical package) for comparative studies as explained below.

Boxplot: A boxplot is a graphical presentation of the five-number summary of a data. It includes the minimum value, the 25th percentile (or 1st quartile), the 50th percentile (or 2nd quartile or median), the 75th percentile (or 3rd quartile) and the maximum value. It also includes the outliers, if any present in the data. Essentially it shows the distribution of the data, i.e., the center (or location), the spread or variation in the data and also the skewness. The median is a measure of center, the length of the box which is the range of the middle 50% of the data is also called the Interquartile range (IQR) and is a very robust measure of variation and the position of the median compared to the 1st and 3rd quartile tells us about the skewness of the data. If the median is equidistant from the 1st and 3rd quartile, then most likely the data is symmetrically distributed, if the median is closer to the 1st quartile than the 3rd quartile then it is skewed to the 'right' (or positively skewed) and if the median is closer to the 3rd quartile than the 1st quartile then the data is said to be skewed to the 'left' (or negatively skewed).

Hence the boxplots were constructed for both mutant and wild-type bacterial counts as obtained from the organs (liver and kidney) and expressed in terms of output cfu per unit input cfu to find out the difference between the colonization levels of the two strains. Boxplots were used for graphical comparison and a more rigorous comparison was done using the paired t-test.

The paired t-test is generally used when measurements are taken from the same subject, which is suited for our data sets as the outputs (in terms of the bacterial count from the infected organs) were obtained by inoculating the same fish with both mutant and wild-type strains. It was appropriate to take into consideration the amount (cfu/fish) of each of the two strains administered to the fish, and it was expressed as output cfu per unit input cfu as the measurement of study. The numbers were log transformed for the ease of analysis.

Statistical Hypotheses: The null hypothesis would be the mean difference between paired observations is zero. This is mathematically equivalent to the null hypothesis of a one-way ANOVA or t-test, that the means of the groups are equal, but because of the paired design of the data, the null hypothesis of a paired t-test is usually expressed in terms of the mean difference. In our case the null hypothesis is that there is no difference in the level of colonization of mutant and wild-type strain in the organs of the infected fish. Where as the research/alternative hypothesis is that the level of colonization of mutant is less than that of wild-type strain.

Assumption: The paired t-test assumes that the differences between pairs are normally distributed which can be easily checked using a histogram or a quantile-quantile plot. If the differences between pair are severely non-normal, it is better to use a non-parametric test. However, the test is robust to small deviations from normality, as is the case with our data sets.

The difference between the observations was calculated for each pair along with the mean and standard error of these differences. The test statistic is then calculated by dividing the mean by the standard error of the mean. The test statistic is t-distributed with degrees of

freedom equal to one less than the number of infected fish. Then the p-value or the probability of observing something more extreme than what we have already observed was computed and employed to obtain the inference. In our experiments, a very small p-value (< 0.05) would indicate that the level of colonization by the mutant is significantly less than the wild-type strain in the infected organs.

Strain	*Specie*	*Relevant Traits*	*Source*
DE3932	*M. marinum*	ATCC 927 (1218R)	Lucia Barker, University of Minnesota
DE4390	*M. marinum*	Human isolate	ATCC (BAA535) Lalita Ramakrishnan (University of Washington)
DE4373	*M. marinum*	DE3932 L5::pDEAM 2 (rfp Kan^R)	This study
DE4374	*M. marinum*	DE3932 L5::pDEAM1 (gfp Kan^R)	This study
DE4433	*M. marinum*	DE3932 L5::pDEAM4 (gfp Hyg^R)	This study
DE4434	*M. marinum*	DE3932 L5::pDEAM5 (rfp Hyg^R)	This study
DE4435	*M. marinum*	DE4390 L5::pDEAM4 (gfp Hyg^R)	This study
DE4436	*M. marinum*	DE4390 L5::pDEAM5 (rfp Hyg^R)	This study
DE4383	*M. marinum*	DE4390 L5::pDEAM2 (rfp Kan^R)	This study
DE4384	*M. marinum*	DE4390 L5::pDEAM1 (gfp Kan^R)	This study
DE4187	*M. marinum*	DE3932/ pSJ27::Bxb1 att p-int (Kan^R)	Laboratory Collection
DE4437	*M. marinum*	DE4187 L5::pDEAM4 (gfp Hyg^R)	This study
DE4438	*M. marinum*	DE4187 L5::pDEAM5 (rfp Hyg^R)	This study
DE4556	*M. marinum*	NTCC 20998/pDEAM2 (rfp Kan^R)	This study
DE4557	*M. marinum*	NTCC 2275/ pDEAM2 (rfp Kan^R)	This study
DE4389	*M. marinum*	iipA mutant	Lian-Yong Gao, University of Maryland, College Park, Maryland
DE4425	*M. marinum*	MelF mutant	Jeffrey D. Cirillo (Texas A&M University Health Sciences Center)

DE4449	*M. marinum*	DE4425/ pDEAM4 (gfp Hyg^R)	This study
DE4450	*M. marinum*	DE4425/ pDEAM5 (rfp Hyg^R)	This study
DE4388	*M. marinum*	Mh3868::Kan (extRD1 mutant)	Lian-Yong Gao, University of Maryland, College Park, Maryland
DE4447	*M. marinum*	DE4388/ pDEAM4 (gfp Hyg^R)	This study
DE4448	*M. marinum*	DE4388/ pDEAM5 (rfp Hyg^R)	This study
DE4331	*M. marinum*	mimI mutant	Jeffrey D. Cirillo (Texas A&M University Health Sciences Center)
DE4516	*M. marinum*	mimD mutant	Jeffrey D. Cirillo (Texas A&M University Health Sciences Center)
DE4517	*M. marinum*	mimH mutant	Jeffrey D. Cirillo (Texas A&M University Health Sciences Center)
DE4558	*M. marinum*	ΔRD1-6	Lalita Ramakrishnan (University of Washington)

Table 2.1 **List of all used bacterial strains**. All *M. marinum* strains used in these studies were derivatives of a fish isolate (ATCC 927 or 1218R) obtained from Lucia Barker (University of Minnesota) or a human isolate (M strain) from the American Type Culture Collections (ATCC). Strains carried different reporter systems on a plasmid or express as a single integrated copy to facilitate tracking of bacterial infections.

Plasmids	Relevant Traits and Derivation	Source
pG13	Kan *g13P-gfp*,M_{ori} Ec_{ori}	Lucia Barker, University of Minnesota (Barker et al, 1999)
pMH94	Kan L5 *int att* Ec_{ori}	Graham Hatfull, University of Pittsburgh
pMSP12-rfp	Kan *msp12P-rfp* , M_{ori} Ec_{ori}	Lalita Ramakrishnan, University of Washington (Cosma et al., 2009)
pMSP12-gfp	Kan *msp12P -gfp* , M_{ori} Ec_{ori}	Lalita Ramakrishnan, University of Washington (Cosma et al., 2009)
pMSP12-*gfp*-Hyg	Hyg *msp12P-gfp,* M_{ori} Ec_{ori}	Lalita Ramakrishnan, University of Washington (Cosma et al., 2009)
pDEAM1	pMH94 *Δ(Aat II/SacI)::msp12P-gfp* L5 *int att* Ec_{ori}, (Kan, Gfp)	This Study
pDEAM2	pMH94 *Δ(Aat II/SacI)::msp12P-rfp* L5 *int att* Ec_{ori}, Kan, Rfp	This Study
pDEAM3	pDEAM1 *NsiI::*Hyg L5 *int att* Ec_{ori}, (Hyg, Rfp)	This Study
pDEAM4	pDEAM1 *NsiI::*Hyg L5 *int att* Ec_{ori}, (Hyg, Gfp)	This Study
pDEAM5	pDEAM2 *NsiI::*Hyg L5 *int att* Ec_{ori}, (Hyg, Rfp)	This Study

Table 2.2 **List of plasmids**. Properties, sources, manipulations and their derivations of all plasmids employed are described in greater detail in Material and Methods section. M_{ori} and Ec_{ori} signify the presence of mycobacterial or *E. coli* origins of replication, respectively on a given plasmid.

CHAPTER THREE: Results

3.1 Efforts to Develop an Antibiotic Regimens against Mycobacteriosis in fish

Frontline anti-TB antibiotics, isoniazid and rifampin were employed to treat medaka that had been chronically infected by *M. marinum*. We wanted to study different end points of antibiotic treatment, like the kinetics of reduction in bacterial burden and possibly gain some insights into the anatomical location of persisters. However proper dosing and delivery was a challenge partially due to lack of previous information. Aquaculture and aquarium trade only poorly documented the effectiveness of their common treatments of aquatic animals with antibiotics (added to aquarium water or in 'medicated food'). Previously attempts were made by our research group to deliver the antibiotics by oral gavage; that is, threading a small bore tube directly into the gut of an infected fish through its mouth. But the bacterial burden did not appear to lessen in these efforts (Broussard 2007 and unpublished data). Moreover this was an invasive and stressful technique for the fish and required them to be anesthetized daily which was considered impractical. In another experimental approach, antibiotics were delivered with fish food. Food (pellets) were soaked in antibiotics, dried and then fed to the fish. But this method was associated with a number of challenges like loss of antibiotics due to leaching into the water when being fed to the fish. Also, the taste and the smell of the antibiotics or solvents like DMSO often did not suit the fish palate. Due to these and other complications, the trial delivery of antibiotics soaked into dried food was considered impractical.

Consequently, developments of alternate regimens were investigated emphasizing on techniques that would disguise the flavor of the drug and/or solvents used to dissolve

antibodies, but nonetheless deliver it efficiently. As a result, we considered the following two approaches:

1. Antibiotic delivery within microparticles
2. Antibiotic delivery within gelatin matrices

3.1.1 Effort to Develop Antibiotic Delivery with Microparticles

In an alternate approach to treat fish with antibiotics, microparticles composed of biodegradable polymers were considered for delivery of drugs. These polymers like polyanhydrides are able to degrade slowly inside biological systems like within the peritoneal cavity or intramuscular region thereby releasing its contents overtime. Such particles are claimed to be an effective approach in drug delivery (or vaccine, protein, DNA etc) and release them at constant rate inside the body (Ulery et al. 2009). We attempted to use Polyanhydride microparticles composed of 20:80 copolymers of 1, 6-bis (p carboxyphenoxy) hexane (CPH) anhydride and sebacic anhydride (SA) developed by our collaborators at Iowa State University. In these pilot experiments the cargo was a fluorescent compound (FITC Dextran), not an antibiotic, in order to monitor spread of particles in translucent animals. These fluorescent loaded particles were mixed with PBS and injected into the peritoneal cavity of See Through (ST) medaka as a pilot experiment to document localization of these particles in live fish. Fish were photographed before IP injection, immediately after, and for three weeks or until they had succumbed. The fluorescent microparticles were found to accumulate in specific viscera of ST fish, especially in the liver. As demonstrated in Figure 3.1 (C and D), a representative ST fish is shown a few minutes after injection of fluorescent particles. In two weeks post-injection, fluorescent particles were observed to become concentrated in the liver (Figure 3.2, C and D). Accumulation of these micropraticles in the

liver is apparently toxic, since the treated ST fish died. Since this approach of antibiotic delivery did not apprear to be useful at this time for our persuits, another oral dosing idea was considered.

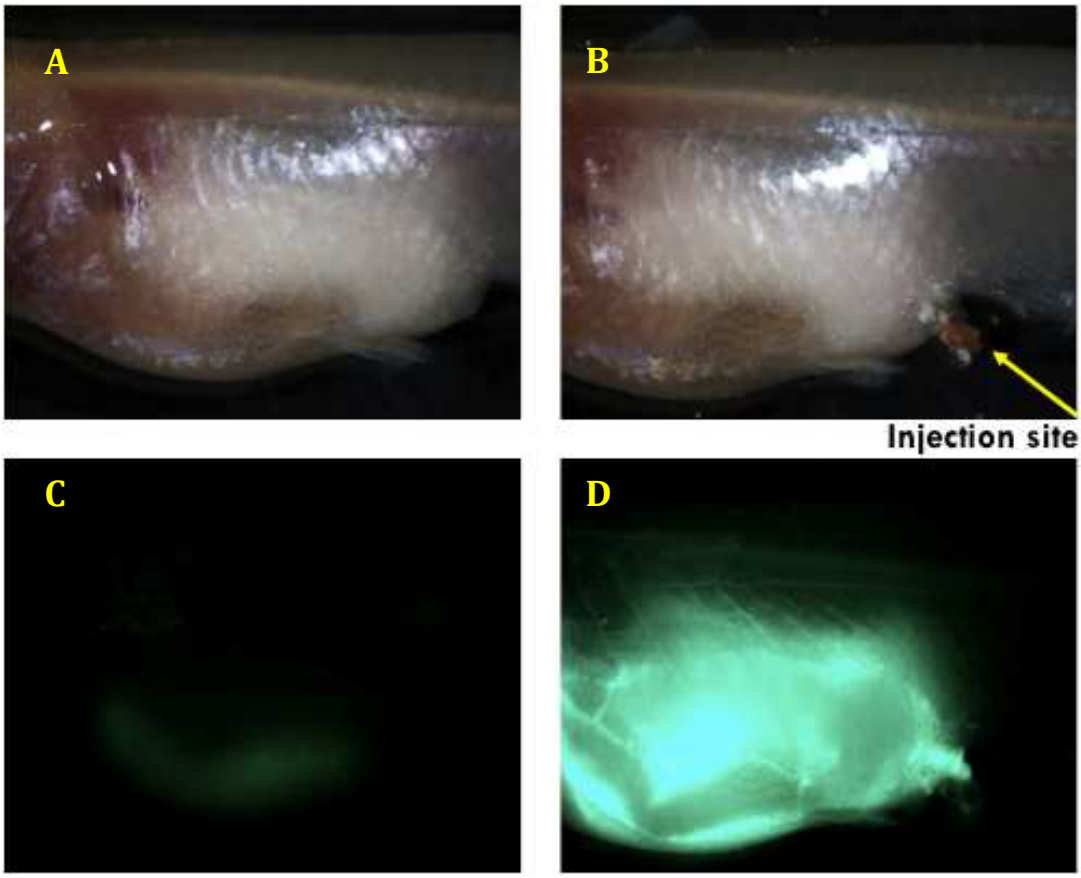

Figure 3.1 **Bright field and the green fluorescent images of a See Though fish a few minutes before and after IP injection with microparticles**. Peritoneal cavity is loaded with fluorescent compound FITC Dextran. Figure 3.1, A and B show the bright field image of the left and right side of the same ST fish before and after injection, respectively. In Figure 3.1 B, the arrow points at the site of injection. Figure 3.1, C and D represents the same field of view as A and B respectively under green fluorescent filter. As shown in Figure 3.1 D, the fluorescent particles have diffused throughout the body cavity of the fish immediately post injection.

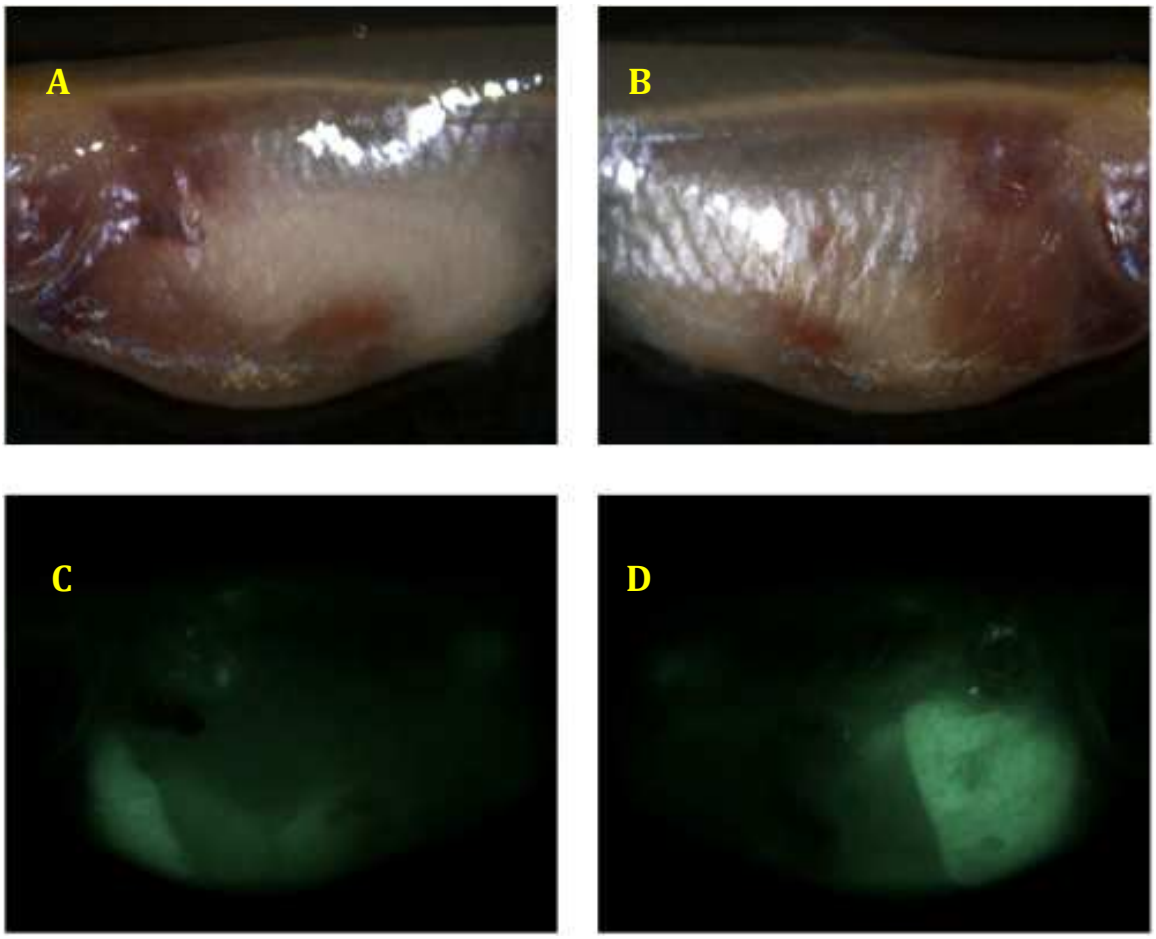

Figure 3.2 **Bright field and the green fluorescent images of a See Though fish three weeks after IP injection with microparticles.** Bright field and the green fluorescent image of the same representative See Though fish as in Figure 3.1 two weeks post-injection. Figure 3.2, A and B show the bright field image of the right and left side of the ST fish respectively. Figure 3.2, C and D represents the same field of view as A and B respectively under green fluorescent filter. Figure 3.2 demonstrates that over time, the fluorescent microparticles have accumulated particularly in the liver; hence it is brightly fluorescing green.

3.1.2 Development of Strategy to Deliver Rifampin

In order to orally deliver antibiotics to fish with the goal of minimizing leaching of the drug into the surrounding water and to make it palatable for the fish, rifampin were embedded gelatin matrix along with attractants like fish food and fish oil. Solidified 20 uL aliquots carrying a known quantity of drug (4 μg) were placed in "Jell-O shots" as shown in Figure 3.3(a). Each shot was cut into four quarters as to be more readily fit and eat with the small mouths of adult medaka. Two quarters of the shots were fed to each fish everyday during the entire treatment period. Figure 3.3(b) shows two Jell-O shots observed by a dissection microscope. Gelatin is a form of hydrolyzed beef collagen extracts consisting of a complex mixture of peptides commonly used as a gelling agent in food and pharmaceutical industries. Here gelatin was thus considered for rifampin delivery purpose in our experiments. The heated liquefied gelatin rapidly solidifies with cooling (at temperature below 35^0C) the natural molecular bond between the collagen fibers brakes down and rearranges more easily within the Jell-O shot, probably helping to trap the ingredients inside the matrix.

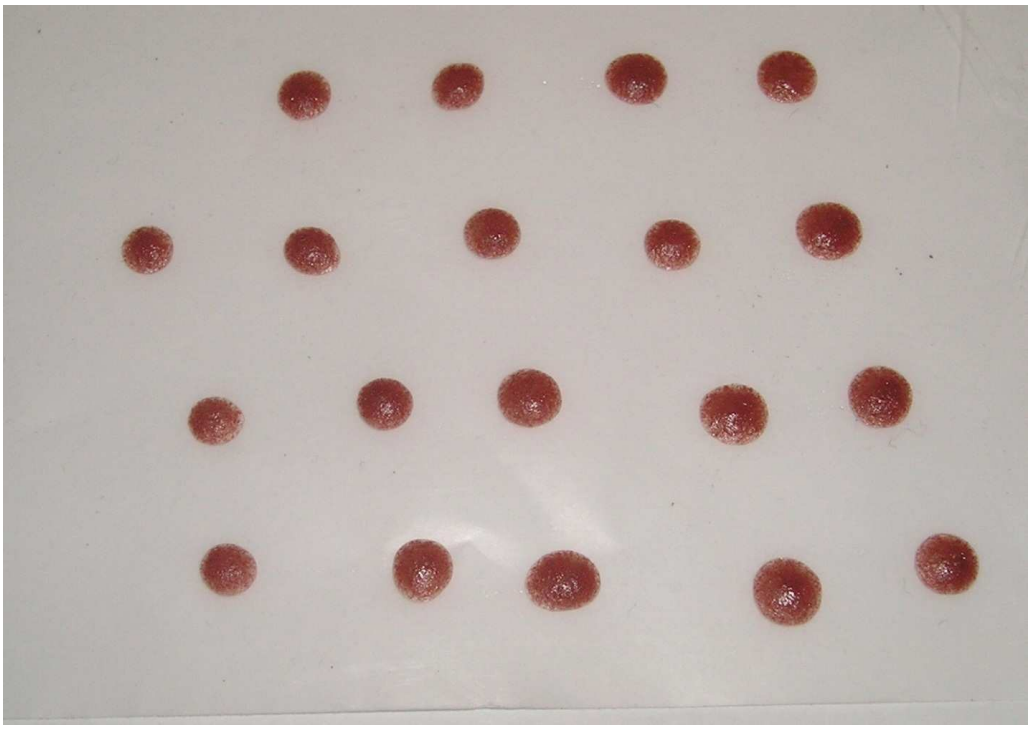

Figure 3.3(a) **20 µl Jell-O shots**; containing rifampin, embedded in gelatin matrix, along with fish food and fish oil.

Figure 3.3(b) **View of two Jell-O shots by a dissection microscope.**

3.1.3 Treatment with Rifampin

Rifampin binds to mycobacterial RNA polymerase near the active site inhibiting RNA synthesis (Wehrli et al. 1971). Rifampin was considered for treatment of fish TB for a number of reasons in particular, it is one of the front line antibiotics used in the treatment of human TB (Jain et al. 2008). *M. marinum* has been shown to be killed by rifampin with MIC_{90} of 0.5 μg/ml (Aubry et al. 2000). Also Rifampin has an intense orange color with a diagnostic λ_{max} and prominent extinction coefficient permitting colorimetric quantification of this antibiotic in aqueous solution. Rifampin standard curve was developed by measuring the absorbance of known concentrations of the antibiotic at 475 nm. This standard curve is useful and diagnostic, allowed us to measure the amount of rifampin present in water. Figure 3.4 shows the rifampin standard curve. The selective concentration used in petri plates for growth of rifampin resistant strains, 0.1 mg/mL and is readily measured by using absorbance and is represented in the graph. Concentrations greater than 0.15 mg/mL become too dark and are no longer linear, thus could not be readily measured by spectrophotometry. This standard curve was used to determine the concentration of rifampin in the Jell-O shots.

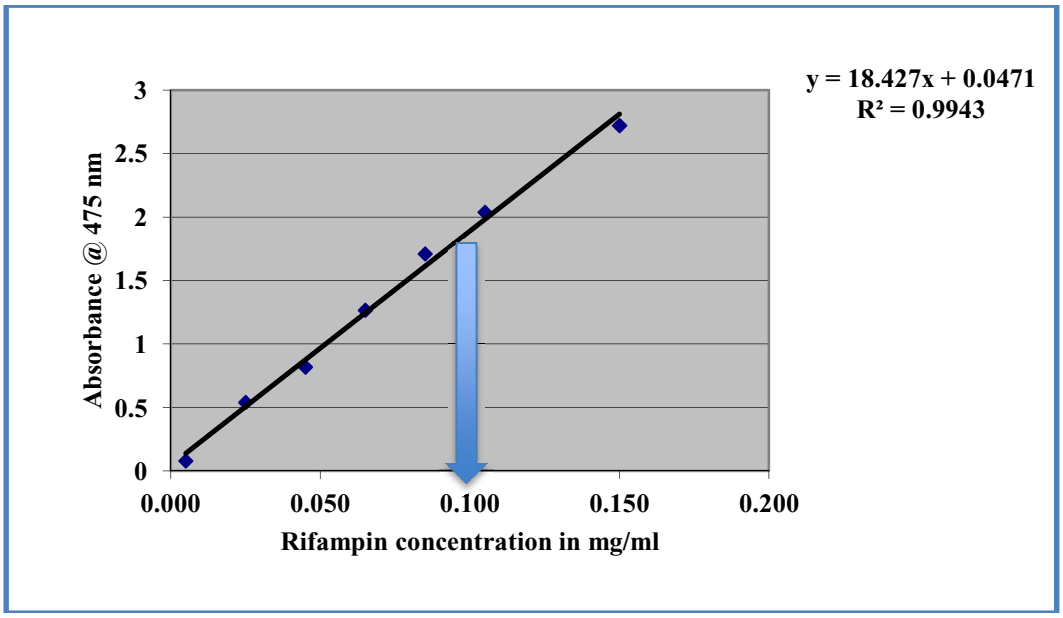

Figure 3.4 **Rifampin standard curve, allows for quantification of rifampin using spectrophotometer.** Known concentrations of rifampin (plotted on X-axis) were used to find their absorbance at 475nm (plotted on Y-axis), as represented in the graph. The standard curve yields an equation (y = 18.427x + 0.0471), used to detect the amount of rifampin present in unknown solutions. The arrow indicates the amount of rifampin (0.1mg/mL) used in plates to grow rifampin resistant mycobacteria.

3.1.4 Quantification of Rifampin Delivered in Jell-O shots

We wanted to quantify the amount of rifampin actually consumed by fish and document the amount of rifampin lost due to leaching into the surrounding water from the Jell-O shot. For this study, two Jell-O shots were cut into four quarters and placed in Eppendorf microfuge tube containing 500 μl of water, and then measured the amount of rifampin leached out into the water at every hour, as represented in Table 3.1 (this study has been repeated atlesast five times, Table 1 is one representative such replicate). The concentration of rifampin in each of the Jell-O shots used were 0.096 mg/ml corresponding to a total amount of 48 μg rifampin (24 μg in each shot). After an hour, 37.5% (30 μg) rifampin had leached out into the surrounding water; a calculated 18 μg of rifampin had been retained in each of the shots. Additional loss of rifampin was apparent; at two hours (62.5%) but little additional loss at, three, four and five hours, 60.42%, 56.25% and 55.21% of rifampin, respectively, was measured in water. It was judged that this high level of loss from shots might not an optimum approach to deliver drugs. However, in our experiments described below, that the fish typically consumed the Jell-O shots within an hour. Thus, we estimate that these fish had been treated with at least 62% rifampin left in shots. The daily dose of medaka (with average body weight of 0.2 gram) would correspond to 2 μg rifampin/fish/day (or 10 mg/kg body weight/day), which is same as the recommended human dose 10 mg rifampin/kg body weight/day for TB treatment. The Jell-O shots were made with the intent of feeding infected fish containing 4 μg of rifampin each; so that each fish would receive daily dosage of approximately 2 μg rifampin, when they consumed half the Jell-O shot.

Hour	Input Rif Concentration in shot	Rif Leached out	% Leached	Rif in shots μg	Rif in solution μg
1	**.096 mg/ml**	**.036 mg/ml**	**37.5%**	**30**	**18**
2	**.096 mg/ml**	**.060 mg/ml**	**62.5%**	**18**	**30**
3	**.096 mg/ml**	**.058 mg/ml**	**60.42%**	**19**	**29**
4	**.096 mg/ml**	**.054 mg/ml**	**56.25%**	**21**	**27**
5	**.096 mg/ml**	**.053 mg/ml**	**55.21%**	**22**	**26**

Table 3.1 **Quantification of Rifampin leaching from Jell-O shot.** For quantification purpose, Jell-O shot were made to contain 24 μg of rifampin in each shot, two such shots (containing 48 μg total rifampin) were cut into quarters and placed into 500 μL water yielding actual rifampin concentration (.096 mg/ml) total in the entire tube. The solutions were allowed to incubate for 1-5 hours and at every hour; absorbance reading was taken, which was then used to calculate the concentration of rifampin (leached out into the surrounding water) from the standard curve. The percentage of rifampin leached out, amount of rifampin left in Jell-O shots and the surrounding water is thus calculated from the above two values for each time point.

3.1.5 Treatment of Infected fish Using Rifampin Containing Jell-O shots

Experiments were performed to test the efficacies of treating infected fish with rifampin embedded in Jell-O shots for different lengths of time, using two different end-points, first, comparing infection burden in target organs and second, survival. Forty, six month-old fish were divided into four groups consisting of ten fish each summarized in Table 3.2. The wild-type strain of *M. marinum* expressing *rfp* and Kan^R marker (DE4373) were used to inject fish by IP ($1.7x\ 10^3$ cfu/fish); these fish were divided into three groups (called 1-3). Group 4 fish were mock infected with PBS at pH 7.4. Group 1 fish received 2 μg dose of rifampin embedded in Jell-O shot per day starting at day 1 post infection. Group 2, rifampin regimen was delayed to 14 days post infection, while control groups 3 and 4 never received any antibiotics during the course of the experiment, they were instead fed with Jell-O shots without the antibiotics. Fish were monitored for nine weeks before they were sacrificed, organs were dissected, homogenized and plated permissively for the detection of *M. marinum* strain. Figure 3.5 shows the survival profile of the fish belonging to all four of these groups. As expected, 100% of the fish uninfected fish control survived (group 4). Group 3 infected fish which did not benefit from antibiotic treatment, yeilded 100% mortality by week five. In contrast, group 1 fish which received rifampin from day 1 post infection showed 50% survival even at week 9 and group 3 fish that received rifampin regimen 14 days after infection had 30% survival at week nine. The survival profile of all fish groups are shown in Figure 3.5 indicates that administration of rifampin did have some positive effects on the survival of the fish. Bacterial loads for fish in groups 1, 2 and 3 were documented at different time points and are expressed in Table 3.3. It also shows data from deceased fish (as and when the fish succumbed), where whole body including the gut was plated for *M. marinum*

detection within 24 hours of death. The data indicate that the level of colonization in fish organs is comparable in all three groups. Therefore it is difficult to document an improvement by this end point, although we also see an evidence of greater survival in fish that benefitted from ingestion of rifampin. In the case of mycobacterial infections, bacteria within an organ are thought to be in variable growth states; including a subset that is refractory to short exposures to antibiotics as well as subsets that are more virulent and actively dividing, causing disease manifestations. We suggest that perhaps the rifampin may be having a disproportional effect on this latter subset and thus, therefore provide protection and less mortality.

These studies suggested that the rifampin regimen used was not having the desired effects of clearing mycobacterial loads as expected. As such, the intent of finding anatomical locations of the persisters seemed like an unobtainable goal and was not persued any further.

Group 1	Group 2	Group 3	Group 4
10 Fish	10 Fish	10 Fish	10 Fish
Infected with a dose of $1.7x10^3$cfu/fish	Infected with a dose of $1.7x10^3$cfu/fish	Infected with a dose of $1.7x10^3$cfu/fish	Control Injection with PBS
Received 2 µg/day Rifampin dose starting on day 1 post infection	Received 2 µg/day Rifampin dose starting on day 14 post infection	No treatment	No treatment

Table 3.2 **An Experimental Design**. The experiment consisted of four groups (1- 4) conataing ten fish in each group. Group 1, 2 and 3 were infected with $1.7x10^3$ cfu of *M. marinum* (DE4373) per fish. Group 4 is control, mock injected with PBS. Group 1 fish were subjected to 2 µg rifampin dose daily in form of Jell-O shot, from day one post infection. Group 2 fish received 2 µg rifampin dose everyday, starting two weeks post infection. Group 3 and 4 fish did not receive any rifampin during the entire time.

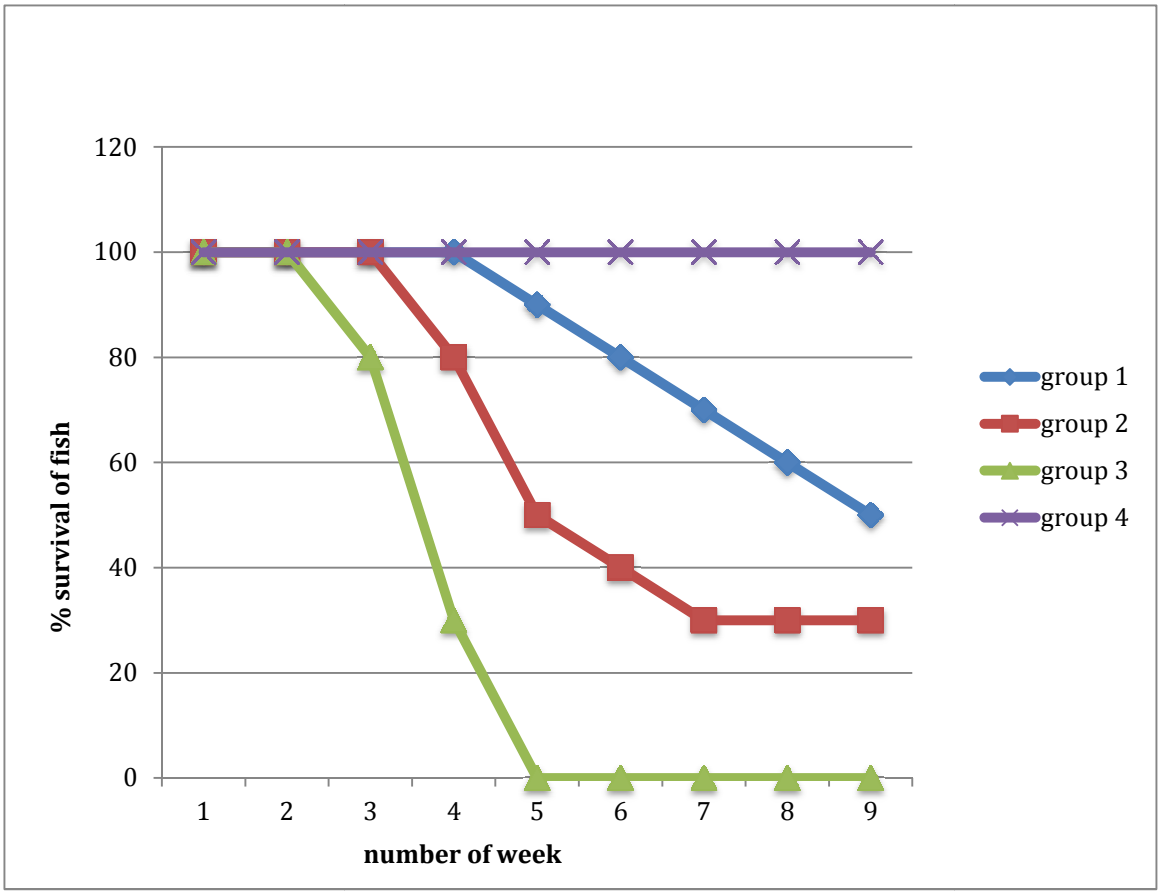

Figure 3.5 **Survival profile of fish, belonging to group 1- 4.** Y- axis represents the percentage survival of the fish and the x-axis, number of weeks. The experiment was monitored for nine-week duration. Control group 4, containing fish were injected with PBS, group 3 fish did not receive any rifampin treatment. Group 1 and 2 received antibiotic regimen (starting one day post infection for group 1 and two week post infection for group 2) seemed to benefit from the drug.

Group 1	Group 2	Group 3
2 week post infection		
Liver: 1x 10^4 Kidney: 2.8x 10^3	Liver: 4x 10^2 Kidney: 4x 10^3	Liver: 2.4x 10^5 Kidney: 5x 10^4
4 week post infection		
Liver: 1.6x 10^4 Kidney: 2.3x 10^5	Liver: 9.6x 10^6 Kidney: 2x 10^6	Liver: 3.4x 10^5 Kidney: 6.8x 10^4
	**Whole body: 4x 10^6	Whole body: 8x 10^7
		Whole body: 7.6x 10^7
		Whole body: 5.2x 10^7
5 week post infection		
Whole body: 1.6x 10^7	Whole body: 6.4x 10^6	Whole body: 7.2x 10^7
	Whole body: 1.6x 10^8	Whole body: 6.4x 10^7
	Whole body: 1.8x 10^7	Whole body: 3.2x 10^8
6 week post infection		
Whole body: 1.6x 10^8	Whole body: 4.6x 10^6	
	Whole body: 3.8x 10^7	
9 week post infection		
Liver: 3.3x 10^6 Kidney: 8.7x 10^5	Liver: 6.5x 10^6 Kidney: 2x 10^6	
Liver: 1.5x 10^3 Kidney: 2.6x 10^4	Liver: 1x 10^6 Kidney: 4.3x 10^6	
Liver: 2.2x 10^6 Kidney: 2.3x 10^5		

Table 3.3 **Bacterial loads in fish organs (liver and kidney), in survivors from group 1, 2 and 3 until week nine**. ** Indicates deceased fish where 'whole body' cavity, after removal of the head and tail, the rest of the fish was homogenized and plated for bacterial count within 24 hours of death.

3.2 Characterization of Activation of Virulence in *Mycobacterium marinum*

3.2.1 Activation of Virulence in *M. marinum* upon Incubation with Mosquito Larvae Extracts: Inoculating Medaka with IP Injection

Previous studies by our lab had consistently documented that *M. marinum* which had passed through mosquito larval gut was more infectious than bacteria grown in culture (Mutoji 2011). This is consistent with other studies that showed that another mycobacteria, *M. avium* grown within caustic environment of amoeba was also shown to have enhanced virulence, compared to bacteria grown in culture, using a murine macrophage infection (Cirillo et al. 1997). In addition, Mutoji (2011) and later Root (2012) observed that *M. marinum* pre-conditioned in Mosquito Larvae Extract (MLE) showed increased virulence when innoculated through ingestion of Jell-O shots. It is plausible that mycobacterial pathogens increased their virulence following passage through a caustic environment that in turn induced virulence gene sets (Tenant et al. 2006)

Although increased virulence of *M. marinum* by MLE incubation was observed by an oral route of infection, we wished to test if MLE exposed bacteria were also more infectious with IP infection. Bacterial cultures and mosquito larval extracts were prepared as previously described (Mutoji 2011). Eight-month old transgenic fish were randomly placed into two groups (groups 1 and 2), and each group included ten animals. Two differentially marked strains of wild-type *M. marinum* (DE3932 expressing no fluorescence and DE4373 carrying both Kan^R and *rfp* markers) were used to perform a competition study. Group 1 fish were IP injected with an equal mixture containing DE4373 bacteria treated with (MLE) and a second strain, DE3932 that was only exposed to neutral PBS at a pH of 7.40. Group 2 was as above, but instead strain DE3932 was treated with MLE and the *rfp*-marked DE4373 cells was mixed in neutral PBS. As per the variation of the CI convention, that we are employing

expresses the competition indices in infection models, strains that received MLE treatment were considered the 'mutant' strains and thus, their colonization values were expressed in the numerators for those ratios (Mutoji 2011). In contrast the 'wild-type' strain, therefore, received only treatment with neutral PBS at a pH of 7.40. To eliminate potential strain bias with the differentially marked bacteria, the study was conducted in two ways, where in one experiment, the *rfp*-marked strain was incubated in MLE and the other, the non-fluorescent strain was incubated. Each fish in either group were IP injected with a volume of 20 µl culture mixture (appropriately diluted to achieve a chronic dose, approximately 10^3cfu) as described before, appropriate dilutions were plated for colony counts. The Input Ratio for group 1 was 1.62 (4373 in MLE: 3932) and group 2 the same two strains with opposite exposures were used. Post injection, the fish were monitored for a period of approximately six weeks (40 days) with weekly water changes. Two fish died from group 1 during the course of the experiment. At termination of the experiment, fish were sacrificed and the dissected livers and kidneys were homogenized and plated for the colony counts for each of the differentially marked *M. marinum* strains. Bacterial loads and competition indices were calculated from each organ in group 1, they are documented in Table 3.4 and group 2 in Table 3.5. Competition indices are also plotted for both the kidney and liver in each fish in Figure 3.6 for group 1 and Figure 3.8 for group 2. Average CI values are plotted for livers and kidneys in Figure 3.7 for group 1 and Figure 3.9 for group 2. Interestingly, the CI values for MLE-incubated mycobacteria were at a minimum unity in most cases was significantly greater than 1.0. For group 1, the average CI value in liver was fifty times greater and for kidney, it was twenty times greater. Alternatively for group 2, average CI values for both livers and kidneys were eighty times higher. The data shows that the level of colonization of

the bacterial strain incubated with MLE was significantly higher; the extreme case was 500 fold greater virulence. These results indicate that the MLE pre-conditioned *M. marinum* was substantially more infectious. These data would suggest that MLE incubation generally activates *M. mar*inum for virulence, and not just potentiating the pathogen for crossing the gut epithelia.

Fish #	Organ	4373 MLE output cfu/organ	3932 output cfu/organ	Output Ratio (4373: 3932)	CI
1	LIVER	3.0×10^5	$<4 \times 10^3$	$<7.5 \times 10$	$**<4.6 \times 10$
	KIDNEY	4.0×10^4	8.0×10^3	0.5×10	0.3×10
2	LIVER	3.1×10^5	4.2×10^5	0.74	4.5×10^{-1}
	KIDNEY	1.9×10^6	2.6×10^4	7.3×10	4.5×10
3	LIVER	1.8×10^6	8.0×10^3	2.3×10^2	1.4×10^2
	KIDNEY	1.2×10^6	4.4×10^4	2.6×10	1.6×10
4	LIVER	1.4×10^5	4.0×10^3	3.6×10	2.2×10
	KIDNEY	9.0×10^4	2.0×10^3	4.0×10	3.0×10
5	LIVER	1.3×10^6	8.0×10^3	1.6×10^2	9.7×10
	KIDNEY	1.0×10^5	5.0×10^4	0.3×10	0.2×10
6	LIVER	2.8×10^5	6.0×10^3	4.7×10	2.9×10
	KIDNEY	8.0×10^4	6.0×10^3	1.0×10	0.8×10
7	LIVER	6.0×10^5	1.2×10^4	5.0×10	3.1×10
	KIDNEY	2.3×10^5	2.0×10^3	1.2×10^2	7.1×10
8	LIVER	2.4×10^5	4.0×10^3	6.1×10	3.7×10
	KIDNEY	1.3×10^6	6.2×10^5	2.1	0.13×10

Table 3.4 **Bacterial loads of Group 1 in a co-infection study using two differentially pre-treated *M. marinum* wild-type strains**. Represented here is the level of bacterial colonization as the total cfu/organ, in liver and kidney recovered from eight fish co-infected by two differentially marked strains of wild-type *M. marinum* (DE3932 expressing no fluorescence and DE4373 expressing Kan^R *rfp*) in a competition study. The strain DE4373 MLE was preconditioned with mosquito larval extracts, where as DE3932 was the control in this study. The output ratio presented here was calculated for liver and kindney from individual fish and used to find the CI values for each organ. The input ratio was 1.62 in this group. The CI values are greater than one, indicating a preference for the MLE treated strain in all cases except for liver of fish 2, which is slightly less than one. ** indicates that the bacterial colonies were not detected at the dilutions used.

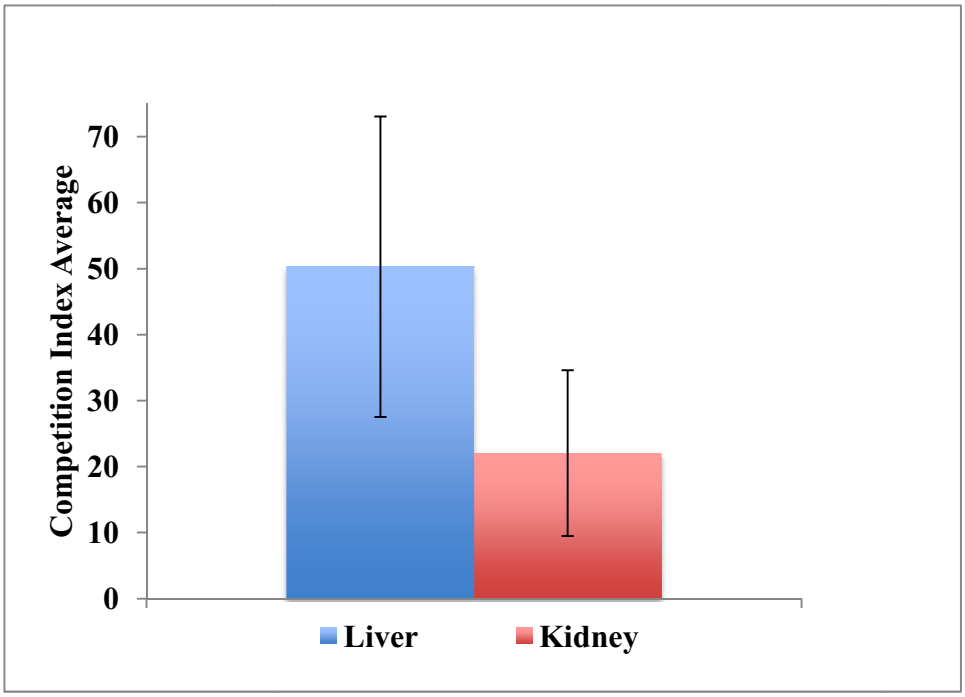

Figure 3.6 **Group 1 Average Competition Index**. Shown here are the mean CI values for kidney and for liver obtained from eight fish infected with two differentially marked and pre-treated strains of *M. marinum*. CI average in both the organ is much greater than one (approximately 50 for livers and 20 fold in case of kidneys), suggesting an increased virulence for the MLE treated *M. marinum* strain. The length of the bar represents one standard deviation of the CI values.

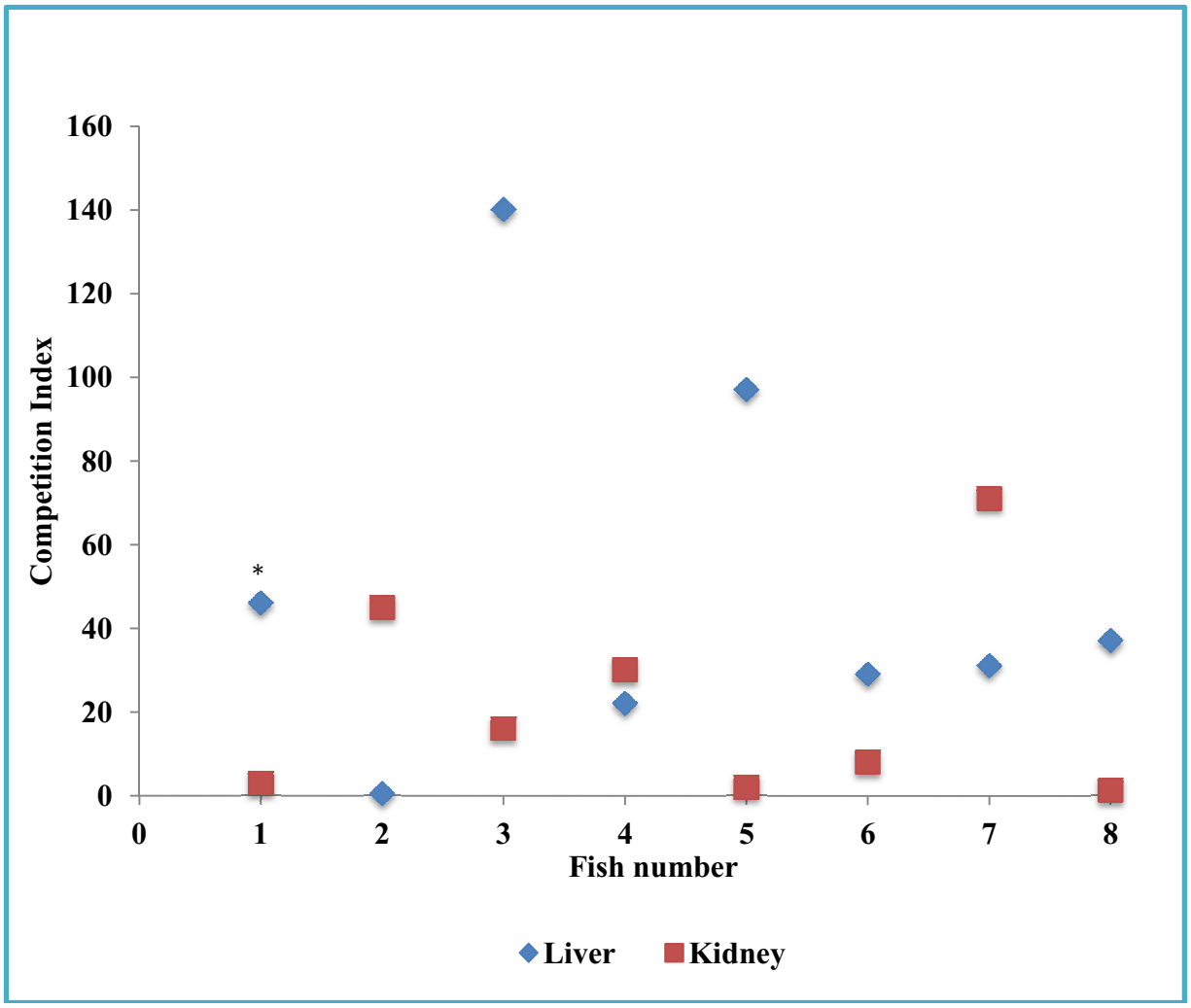

Figure 3.7 **Competition Index of individual organ in Group 1.** Shown here are the CI values of individual livers and kidneys of the eight fish in Group 1. Each Competition Index is represented on y-axis, while individual fish number x-axis. CIs close to one indicate equal colonization between the two differentially treated wild-type strains. In almost all instances, the CI values were above unity suggesting the untreated bacteria were not as infectious as the treated strain at colonizing the organs. * indicates no colonies of the untreated strain were recovered from the organs at the particular dilution, and thus would be a CI value greater than 4.6 x 10.

Fish #	Organ	3932 MLE output cfu/organ	4373 output cfu/organ	Output Ratio (3932:4373)	CI
1	LIVER	$<4 \times 10^3$	6×10^3	<1.5	**<2
	KIDNEY	8×10^3	2.2×10^4	2.8	4
2	LIVER	$<4 \times 10^3$	$<4 \times 10^3$	ND	ND
	KIDNEY	$<4 \times 10^3$	1.3×10^5	<3.3 x 10	**<53
3	LIVER	$<4 \times 10^4$	1.5×10^6	<3.8 x 10	**<62
	KIDNEY	$<4 \times 10^3$	5.8×10^4	<1.5 x 10	**<24
4	LIVER	$<4 \times 10^3$	3.9×10^5	<9.9 x 10	**<160
	KIDNEY	$<2.2 \times 10^4$	5.9×10^6	$<2.7 \times 10^2$	**<435
5	LIVER	$<4 \times 10^3$	8×10^4	<2.1 x 10	**<33
	KIDNEY	$<1.6 \times 10^4$	2.9×10^4	<1.8	**<3
6	LIVER	2×10^4	3×10^4	1.3	2
	KIDNEY	8×10^3	1.7×10^5	2.2 x 10	35
7	LIVER	6.1×10^5	8.0×10^6	1.3 x 10	21
	KIDNEY	3.6×10^6	2.6×10^7	7.3	12
8	LIVER	2.8×10^4	8.2×10^6	2.9×10^2	475
	KIDNEY	1.0×10^5	1.3×10^7	1.2×10^2	203
9	LIVER	$<4 \times 10^3$	1×10^5	<2.7 x 10	**<43
	KIDNEY	8×10^3	8×10^4	1 x 10	16
10	LIVER	6×10^3	3.8×10^5	6.4 x 10	104
	KIDNEY	6×10^3	2.7×10^5	4.5 x 10	74
11	LIVER	4.8×10^4	9.3×10^5	1.9 x 10	31
	KIDNEY	5.3×10^4	2.4×10^6	4.4 x 10	72

Table 3.5 **Bacterial loads of Group 2 in a co-infection study using two differentially pre-treated *M. marinum* wild-type strains**. Represented here is the level of bacterial colonization as the total cfu/organ, in liver and kidney recovered from eleven fish co-infected by two differentially marked strains of wild-type *M. marinum* (DE3932 expressing no fluorescence and DE4373 expressing *Kan*^{R} *rfp*) in a competition study. The strain DE3932 were treated with mosquito larval extracts where as DE4373 was control that received treatment with PBS in this study. The output ratio presented here was calculated for liver and kindney from individual fish and used to find the CI values for each organ. The input ratio was 0.6 in this group. The CI values are greater than one; ranging from <2 to 475, indicating an advantage for the MLE treated strain in all cases. ** indicates that the bacterial colonies were not detected at the particular dilution. ND indicates values not determined.

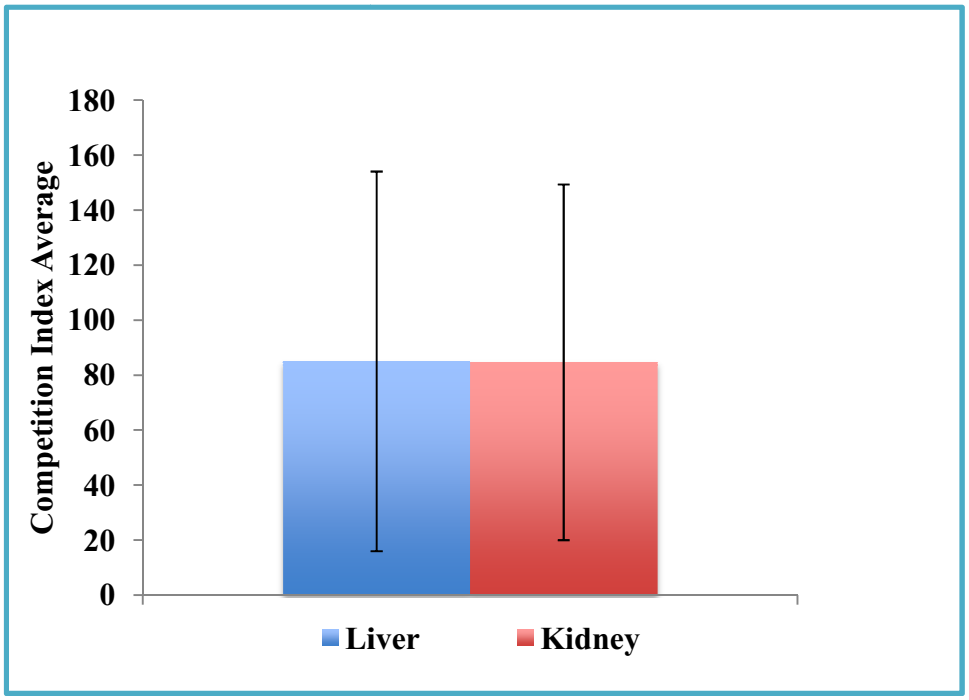

Figure 3.8 **Group 2 Average Competition Index**. Shown here are the mean of CI of kidney and liver obtained from eleven fish infected with two differentially marked and pre-treated strains of *M. marinum*. CI average in both the organs are much greater than one (80 in case of liver and kidney), suggesting an increased virulence for the MLE treated *M. marinum* strain. The length of the bar represents one standard deviation of the CI values.

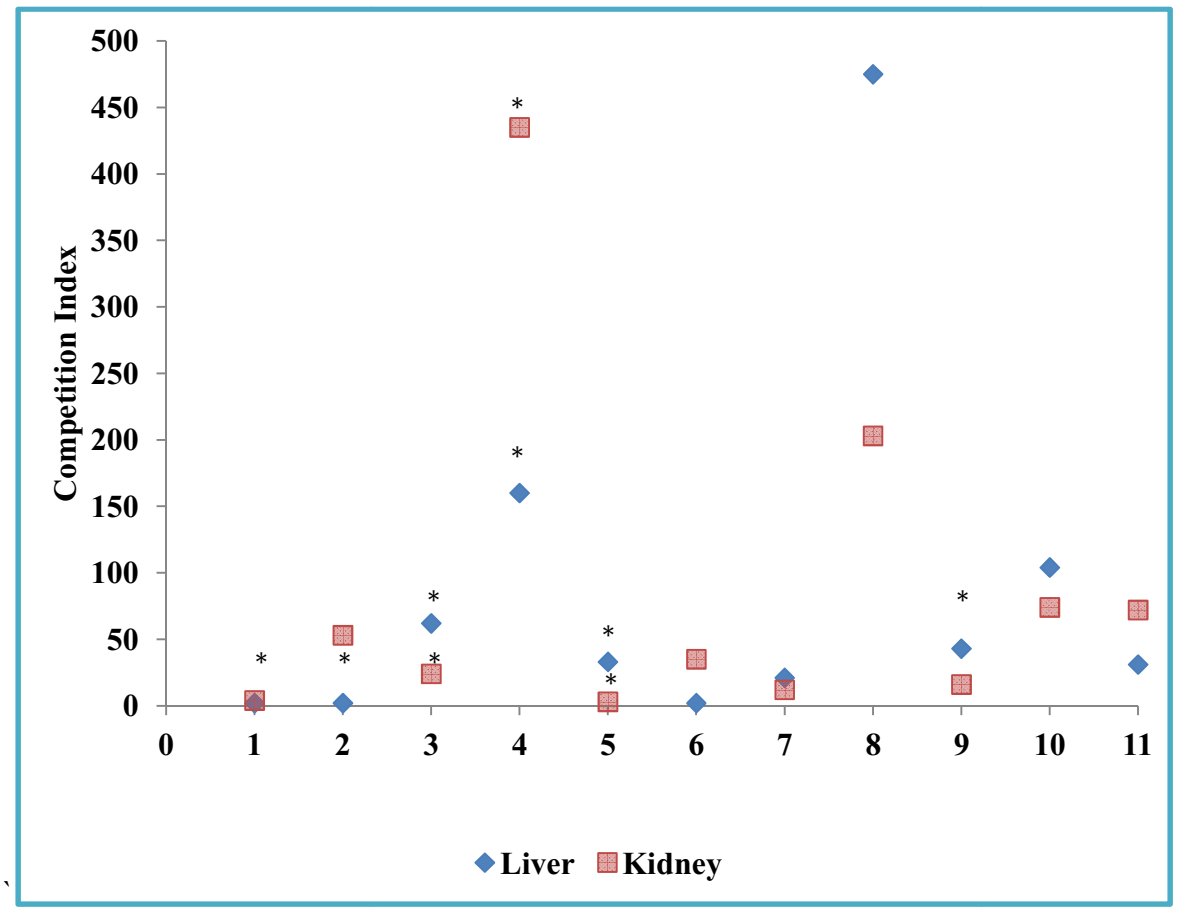

Figure 3.9 **Competition Index of individual organs in Group 2.** Shown here are the CIs of liver and kidney of the eleven fish in Group 2. Competition Index is represented on y-axis, while individual fish number x-axis. CIs close to a value of one indicate equal colonization between the two differentially treated wild-type strains. In all instances, the points are above the line suggesting the untreated bacteria were not as infectious as the wild-type strain at colonizing the organs. * indicates CI values are estimates, no colonies were recovered from the homogenized organs of untreated strain at the dilution employed; thus each CI is less than the value shown.

3.2.2 Effect of pH on *M. marinum* Virulence

As observed in previous studies (section 3.2.1) and augmented by other findings in our group (Mutoji 2011; Root 2012), that the passage of bacteria through mosquito larval gut or incubation in MLE greatly enhanced virulence compared to bacteria grown in culture. In contrast to the mammalian stomachs, the mosquito larval gut harbor an extreme alkaline pH (example, pH 8-11) (Onken et al. 2009; Boudko et al. 2001) and studies have shown that the genetic relatives of *M. avium -M. paratuberculosis* complex (MAP) when preconditioned in acidic pH, had enhanced virulence (Bodmer et al. 2000). These studies have led us to hypothesize that preconditioning of *M. marinum* at high or low pH extremes might also enhance virulence or by pre-adapting mycobacteria to encounter the caustic gastrointestinal tract of medaka.

In this experiment, mycobacteria were incubated in either low or high pH prior to infecting medaka by IP injection. Differentially marked strains of wild-type *M. marinum* (DE3932 expressing no fluorescence and DE4373 carrying both Kan^R and *rfp* markers) were again used for the competition study, but here as an internal comparison of pH-exposed and unexposed bacteria in each animal. This experiment had four medaka treatment groups each containing ten, six-month-old fish. In group 1, fish were IP injected with an approximately equal mixture of bacterial strains containing DE4373 bacteria pre incubated in basic PBS at a pH of 9 and DE3932 that received treatment with neutral PBS at a pH of 7.40. Group 2 comprised of fish IP injected with an equal mixture of DE4373 bacteria exposed to acidic PBS at a pH of 5 and DE3932 cells treated with neutral PBS. Groups 3 and 4 contained IP injected fish where, DE3932 cells received treatment with high (pH 9) and low (pH 5) pH respectively, mixed in equal ratio with DE4373 bacteria that were treated in neutral pH. In

this experiment, strains that received either high or low pH treatment as per CI convention were considered the 'mutant' strains, hence, the 'wild-type' strain received only treatment with neutral PBS at a pH of 7.40 at all times. The strains were incubated in their respective pH for an hour prior to injection and 20 µl culture mixture was used for IP injection as described before. The infective dose of DE3932 and DE4373 were 3.4×10^1 cfu/fish and 3.5×10^1 cfu/fish respectively, the input ratios were thus calculated to be 1:1.03 for group 1 and 2; 1.03:1 for group 3 and 4.

Survival of the fish was monitored for a period of seven weeks with weekly water changes, at which time animals were sacrificed for organ colony counts. During this time, three fish in group 1, two fish in group 2 and four fish in group 3 died so the data shown here represents only the survivors. For each group, the bacterial loads, output ratios and competition index were calculated from respective organs and then log transformed. Figures 3.10, 3.11, 3.12 and 3.13 show the range of competition index of the organs for each individual fish. The data indicated that for bacteria exposed to pH 9, a small decline in virulence was noted (Figures 3.10 and 3.12); interestingly an even greater decline was apparent with pre-incubation at pH 5 (Figures 3.11 and 3.13). In all of these conditions there was no enhanced virulence due to exposures in higher or lower pH; instead, these exposures likely reduced fitness of the bacteria in mounting infections.

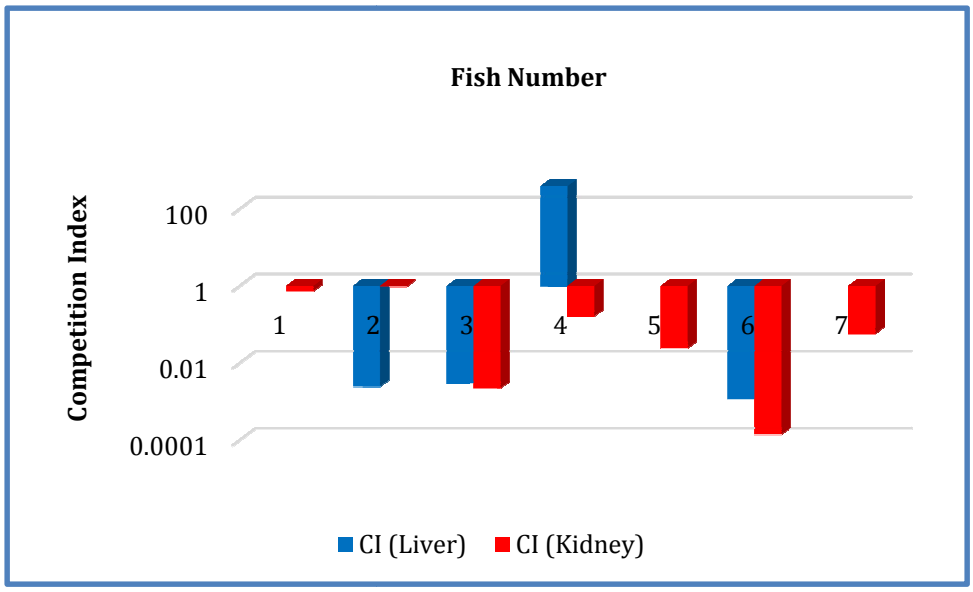

Figure 3.10 **Competition Index of individual organs in Group 1.** Shown here are the CIs of liver and kidney of the seven fish in Group 1 co-infected by two differentially marked strains of wild-type *M. marinum* (DE3932 expressing no fluorescence and DE4373 expressing Kan^R *rfp*) in the competition study. Here, DE4373 bacteria were pre-treated in high pH (pH 9) where as DE3932 were control that received treatment with PBS at normal pH (pH 7.4). Competition Index is represented on y-axis, while individual fish number x-axis. CIs close to one indicate equal colonization between the two differentially treated wild-type strains. In almost all instances, the points are well below one, so treatment at high pH does not render any advantage to the bacteria.

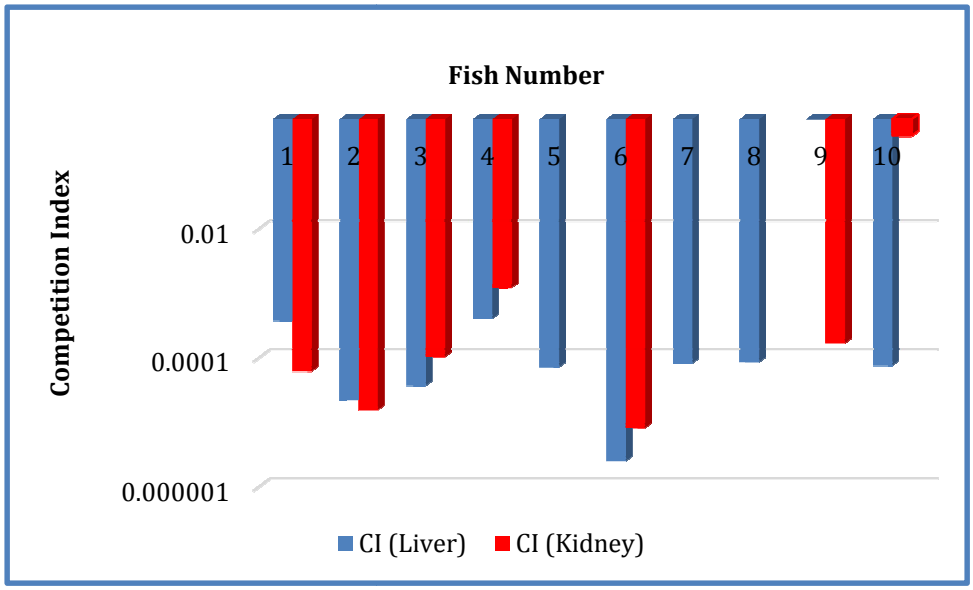

Figure 3.11 **Competition Index of individual organs in Group 2.** Shown here are the CIs of liver and kidney of the ten fish in Group 2, co-infected by two differentially marked strains of wild-type *M. marinum* (DE3932 expressing no fluorescence and DE4373 expressing *Kan*^{R} *rfp*) in the competition study. Here, DE4373 bacteria were pre treated in low pH (pH 5) where as DE3932 were control that received treatment with PBS at normal pH (pH 7.4). Competition Index is represented on y-axis, while individual fish number x-axis. CIs close to one indicate equal colonization between the two differentially treated wild-type strains. In almost all instances, the points are substantially below one, hence, treatment at low pH does not render any advantage to the bacteria.

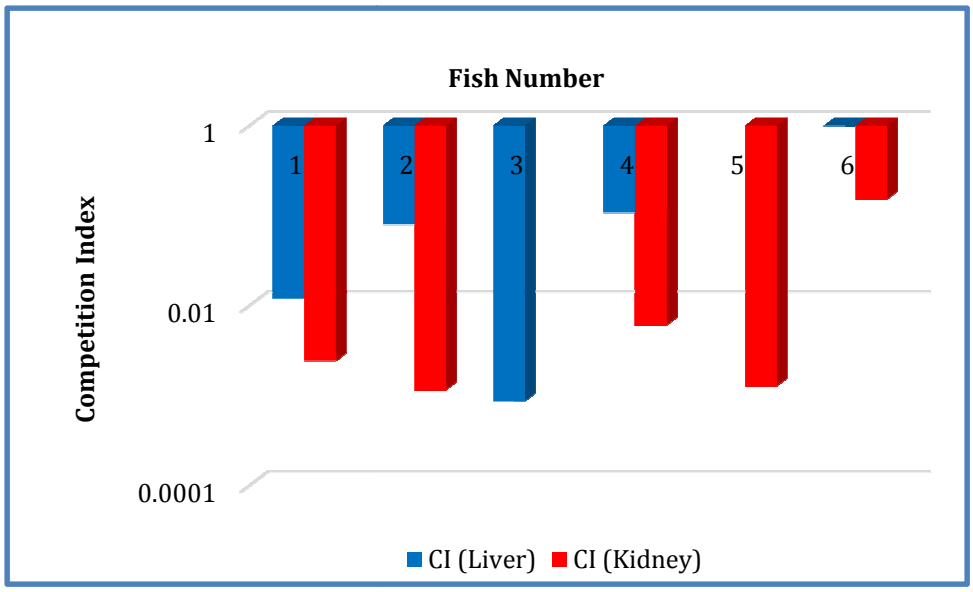

Figure 3.12 **Competition Index of individual organs in Group 3.** Shown here are the CIs of liver and kidney of the six fish in Group 3, co-infected by two differentially marked strains of wild-type *M. marinum* (DE3932 expressing no fluorescence and DE4373 expressing *Kan*^{R} *rfp*) in the competition study. Here, DE3932 bacteria were pre treated in high pH (pH9) where as DE4373 were control that received treatment with PBS at normal pH (pH7.4). Competition Index is represented on y-axis, while individual fish number x-axis. CIs close to one indicate equal colonization between the two differentially treated wild-type strains. In almost all instances, the points are below one, so treatment at high pH does not render any advantage to the bacteria.

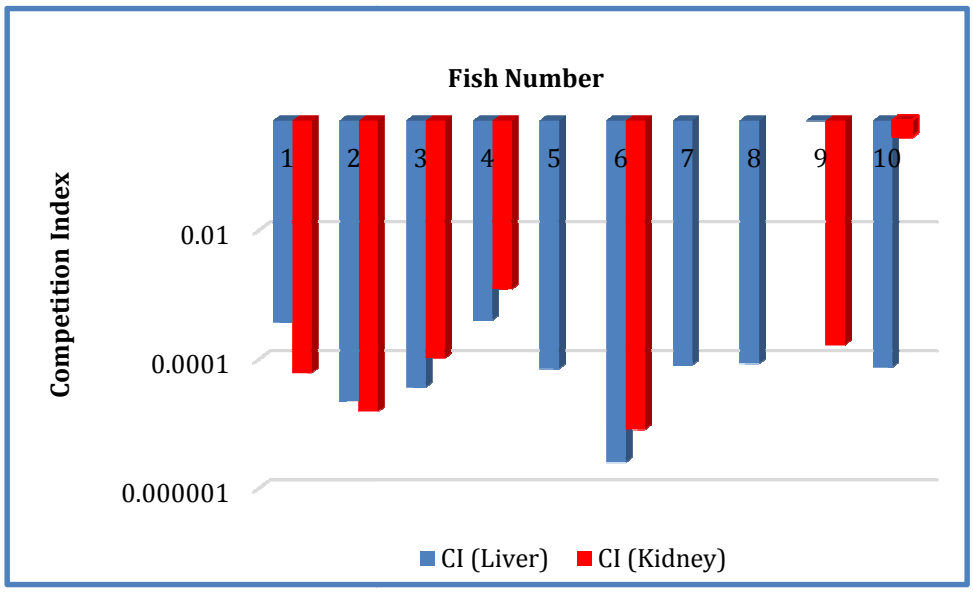

Figure 3.13 **Competition Index of individual organs in Group 4.** Shown here are the CIs of liver and kidney of the ten fish in Group 4 co-infected by two differentially marked strains of wild-type *M. marinum* (DE3932 expressing no fluorescence and DE4373 expressing *Kan*^{R} *rfp*) in the competition study. Here, DE3932 bacteria were pre treated in low pH (pH 5) where as DE4373 were control that received treatment with PBS at normal pH (pH 7.4). Competition Index is represented on y-axis, while individual fish number x-axis. CIs close to zero indicate equal colonization between the two differentially treated wild-type strains. In almost all instances, the points are below one, so treatment at low pH does not render any advantage to the bacteria.

3.3 Experimental Investigations of Established and Novel *Mycobacterium marinum* Mutants in a Chronic *in vivo* Model

3.3.1 *In vivo* Analysis of *M. marinum* Mutants by IP Infections

Our research group has worked to develop an infection model using *M. marinum* as the pathogen and a small laboratory fish Japanese medaka (*Oryzias latipes*) as a host to study TB pathogenesis. Both acute and chronic infections are inducible in this fish model in a dose-dependent manner (Broussard et al. 2007). Here we have used this medaka-*M. marinum* model to study the fitness of mutants carrying defects in established virulence genes as well as novel mutant strains when compared to a wild-type reference strain. As an internal reference, the virulence of each mutant is compared to a differentially marked parental wild-type strain following IP injection at equal ratios in an individual animal.

3.3.1.1 *In vivo* Analysis of Established *M. marinum iipA* Avirulent Mutant by IP Infections

A *Mycobacterium marinum* mutant strain, with a an insertion marked by a kanamycin resistance cassette (Kan^R) in the *iipA* gene, previously characterized as defective in both invasion and intracellular survival in macrophages in vitro, and was completely avirulent in zebrafish infection as well (Gao et al. 2006). Both *in vivo* and *in vitro* defects were completely complemented by expression of *M. tuberculosis* ortholog of *iipA*, *Rv1477* (Gao et al. 2006). Since our *M. marinum*-medaka is a chronic infection model at lower doses, we wished to compare colonization of organs of this known mutant to a wild-type control, as an experimental end-point, which is not possible in an acute model.

As stated above, this experiment employs a competition approach, using both wild-type strain (DE4436) and *iipA* mutant (DE4489) to evaluate relative virulence. Cultures were prepared in Middlebrook broth and ten, five months old fish were IP injected with an equal

ratio of wild-type and the mutant strain according to the protocol discussed above. The input Ratio of mutant/wild-type was calculated to be 1.04: 1 (1.13×10^2 cfu/fish: 1.08×10^2 cfu/fish). Fish were monitored for general health for eight weeks and two days before they were sacrificed; the dissected organs were homogenized and plated permissively for the detection of both *M. marinum* strains. Three of ten fish were observed to succumb in duration of the experiment. Bacterial loads in the surviving test animals for each strain detected are expressed in Table 3.6. Unlike the wild-type strain, no colonies from the mutant strain could be retrieved in any of the seven surviving fish even at the lowest dilutions, thus the output ratios were substantially in favor of the wild-type strain for all these infections. As such, the CI values and statistical tests were performed considering their number to be less than ten cfu for the *iipA* mutant. Comparative box plots of output colonization per unit input (in log scale) of mutant and wild-type for both liver and kidney are shown in Figure 3.14. It is evident from this plot that the *iipA* mutant is significantly less infectious than the wild-type strain *in-vivo* for both the organs, consistent with the findings in the zebrafish model. The individual log transformed CI values from the organs for each individual fish is plotted in Figure 3.15.

Statistical analysis was performed on the log of output colonization per unit input values for kidney and liver to determine if on an average the difference between mutant and wild-type were less than zero. Paired t-tests applied on the data showed that the average difference between colonization of mutant and wild-type are significantly less than zero with p-values less than 0.00001 for both liver and kidney, indicating the wild-type strain as being significantly more infectious than the mutant strain.

Fish #	Organ	*iipA* Mutant output cfu/organ	Wild-Type output cfu/organ	Output Ratio (Mutant:Wild-type)	CI
1	LIVER	<10	2.0×10^{7}	$<5.0\times 10^{-7}$	$<4.8\times 10^{-7}$
	KIDNEY	<10	3.6×10^{6}	$<2.8\times 10^{-6}$	$<2.7\times 10^{-6}$
2	LIVER	<10	3.5×10^{5}	$<2.9\times 10^{-5}$	$<2.8\times 10^{-5}$
	KIDNEY	<10	6.6×10^{5}	$<1.5\times 10^{-5}$	$<1.4\times 10^{-5}$
3	LIVER	<10	4.8×10^{3}	$<2.1\times 10^{-3}$	$<2.0\times 10^{-3}$
	KIDNEY	<10	5.3×10^{4}	$<1.9\times 10^{-4}$	$<1.8\times 10^{-4}$
4	LIVER	<10	5.3×10^{5}	$<1.9\times 10^{-5}$	$<1.8\times 10^{-5}$
	KIDNEY	<10	1.0×10^{5}	$<1.0\times 10^{-4}$	$<9.6\times 10^{-5}$
5	LIVER	<10	3.1×10^{6}	$<3.2\times 10^{-6}$	$<3.1\times 10^{-6}$
	KIDNEY	<10	2.5×10^{6}	$<4.0\times 10^{-6}$	$<3.8\times 10^{-6}$
6	LIVER	<10	1.7×10^{6}	$<5.9\times 10^{-6}$	$<5.7\times 10^{-6}$
	KIDNEY	<10	2.7×10^{6}	$<3.7\times 10^{-6}$	$<3.6\times 10^{-6}$
7	LIVER	<10	4.1×10^{5}	$<2.4\times 10^{-5}$	$<2.3\times 10^{-5}$
	KIDNEY	<10	1.6×10^{6}	$<6.3\times 10^{-6}$	$<6.1\times 10^{-6}$

Table 3.6 **Bacterial loads of co-infection experiment using *M. marinum* wild-type and *iipA* mutant**. Expressed here is the bacterial load in liver and kidney recovered from seven fish co-infected by *iipA* mutant (expressing no fluorescence) strain and wild-type *M. marinum* (expressing Hyg^{R} *rfp*) in a competition study. The input Ratio of mutant/wild-type was 1.04:1; accordingly, the output Ratio and CI values for liver and kidney of each individual fish were calculated and shown here. The cfu count of the wild-type strain from the organs ranged from 10^{3} to 10^{7} whereas, colonies of the mutant strain were below the detection level even at lowest dilutions, as such their values were considered to be less than ten.

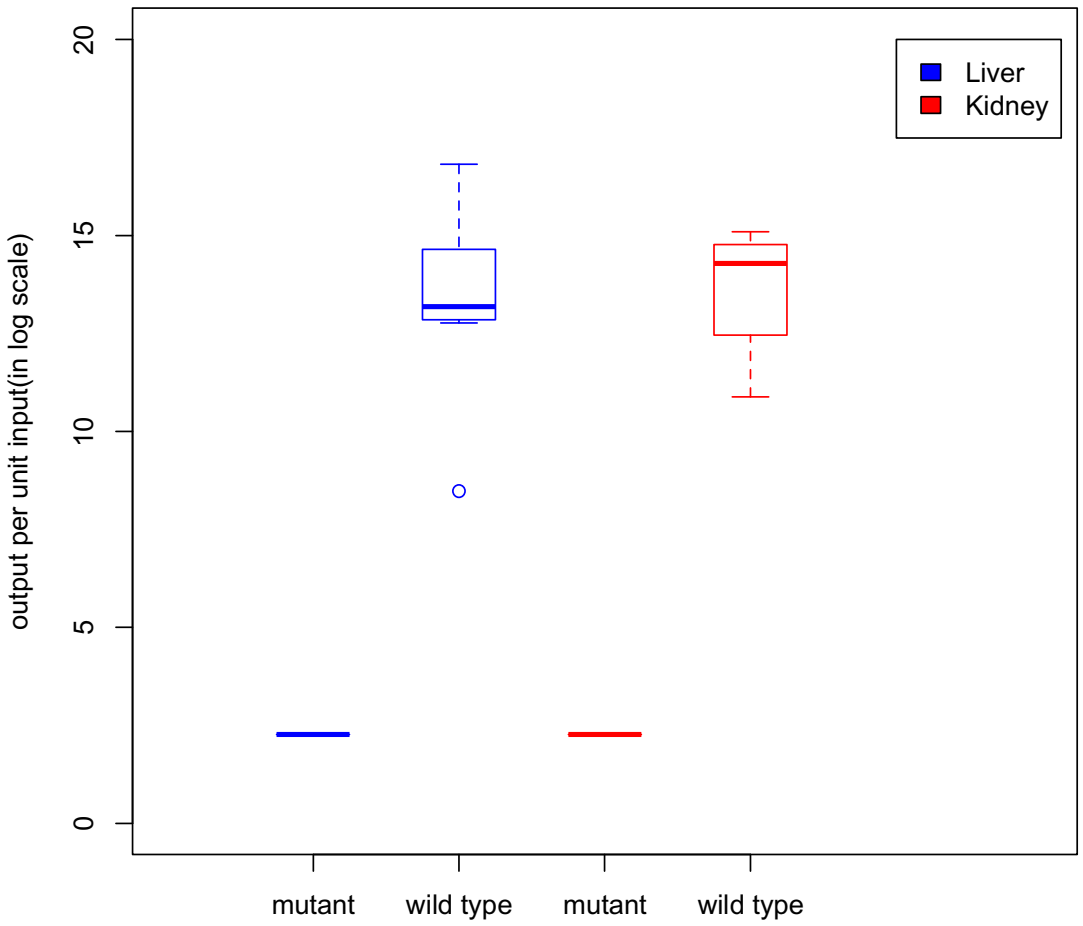

Figure 3.14 **The comparative box plot of output colonization per unit input (in log scale) of co-infection experiment using *M. marinum* wild-type and *iipA* mutant**. Shown here are the minimum, first quartile, median (bar in bold), third quartile and the maximum. The outliers (if present) are denoted by a dot. Log of output colonization per unit input is presented on the y-axis. In this experiment, for the mutant strain, no colonies were recovered from the organs at lowest dilution, as such their values were considered to be ten for the analysis. Through paired t-test for the above data, the p-values were determined to be less than 0.00001 for both liver and kidney.

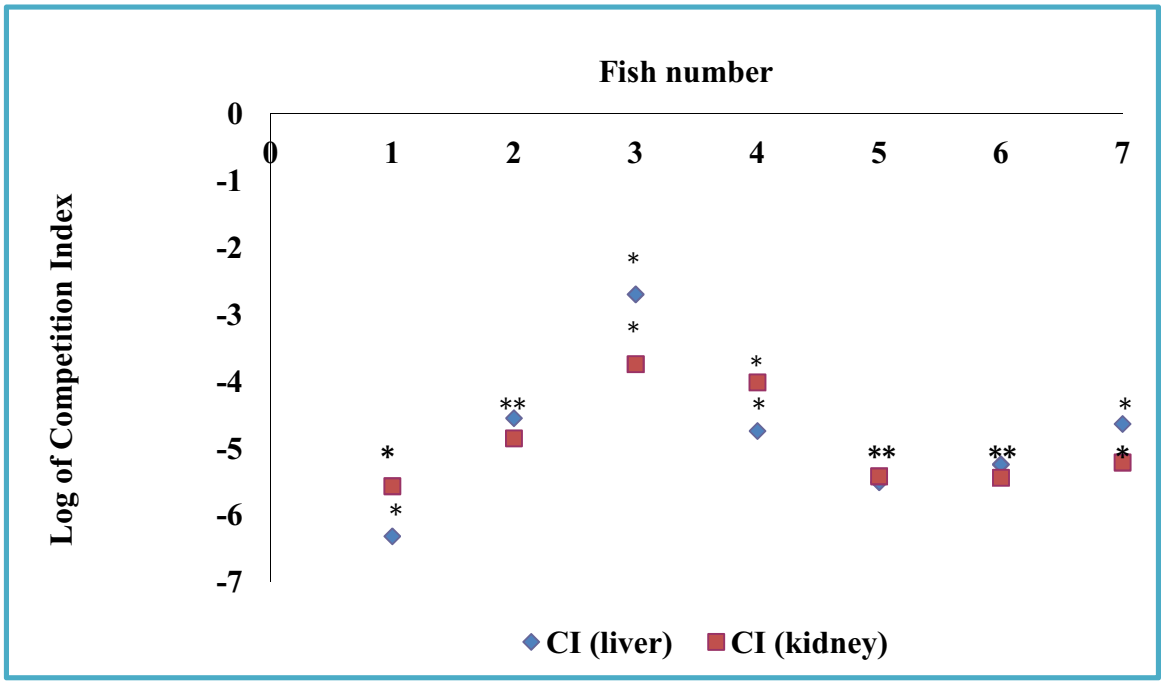

Figure 3.15 **Competition Index of individual organs in fish co-infected with *M. marinum* wild-type and *iipA* mutant.** Shown here are the log transformed values of CIs of liver and kidney of the seven co-infected fish in the competition study using the *iipA* mutant and wild-type strain. Log of Competition Index is represented on y-axis, while and on x-axis is fish number from 1-7. CIs close to zero on log scale indicate equal colonization between the two strains. In all instances, the points are greater than zero (in log scale) suggesting that the *iipA* mutant is deficient in establishing infections than the wild-type strain. * indicates no colonies were recovered from the organs for the *iipA* mutant and the CIs were calculated using the mutant strain count from the organs to be less than ten, thus the estimated CIs may even be ten-fold lower.

3.3.1.2 *In vivo* Analysis of an Established *M. marinum* Aviruent Mutant (*Mh3868*) by IP Infection

An insertion mutant within the uncharacterized gene *Mh3868* that is within the extended *RD1* virulence region of *M. marinum* (DE4388) was characterized by Gao et al. (2004). This strain contains an insertion mutation in one of the genes that is homologous to the extended RD1 region (a known virulence gene cluster) in *M. tuberculosis*. These *extRD1* genes in *M. marinum* (as well as in *M. tuberculosis*) are required for secretion of ESAT-6 protein (an important antigenic factor) and loss of this protein showed decreased virulence in the acute zebrafish model. We wanted to compare this mutant for its ability to colonize the organs in the chronic medaka model, using the wild-type mycobacterial strain in a competition as internal comparison. This competition study involved ten, five month old fish, cultures were prepared in standard media and fish were IP injected with equal ratio of wild-type and the mutant strain as per the protocol discussed above. The input Ratio of mutant/wild-type was calculated to be 0.8:1 (5.22×10^2 mutant cfu/fish to 6.47×10^2 wild-type cfu/fish). Fish were monitored for eight weeks and two days, all surviving fish were sacrificed, the target organs dissected, homogenized and then plated permissively for the detection of both *M. marinum* strains. Bacterial loads for both strain detected and the CI values are expressed in Table 3.7, showing output ratios substantially in favor of the wild-type strain for all experimentally infected animals. Comparative box plots of output colonization per unit input (in log scale) of mutant and wild-type for both liver and kidney are shown in Figure 3.16 and the individual log transformed CI values from the organs for each individual fish is plotted in Figure 3.17. These plots strongly indicate that the *extRD1* mutant is substantially less infectious than the wild-type strain using colonization as an end-point in medaka and is consistent with the zebrafish studies. Statistical analysis was performed on the log of output colonization per unit

input values for kidney and liver to determine if on an average the difference between mutant and wild-type were less than zero. Paired t-tests applied on the data showed that the average difference between colonization of mutant and wild-type are significantly less than zero with p-value 0.00001 for both livers and kidneys. These results indicate that the mutant strain is avirulent or inept in infecting the organs as compared to the wild-type strain. In most of the cases, the mutant strain could not be recovered from the organs at the lowest dilution, so CI values were calculated considering their value to be ten, even though the actual value were less than ten.

Fish #	Organ	*Mh3868* Mutant output cfu/organ	Wild-type output cfu/organ	Output Ratio (Mutant:WildType)	CI
1	LIVER	<10	1.40×10^{5}	7.14×10^{-5}	$<3.57\times10^{-4}$
	KIDNEY	<10	3.00×10^{4}	3.33×10^{-4}	$<1.67\times10^{-3}$
2	LIVER	<10	4.90×10^{5}	2.04×10^{-5}	$<1.02\times10^{-4}$
	KIDNEY	4.00×10^{3}	1.20×10^{4}	3.33×10^{-1}	1.67
3	LIVER	4.00×10^{4}	3.58×10^{6}	1.12×10^{-2}	5.59×10^{-2}
	KIDNEY	2.00×10^{3}	4.88×10^{5}	4.10×10^{-3}	2.05×10^{-2}
4	LIVER	<10	2.00×10^{4}	5.00×10^{-4}	$<2.50\times10^{-3}$
	KIDNEY	<10	7.40×10^{4}	1.35×10^{-4}	$<6.76\times10^{-4}$
5	LIVER	<10	1.02×10^{5}	9.80×10^{-5}	$<4.90\times10^{-4}$
	KIDNEY	<10	4.00×10^{3}	2.50×10^{-3}	$<1.25\times10^{-2}$
6	LIVER	<10	3.20×10^{4}	3.13×10^{-5}	$<1.56\times10^{-4}$
	KIDNEY	<10	4.00×10^{3}	2.50×10^{-3}	$<1.25\times10^{-2}$
7	LIVER	2.00×10^{5}	4.68×10^{5}	4.27×10^{-3}	2.14×10^{-2}
	KIDNEY	<10	1.00×10^{5}	1.00×10^{-4}	$<5.00\times10^{-4}$
8	LIVER	<10	2.40×10^{5}	4.17×10^{-5}	$<2.08\times10^{-4}$
	KIDNEY	<10	2.40×10^{4}	4.17×10^{-4}	$<2.08\times10^{-3}$
9	LIVER	<10	4.00×10^{4}	2.50×10^{-4}	$<1.25\times10^{-3}$
	KIDNEY	<10	1.34×10^{5}	7.46×10^{-5}	$<3.73\times10^{-4}$
10	LIVER	<10	1.20×10^{6}	8.33×10^{-6}	$<4.17\times10^{-5}$
	KIDNEY	<10	4.48×10^{5}	2.23×10^{-5}	$<1.12\times10^{-4}$

Table 3.7 **Bacterial loads of co-infection experiment using *M. marinum* wild-type and *Mh3868* mutant**. Expressed here is the bacterial load in liver and kidney recovered from ten fish co-infected by *Mh3868* mutant (expressing no fluorescence) strain and wild-type *M. marinum* (expressing Hyg^{R} *rfp*) in a competition study. The input Ratio of mutant/wild-type was 0.8:1; accordingly, the output Ratio and CI values for liver and kidney of each individual fish were calculated and shown here. The cfu count of the wild-type strain from the organs ranged from 10^{3} to 10^{6} whereas, colonies of the mutant strain in most organs were below the detection level even at lowest dilutions, as such their values were considered to be less than ten.

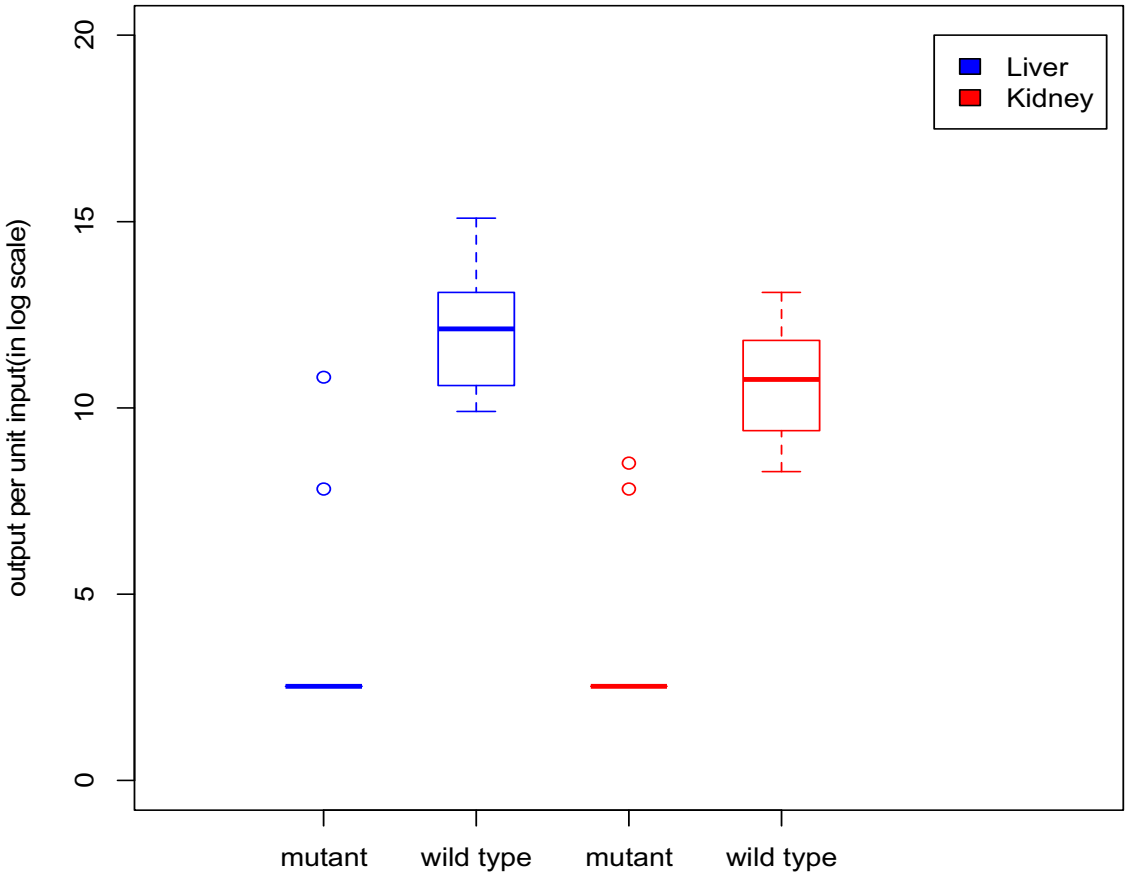

Figure 3.16 **The comparative box plot of output colonization per unit input (in log scale) of co-infection experiment using *M. marinum* wild-type and *Mh3868* mutant**. Shown here are the minimum, first quartile, median (bar in bold), third quartile and the maximum. The outliers (if present) are denoted by a dot. Log of output colonization per unit input is presented on the y-axis. In this experiment, for the mutant strain, no colonies were recovered from the organs at lowest dilution except in four out of twenty organs, as such their values were considered to be ten for the analysis. Through paired t-test for the above data, the p-values were determined to be 0.00001 for both liver and kidney.

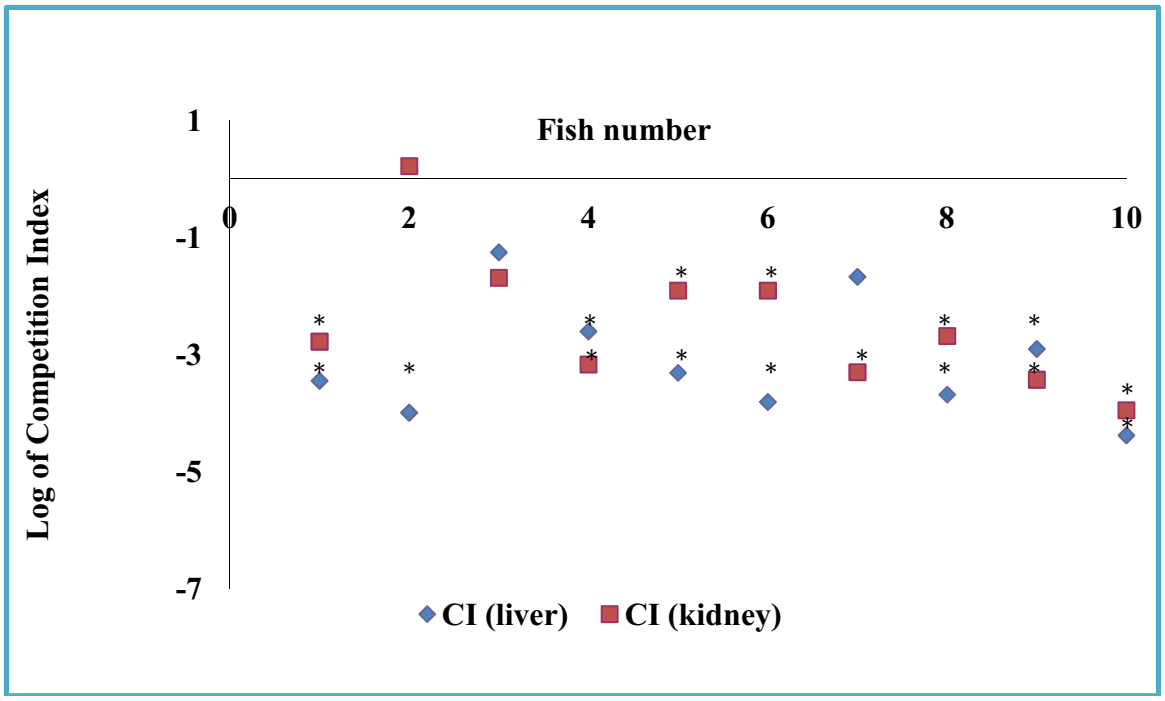

Figure 3.17 **Competition Index of individual organs in fish co-infected with *M. marinum* wild-type and *Mh3868* mutant.** Shown here are the log transformed values of CIs of liver and kidney of the ten co-infected fish in the competition study using mutant and wild-type strain. Log of Competition Index is represented on y-axis, while and on x-axis is fish number from 1-10. CIs close to zero on log scale indicate equal colonization between the two strains. In almost all instances, the points are less than zero (in log scale) suggesting that the *RD1* mutant is deficient in establishing infections than the wild-type strain. * indicates no colonies were recovered from the organs and the CIs were calculated using the mutant strain count from the organs to be less than ten.

3.3.1.3 *In vivo* Analysis of *M. marinum MelF* Aviruent Mutant by IP Infection

El -Etr et al. (2004) isolated a 'new' avirulent insertion mutant in *M. marinum,* they called *melF* (Mycobacterial Enhanced infection Loci F), and showed by *in vitro* virulence assays that is was defective in the ability to infect the murine and fish macrophage cell lines. Analysis of mycobacterial genome showed that *M. tuberculosis* shared a closely related gene, which was shown to be functionally homologous, since the *M. tuberculosis* orthologous gene *Rv1936* complemented the *melF* defect in *M. marinum.* Although *melF* mutants have a clear defect in mounting an infection *in vitro*, its effect *in vivo* was not known. In these experiments we aimed to test the effect of *melF* mutant on virulence in medaka infection model, using a competition approach. Cultures of both mutant and wild-type strains were prepared in laboratory conditions, for IP injection in an equal ratio for ten, five months old fish in a competition study. The input Ratio of mutant/wild-type was calculated to be 0.7:1 (1.51×10^2 *melF* cfu/fish: 2.03×10^2 wild-type cfu/fish). Fish were monitored for eight weeks and two days before the eight survivors were sacrificed and the dissected organs were plated permissively for the detection of both *M. marinum* strains. Bacterial load for each strain from the organs is expressed in Table 3.8. The output ratios and CI values ranging from about 0.5 to $<10^{-6}$ are substantially in favor of the wild-type strain for all the experimental animals. Comparative box plots of output colonization per unit input (in log scale) of mutant and wild-type for both liver and kidney are shown in Figure 3.18 and the individual log transformed CI values from the organs for each individual fish is plotted in Figure 3.19. The colonization patterns of the wild-type and mutant strain in the infected organs as shown in these figures, clearly indicate that the *melF* mutant less virulent in medaka. Statistical analysis was performed on the log of output colonization per unit input values for kidney and liver to

determine if on an average the difference between mutant and wild-type were less than one. Paired t-tests applied on the data showed that the average difference between colonization of mutant and wild-type are significantly less than zero with p-value 0.0199 for livers and 0.0069 for kidneys, indicating the mutant strain was less infectious than the wild-type strain. The colonization by the mutant strain were below the detection level in some instances (six out of fourteen organs) even at lowest dilutions and their values were considered to be less than ten, as such the estimated CI values are even less, however the wild-type strain in the same organs were 10^5 to 10^7. These *in vivo* studies suggest that indeed the *melF* mutant is less virulent than the wild-type parental strain, but this defect is moderate compared to other avirulent strains described above (i.e., *iipA* or *Mh3868*).

Fish #	Organ	*melF* Mutant output cfu/organ	Wild-type output cfu/ organ	Output Ratio (4425: 4436)	CI
1	LIVER	2.1×10^{5}	5.9×10^{5}	3.6×10^{-1}	4.9×10^{-1}
	KIDNEY	2.2×10^{5}	7.8×10^{6}	2.8×10^{-2}	3.8×10^{-2}
2	LIVER	<10	1.3×10^{7}	$<7.7\times 10^{-7}$	$<1.1\times 10^{-6}$
	KIDNEY	5.4×10^{5}	6.0×10^{6}	9.0×10^{-2}	1.2×10^{-1}
3	LIVER	<10	8.7×10^{6}	$<1.1\times 10^{-6}$	$<1.5\times 10^{-6}$
	KIDNEY	<10	1.0×10^{5}	$<1.0\times 10^{-4}$	$<1.4\times 10^{-4}$
4	LIVER	1.3×10^{5}	2.9×10^{6}	4.5×10^{-2}	6.1×10^{-2}
	KIDNEY	<10	1.1×10^{7}	$<9.1\times 10^{-7}$	$<1.2\times 10^{-6}$
5	LIVER	<10	2.6×10^{7}	$<3.8\times 10^{-7}$	$<5.1\times 10^{-7}$
	KIDNEY	<10	6.5×10^{6}	$<1.5\times 10^{-6}$	$<2.0\times 10^{-6}$
6	LIVER	ND	ND	ND	ND
	KIDNEY	2.2×10^{3}	1.4×10^{5}	1.6×10^{-2}	2.2×10^{-2}
7	LIVER	ND	ND	ND	ND
	KIDNEY	4.0×10^{3}	1.4×10^{5}	2.9×10^{-2}	3.9×10^{-2}

Table 3.8 **Bacterial loads of co-infection experiment using *M. marinum* wild-type and *melF* mutant**. Expressed here is the bacterial load in liver and kidney recovered from seven fish co-infected by *melF* mutant (expressing no fluorescence) strain and wild-type *M. marinum* (expressing Hyg^{R} *rfp*) in a competition study. The input Ratio of mutant/wild-type was 0.7:1; accordingly, the output Ratio and CI values for liver and kidney of each individual fish were calculated and shown here. The cfu count of the wild-type strain from the organs ranged from 10^{5} to 10^{7} whereas, colonies of the mutant strain were below the detection level in some instances even at lowest dilutions, as such their values were considered to be less than ten. ND specifies the cases where contaminating bacteria had outgrown *M. marinum* on the plates, hence their count was Not Determined (ND).

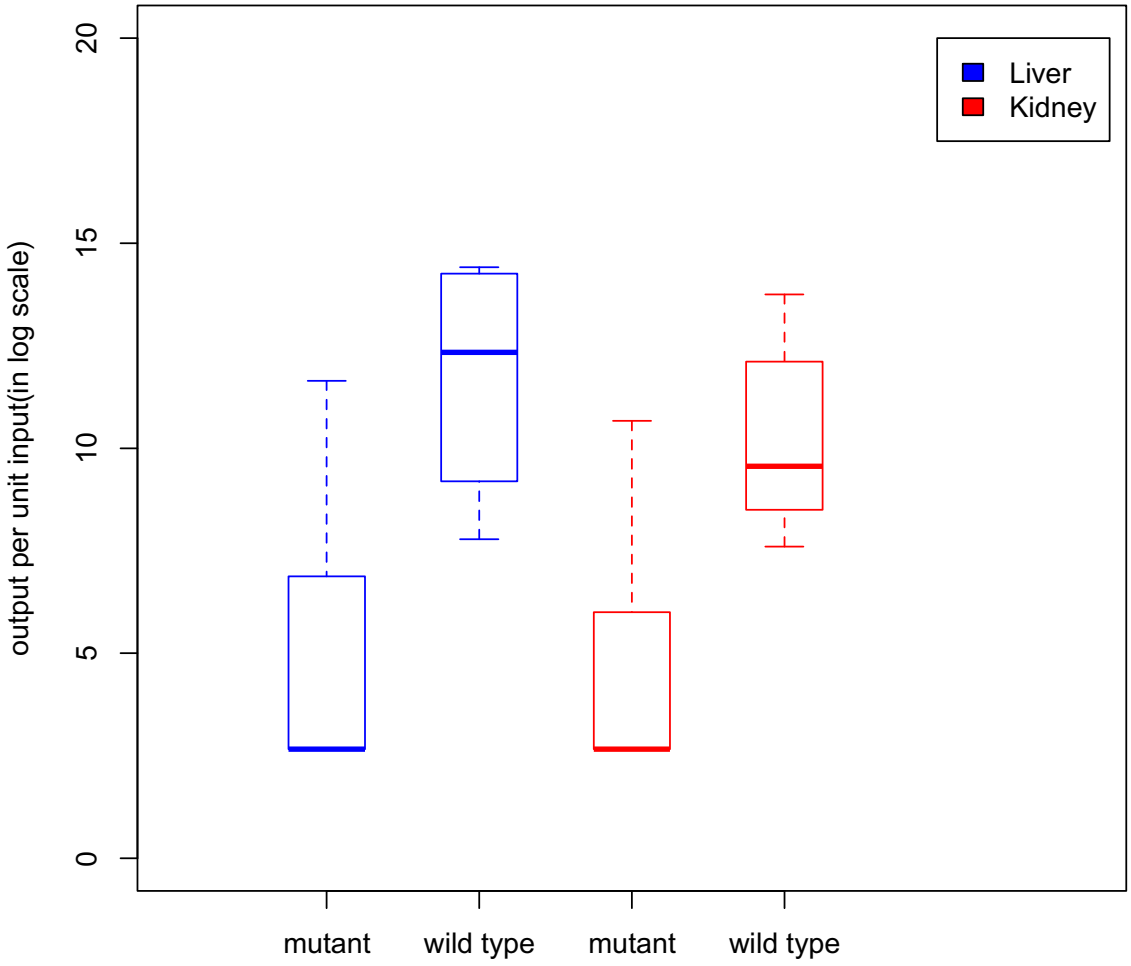

Figure 3.18 **The comparative box plot of output colonization per unit input (in log scale) of co-infection experiment using *M. marinum* wild-type and *melF* mutant**. Shown here are the minimum, first quartile, median (bar in bold), third quartile and the maximum. The outliers (if present) are denoted by a dot. Log of output colonization per unit input is presented on the y-axis. In this experiment, for the mutant strain, no colonies were recovered from the organs at lowest dilution except in four out of twenty organs, as such their values were considered to be ten for the analysis. Through paired t-test for the above data, the p-values were determined to be 0.0199 for liver and 0.0069 for kidney.

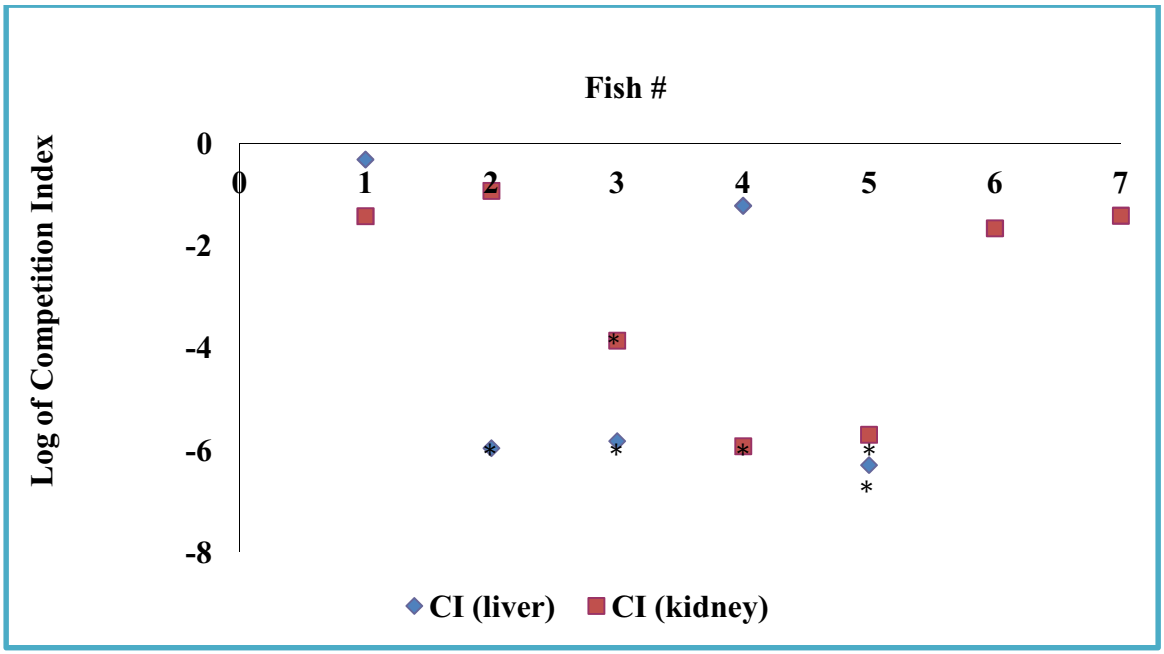

Figure 3.19 **Competition Index of individual organs in fish co-infected with *M. marinum* wild-type and *melF* mutant.** Shown here are the log of CIs of liver and kidney of the seven co-infected fish in the competition study using mutant and wild-type strain. Log of Competition Index is represented on y-axis, while and on x-axis is fish number from 1-7. CIs close to zero on log scale indicate equal colonization between the two strains. In all instances, the points are greater than zero (in log scale) suggesting that the *melF* mutant is deficient in establishing infections than the wild-type strain. * indicates no colonies were recovered from the organs and the CIs were calculated using a less than estimate for the mutant strain count from the organs to be less than ten cfu in the sample.

3.3.1.4 Investigation of Novel *Mycobacterium marinum* Macrophage Infection Mutants in a Chronic *in vivo* Model

Mehta et al. 2006 isolated and characterized a number of *M. marinum* mutants obtained by an open-ended transposon mutagenesis 'hunt' and then screened isolates in murine macrophage infection assay. These macrophage infection mutants (Mim) were conceptually divided into three groups: 1) defective in macrophage binding, 2) defective in intracellular survival, 3) defective in both the above. The experiments described here, investigated some of these mutants in our *in vivo* chronic infection model to gain valuable insights of their role in TB pathogenesis by accessing their ability to colonize the organs in medaka. As was described previously, we have used medaka-*M. marinum* model to study the fitness of mutants carrying defects in established virulence genes compared to wild-type reference strain. Here we aimed to characterize the *in vivo* effect of three novel mutants: *mimI, mimD* and *mimH,* identified in the above macrophage studies using this model. We have compared the virulence of these mutants by both IP injection and oral infection route, the latter being a natural mode of infection.

3.3.1.4.1 *In vivo* Analysis of *M. marinum mimI* Mutant by IP Infection

In vitro studies using cultured murine macrophages have shown that *mimI* is defective in both cell association and ability to survive inside the macrophages (Mehta et al, 2006). In this experiment we aimed to investigate fitness of the mutant strain in comparison to the wild-type parental bacteria when inoculated in essentially an equal ratio through IP injections into the animal. Bacterial cultures were prepared using standard laboratory culture and IP injected into the fish using the same method as described above for other mutants. This competition study was repeated several times, and the outcome from each experiment followed the same trend of substantial reduced virulence. Shown here are two representative experiments (called

group 1 and group 2). Both the groups have employed ten five months old fish. The input Ratio of mutant/wild-type was calculated to be 1.3:1 (6.8×10^1 mutant cfu/fish: 5.2×10^1 wild-type cfu/fish) for group 1 and 1.01:1 (1.70×10^2 mutant cfu/fish: 1.67×10^2 wild-type cfu/fish) for group 2. Fish were monitored for approximately six weeks before they were sacrificed and the homogenized dissected organs were plated permissively for the detection of both *M. marinum* strains. Four and seven fish were lost in groups 1 and 2 respectively. Bacterial loads from the organs for each group is shown in Table 3.9 (A and B). Since there was considerable mortality in both the groups, the analysis of CI values of the liver and kidney from fish in the both groups were compromised and were instead averaged, log transformed and shown in Figure 3.21. Similarly, comparative box plots of output colonization per unit input (in log scale) of mutant and wild-type for both liver and kidney are shown in Figure 3.20. The output ratios and the consequently the CI values are significantly in favor of the wild-type strain for all instances of infection, ranging from 3.4×10^{-2} to $<8.1 \times 10^{-6}$, strongly indicating that the *mimI* mutant is substantially less virulent than the wild-type strain. Statistical analysis was performed on the log of output colonization per unit input values for kidney and liver to determine if on an average the difference between mutant and wild-type were less than zero. Paired t-tests applied on the data showed that the average difference between colonization of mutant and wild-type are significantly less than zero with p-value 0.00019 for livers and 0.00079 for kidneys. This data are in strong support of the conclusion that *mimI* strain is substantially less infectious than the wild-type strain. However, in all the instances when the mutant strain was found to be present below the detection level even at lowest dilution, the CI values and statistical tests were performed considering their number to be less than ten, as such the estimated CI values are actually an underestimation of the loss of

virulence. These *in vivo* data are in agreement with the initial characterization of *mimI* using cultured murine macrophages, but offers a direct comparison of mutant to wild-type in a relevant fish model.

A)

Fish #	Organ	*mimI* Mutant output cfu/organ	Wild-type output cfu/organ	Output Ratio (Mutant:Wild-type)	CI
1	LIVER	8.0×10^{4}	1.82×10^{6}	4.4×10^{-2}	3.4×10^{-2}
	KIDNEY	< 10	1.5×10^{5}	$< 6.8 \times 10^{-5}$	$<5.2 \times 10^{-5}$
2	LIVER	< 10	1.0×10^{5}	$< 1.0 \times 10^{-4}$	$<7.7 \times 10^{-5}$
	KIDNEY	8.0×10^{3}	2.0×10^{4}	4.0×10^{-1}	3.1×10^{-1}
3	LIVER	< 10	1.6×10^{6}	$<6.4 \times 10^{-6}$	$<4.9 \times 10^{-6}$
	KIDNEY	< 10	9.4×10^{5}	$< 1.06 \times 10^{-5}$	$<8.1 \times 10^{-6}$
4	LIVER	4.60×10^{4}	1.5×10^{6}	3.01×10^{-2}	2.3×10^{-2}
	KIDNEY	3.0×10^{4}	2.2×10^{5}	1.25×10^{-1}	9.6×10^{-3}
5	LIVER	< 10	5.2×10^{5}	$< 1.91 \times 10^{-5}$	$< 1.5 \times 10^{-5}$
	KIDNEY	< 10	1.0×10^{4}	$< 7.14 \times 10^{-4}$	$< 5.5 \times 10^{-4}$

Group 1

B)

Fish #	Organ	*mimI* Mutant output cfu/organ	Wild-type output cfu/organ	Output Ratio (Mutant:Wild-type)	CI
6	LIVER	< 10	8×10^{3}	$<1.3 \times 10^{-3}$	$<1.3 \times 10^{-3}$
	KIDNEY	< 10	1.0×10^{4}	$<1.0 \times 10^{-3}$	$<1.0 \times 10^{-3}$
7	LIVER	< 10	2.4×10^{3}	$<4.2 \times 10^{-3}$	$<4.2 \times 10^{-3}$
	KIDNEY	< 10	2.4×10^{3}	$<4.2 \times 10^{-3}$	$<4.2 \times 10^{-3}$
8	LIVER	< 10	1.2×10^{4}	$<8.3 \times 10^{-4}$	$<8.3 \times 10^{-4}$
	KIDNEY	< 10	2.0×10^{3}	$<5.0 \times 10^{-3}$	$<5.0 \times 10^{-3}$

Group 2

Table 3.9 **Bacterial loads of co-infection experiment using *M. marinum* wild-type and *mimI* mutant**. Expressed here is the bacterial load in liver and kidney recovered from eight fish, belonging to A) group 1 (1-5) and B) group 2 (6-8), co-infected by *mimI* mutant (expressing no fluorescence) strain and wild-type *M. marinum* (expressing Hyg^{R} *rfp*) in a competition study. The input Ratio of mutant/wild-type was 1.3:1 and 1.01:1 for group 1 and 2 respectively; accordingly, the output Ratio and CI values for liver and kidney of each individual fish were calculated and shown here. The cfu count of the wild-type strain from the organs ranged from 10^{3} to 10^{6} whereas, colonies of the mutant strain were often below the detection level even at lowest dilutions in some cases, as such their values were considered to be less than ten.

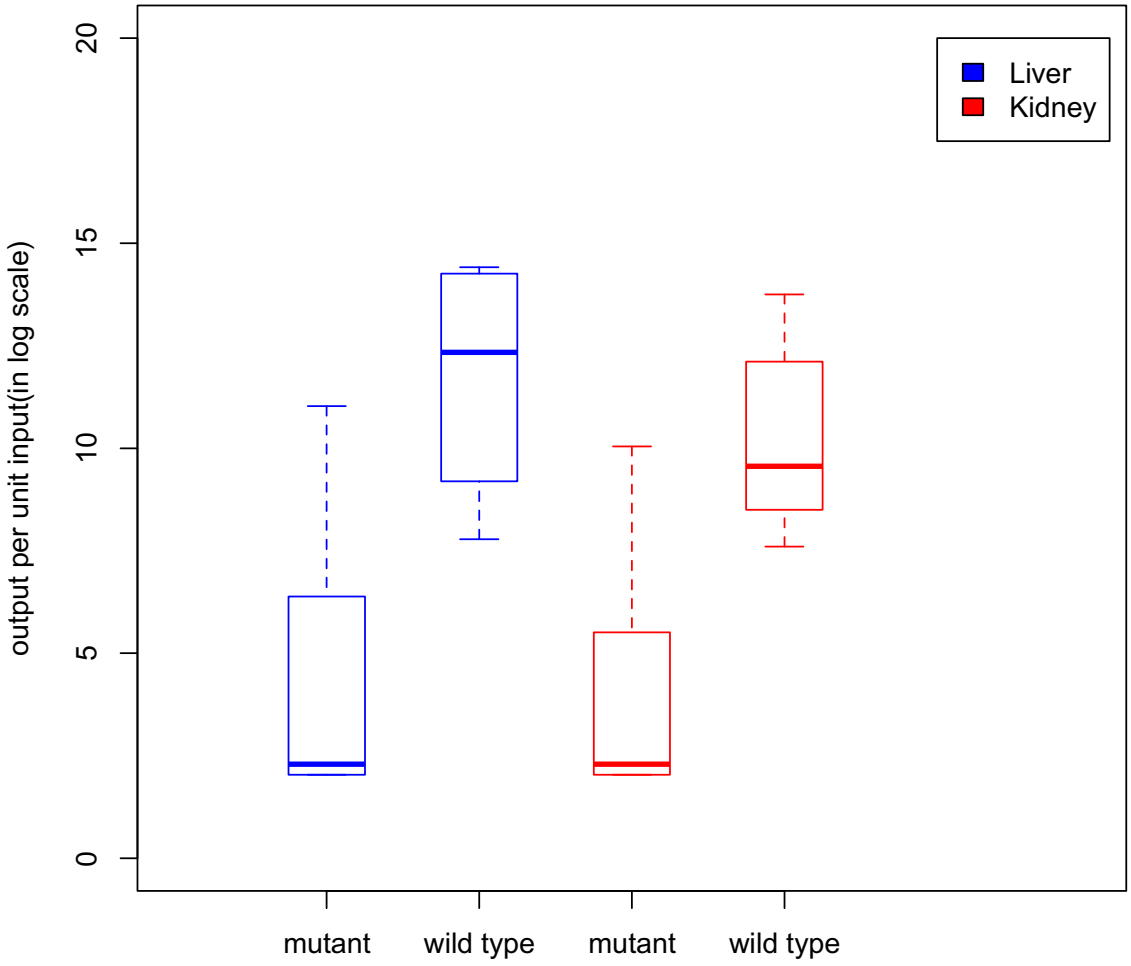

Figure 3.20 **The comparative box plot of output colonization per unit input (in log scale) of co-infection experiment using *M. marinum* wild-type and *mimI* mutant**. Shown here are the minimum, first quartile, median (bar in bold), third quartile and the maximum. Log of output colonization per unit input is presented on the y-axis. In this experiment, for the mutant strain, no colonies were recovered from the organs at lowest dilution except in four out of sixteen organs, as such their values were considered to be ten for the analysis. Through paired t-test for the above data, the p-values were determined to 0.00019 for liver and 0.00079 for kidney.

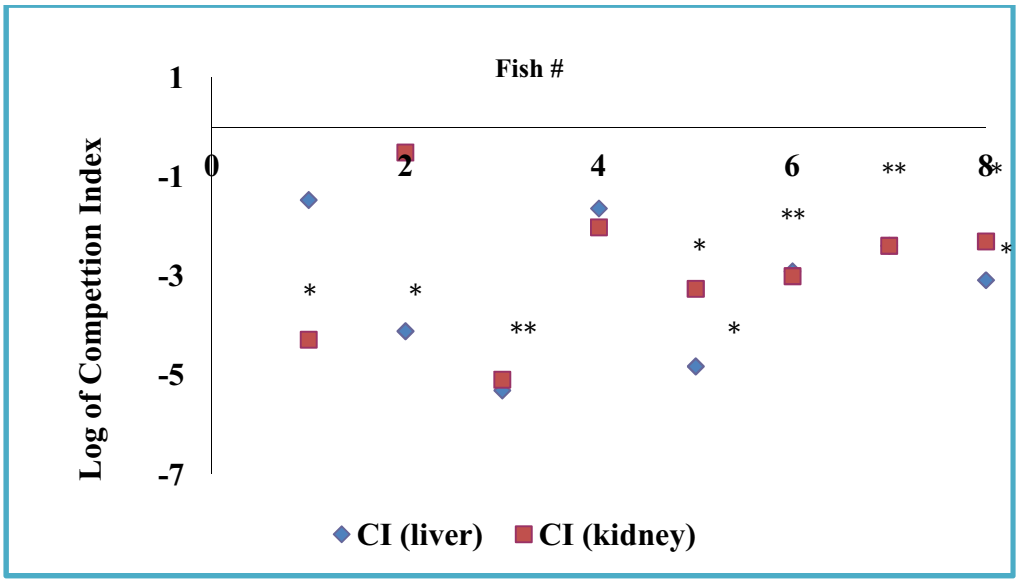

Figure 3.21 **Competition Index of individual organs in fish co-infected with *M. marinum* wild-type and *mimI* mutant.** Shown here are the log of CIs for livers and kidneys of the eight co-infected fish in the competition study using mutant and wild-type strain. Log of Competition Index is represented on y-axis, while and on x-axis is fish number from 1-8 (belonging to both group1 and 2). CIs close to zero on log scale indicate equal colonization between the two strains. In all instances, the points are greater than zero (in log scale) suggesting that the *mimI* mutant is deficient in establishing infections than the wild-type strain. * indicates no *mimI* colonies were recovered from the organs and the CIs were calculated using the mutant strain count from the organs to be less than ten.

3.3.1.4.2 *In vivo* Analysis of *M. marinum mimD* Mutant by IP Infection

The *mimD* mutant was initially characterized *in vitro* and shown to be defective in its ability to survive inside murine macrophages (Mehta et al, 2006). To extend the earlier *in vitro* studies we aimed to investigate fitness of the mutant strain in comparison to the wild-type parent bacteria when inoculated in equal ratio through IP injections into the animal. Bacterial cultures were prepared and IP injected into the fish using the same method as described above for other mutants. This competition study utilized eleven five months old fish; the input ratio of mutant/wild-type was calculated to be 1.32:1 (4.38×10^2 mutant cfu/fish: 3.32×10^2 wild-type cfu/fish). Infected fish were monitored for approximately six weeks before they were sacrificed and the organs were plated permissively for the detection of both *M. marinum* strains. None of the fish were lost for the duration of the experiment but *M. marinum* could not be isolated from four of the eleven fish (data not included). Bacterial loads from the organs of each fish and calculated CI values are expressed in Table 3.10. Comparative box plots of output colonization per unit input (in log scale) of mutant and wild-type for both liver and kidney are shown in Figure 3.22. Individual log transformed CI values from the organs for each fish are plotted in Figure 3.23. The output ratios and the CI values are slightly in favor of the wild-type strain for all infected animal, suggesting that the mutant strain is somewhat less infectious than the wild-type strain. Similar trend is also seen in the box plot, where the difference between the median of wild-type and *mimD* mutant is visible but comparatively less pronounced than the mutants studied thus far. Statistical analysis was performed on the log of output colonization per unit input values for kidney and liver to determine if on an average the difference between mutant and wild-type were less than zero. Paired t-tests applied on the data showed that the average difference between colonization of

mutant and wild-type are significantly less than zero with p-value 0.0212 for livers and 0.0251 for kidneys, thus supporting the impression that wild-type strain as being more infectious than the mutant strain. These data obtained in a relevant fish model offer support to previous *in vitro* murine macrophage studies, but indicate that inactivation of the *mimD* gene has modest effects on virulence.

Fish #	Organ	*mimD* Mutant cfu/organ	Wild-type output cfu/organ	Output Ratio (Mutant:Wild-type)	CI
1	LIVER	1.4×10^{6}	3.1×10^{6}	4.6×10^{-1}	3.5×10^{-1}
	KIDNEY	2.4×10^{6}	1.4×10^{7}	1.7×10^{-1}	1.3×10^{-1}
2	LIVER	< 10	4.6×10^{5}	$< 2.2 \times 10^{-5}$	$<1.7 \times 10^{-5}$
	KIDNEY	< 10	5.3×10^{5}	$< 1.9 \times 10^{-5}$	$<1.4 \times 10^{-5}$
3	LIVER	2.2×10^{5}	2.0×10^{5}	1.1	8.3×10^{-1}
	KIDNEY	8.0×10^{3}	3.4×10^{4}	2.4×10^{-1}	1.8×10^{-1}
4	LIVER	4.0×10^{3}	1.4×10^{5}	2.8×10^{-2}	2.1×10^{-2}
	KIDNEY	8.0×10^{3}	1.0×10^{5}	7.8×10^{-2}	5.9×10^{-2}
5	LIVER	2.0×10^{4}	2.0×10^{5}	7.8×10^{-2}	5.9×10^{-2}
	KIDNEY	4.6×10^{4}	2.1×10^{5}	2.2×10^{-1}	1.7×10^{-1}
6	LIVER	5.4×10^{5}	5.7×10^{6}	9.5×10^{-2}	7.2×10^{-2}
	KIDNEY	7.3×10^{5}	1.5×10^{6}	4.7×10^{-1}	3.6×10^{-1}
7	LIVER	2.9×10^{5}	3.6×10^{6}	8.2×10^{-2}	6.2×10^{-2}
	KIDNEY	4.0×10^{3}	3.0×10^{4}	1.2×10^{-1}	9.1×10^{-2}

Table 3.10 **Bacterial loads of co-infection experiment using *M. marinum* wild-type and *mimD* mutant**. Expressed here is the bacterial load in liver and kidney recovered from seven fish co-infected by *mimD* mutant (expressing no fluorescence) strain and wild-type *M. marinum* (expressing Hyg^{R} *rfp*) in a competition study. The input Ratio of mutant/wild-type was 1.32:1; accordingly, the output Ratio and CI values for liver and kidney of each individual fish were calculated and shown here. The cfu count of the wild-type strain from the organs ranged from 10^{4} to 10^{7} whereas, colonies of the mutant strain ranged from 10^{3} to 10^{6}. In case of one fish, the mutant strain count was below the detection level even at lowest dilutions, as such their values were considered to be less than ten.

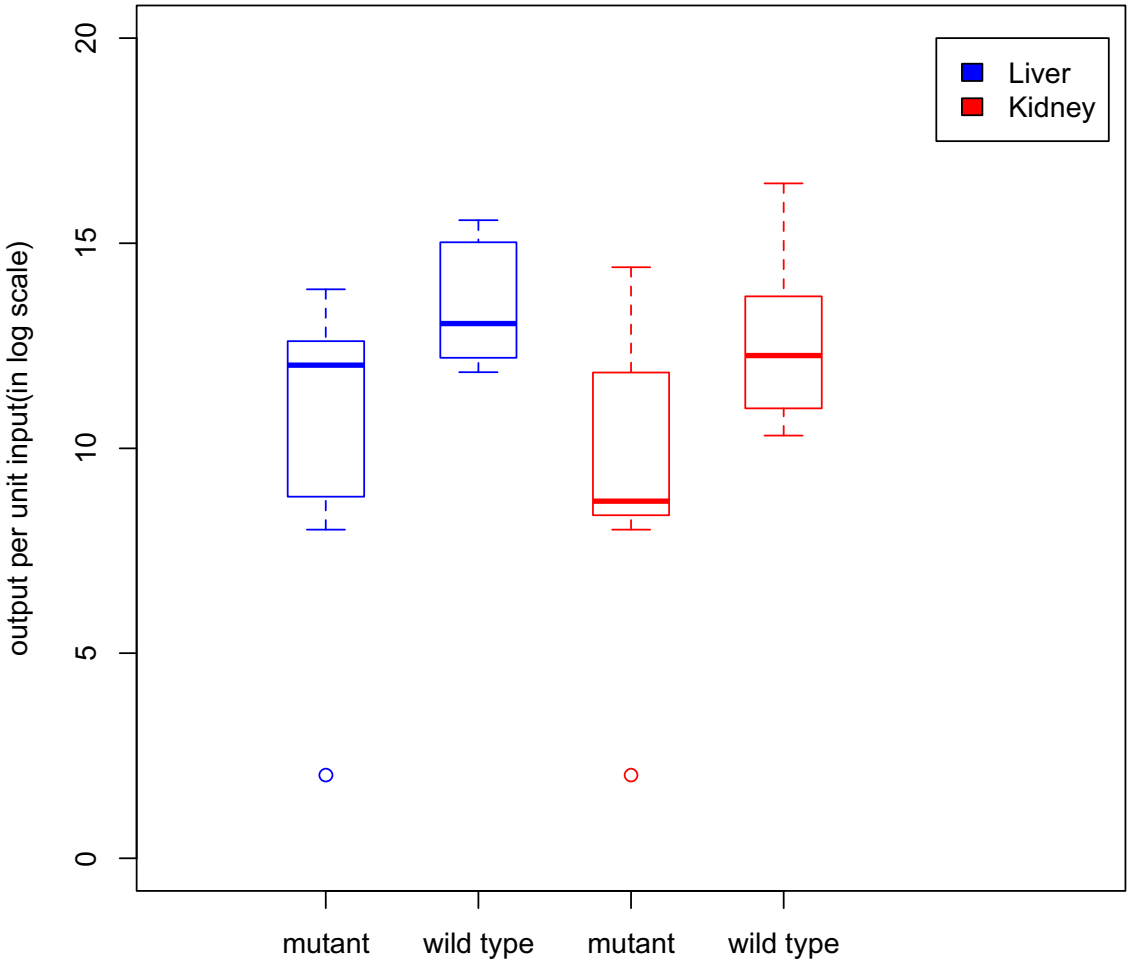

Figure 3.22 **The comparative box plot of output colonization per unit input (in log scale) of co-infection experiment using *M. marinum* wild-type and *mimD* mutant**. Shown here are the minimum, first quartile, median (bar in bold), third quartile and the maximum. Log of output colonization per unit input is presented on the y-axis. The outliers (if present) are denoted by a dot. In this experiment, for the mutant strain, no colonies were recovered from the organs at lowest dilution for only two out of twenty organs, as such their values were considered to be ten for the analysis. Through paired t-test for the above data, the p-values were determined to be 0.0212 for liver and 0.0251 for kidney.

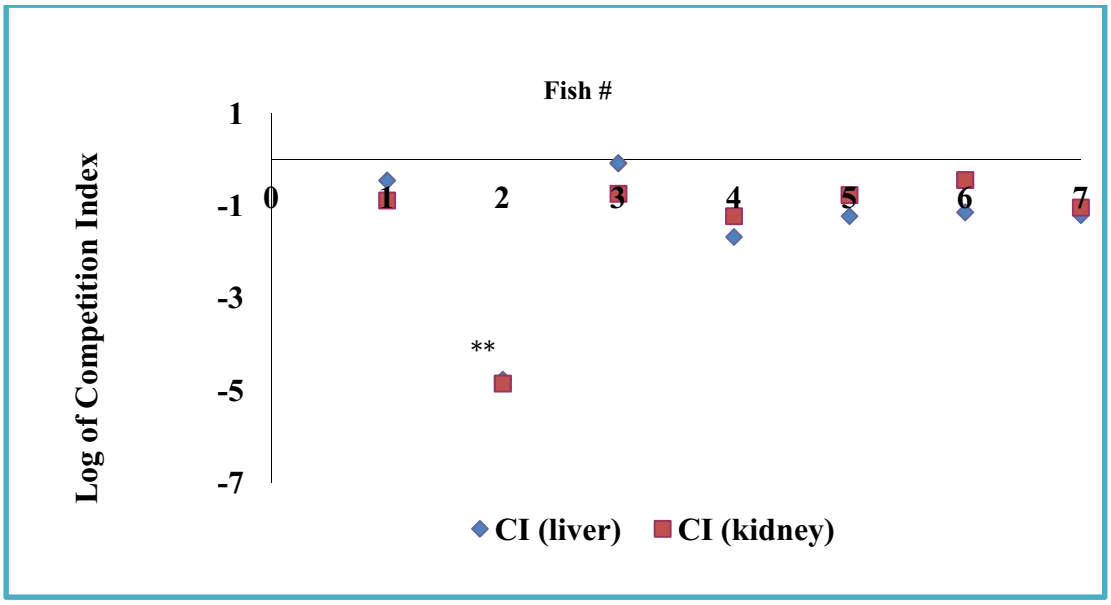

Figure 3.23 **Competition Index of individual organs in fish co-infected with *M. marinum* wild-type and *mimD* mutant.** Shown here are the log of CIs of liver and kidney of the seven co-infected fish in the competition study using mutant and wild-type strain. Log of Competition Index is represented on y-axis, while and on x-axis is fish number from 1-7. CIs close to zero on log scale indicate equal colonization between the two strains. In most instances, the points are greater than zero (in log scale) suggesting that the *mimD* mutant is deficient in establishing infections than the wild-type strain. * indicates no *mimD* colonies were recovered from the organs and the CIs were calculated using the mutant strain count from the organs to be less than ten.

3.3.1.4.3 *In vivo* Analysis of *M. marinum mimH* Mutant by IP Infection

Mehta et al. (2006) have shown *in vitro* using murine macrophages that a *mimH* mutant is defective in binding to the macrophages, thought to be an important step for mycobacterial virulence. In this experiment we aimed to investigate fitness of the *mimH* mutant strain in comparison to the wild-type parent strain when inoculated in equal ratio through IP injections into fish hosts. Bacterial cultures were prepared and IP injected into the fish using the same approaches as described above for the other mutants. This competition study utilized ten five months old fish; the input ratio of mutant/wild-type was calculated to be 0.86:1 (2.64×10^2 mutant cfu/fish: 3.04×10^2 wild-type cfu/fish). Fish were monitored for about six weeks before they were sacrificed and the organs were homogenized and plated permissively for the detection of both *M. marinum* strains. Two fish were lost during the experiment and *M. marinum* could not be isolated from one fish (data not included). Bacterial loads from the organs of each fish and calculated CI value are expressed in Table 3.11. Comparative box plots of output colonization per unit input (in log scale) of mutant and wild-type for both liver and kidney are shown in Figure 3.24. Individual log transformed CI values from the organs for each fish are plotted in Figure 3.25. The data indicates that the *mimH* mutant is somewhat less virulent than the wild-type strain. As another indication of reduced virulence, the *mimH* mutant was retrieved from only three of the fourteen dissected organs even at lowest dilution. To strengthen this conclusion that the mutant is less virulent, statistical analysis was performed on the log of output colonization per unit input values for kidney and liver to determine if on an average the difference between mutant and wild-type were less than zero. Paired t-tests applied on the data showed that the average difference between colonization of mutant and wild-type are significantly less than zero with p-value 0.0089 for

livers and 0.00039 for kidneys as expected, thus supporting the idea that the wild-type strain is more infectious than the mutant.

Fish #	Organ	*mimH* Mutant cfu/organ	Wild-type cfu/organ	Output Ratio (Mutant:Wild-type)	CI
1	LIVER	< 10	6.0×10^{3}	$< 1.7 \times 10^{-3}$	$<2.0 \times 10^{-3}$
	KIDNEY	< 10	1.0×10^{4}	$< 8.3 \times 10^{-4}$	$<9.6 \times 10^{-4}$
2	LIVER	< 10	5.6×10^{4}	$< 1.8 \times 10^{-4}$	$<2.1 \times 10^{-4}$
	KIDNEY	< 10	9.8×10^{4}	$< 1.0 \times 10^{-4}$	$<1.2 \times 10^{-4}$
3	LIVER	< 10	8.0×10^{3}	$< 1.0 \times 10^{-3}$	$<1.2 \times 10^{-3}$
	KIDNEY	< 10	2.6×10^{4}	$< 3.8 \times 10^{-4}$	$<4.4 \times 10^{-4}$
4	LIVER	7.2×10^{5}	1.6×10^{5}	4.4	5.1
	KIDNEY	< 10	1.0×10^{4}	$< 7.0 \times 10^{-4}$	$< 8.1 \times 10^{-4}$
5	LIVER	2.0×10^{4}	3.0×10^{4}	6.0×10^{-1}	6.9×10^{-1}
	KIDNEY	< 10	< 10	ND	ND
6	LIVER	< 10	6.6×10^{4}	$< 1.5 \times 10^{-4}$	$<1.7 \times 10^{-4}$
	KIDNEY	< 10	< 10	ND	ND
7	LIVER	2.0×10^{4}	7.5×10^{6}	2.7×10^{-3}	3.1×10^{-3}
	KIDNEY	< 10	< 10	ND	ND

Table 3.11 **Bacterial loads of co-infection experiment using *M. marinum* wild-type and *mimH* mutant**. Expressed here is the bacterial load in liver and kidney recovered from seven fish co-infected by *mimH* mutant (expressing no fluorescence) strain and wild-type *M. marinum* (expressing Hyg^{R} *rfp*) in a competition study. The input Ratio of mutant/wild-type was 0.86:1; accordingly, the output Ratio and CI values for liver and kidney of each individual fish were calculated and shown here. The cfu count of the wild-type strain from the organs ranged from 10^{3} to 10^{6} whereas, colonies of the mutant strain were below the detection level even at lowest dilutions for most dissected organs, as such their values were considered to be less than ten. Also, for the kidney of one fish neither the mutant nor the wild-type count could be determined, shown here as ND.

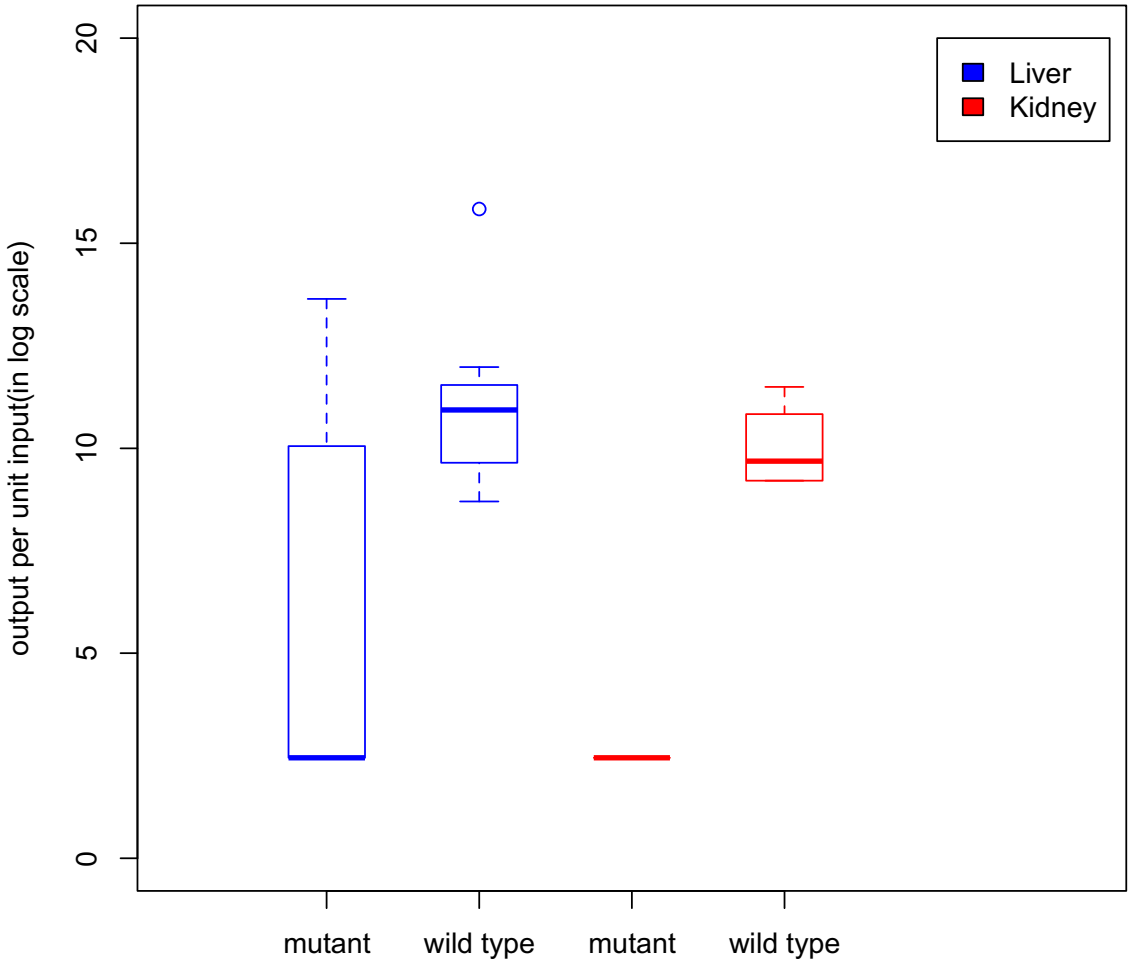

Figure 3.24 **The comparative box plot of output colonization per unit input (in log scale) of co-infection experiment using *M. marinum* wild-type and *mimH* mutant**. Shown here are the minimum, first quartile, median (bar in bold), third quartile and the maximum. The outliers (if present) are denoted by a dot. Log of output colonization per unit input is presented on the y-axis. In this experiment, for the mutant strain, no colonies were recovered from eleven out of fourteen organs at lowest dilution, as such their values were considered to be ten for the analysis. Through paired t-test for the above data, the p-values were determined to be 0.0089 for liver and 0.00039 for kidney.

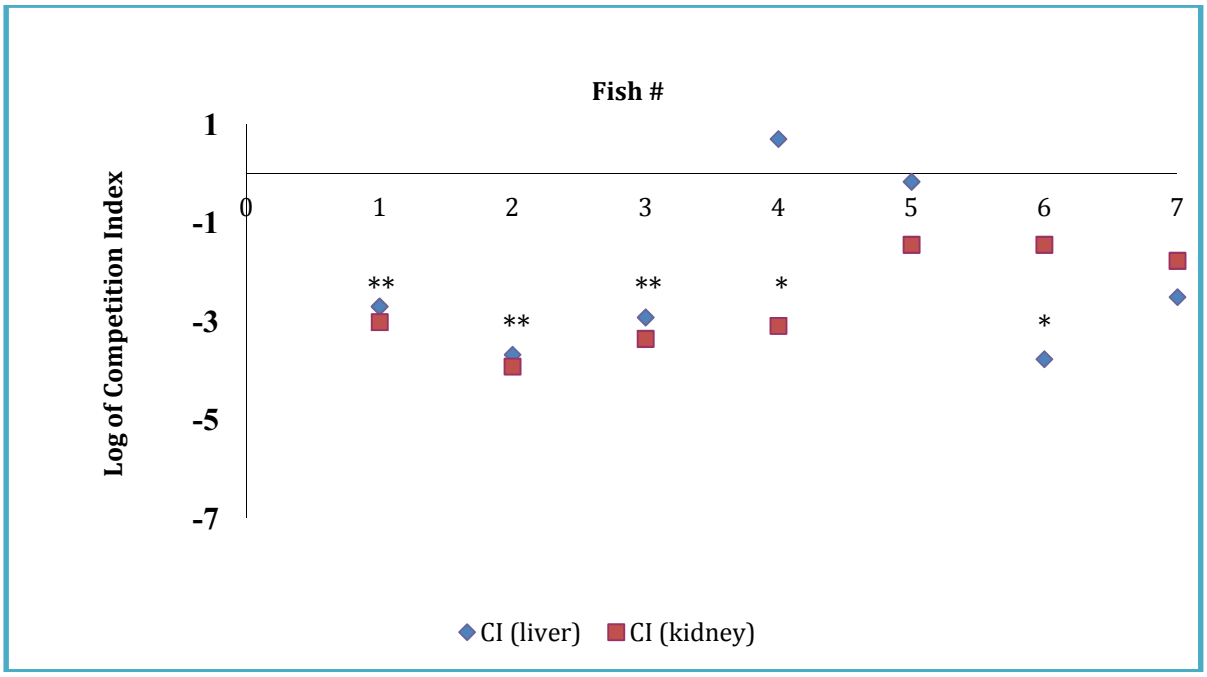

Figure 3.25 **Competition Index of individual organs in fish co-infected with *M. marinum* wild-type and *mimH* mutant.** Shown here are the log of CIs of liver and kidney of the seven co-infected fish in the competition study using mutant and wild-type strain. Log of Competition Index is represented on y-axis, while and on x-axis is fish number from 1-7. CIs close to zero on log scale indicate equal colonization between the two strains. In most instances, the points are greater than zero (in log scale) suggesting that the *mimH* mutant is moderately deficient in establishing infections than the wild-type strain. * Indicates no *mimH* colonies were recovered from the organs and the CIs were calculated using the mutant strain count to be less than ten.

3.3.2 *In vivo* Analyses of *M. marinum* Macrophage Infection Mutants (mim) Following Infection by an Oral Route

The three macrophage infection mutants (*mimI, mimD* and *mimH*) were also investigated by competition study using ingestion of pathogen carried in larvae, a more natural mode of infection, as inoculation by IP injections is unnatural and invasive. Data obtained from infections administered through IP injections, suggested significant reduced fitness for many of these mutants, in particular for the *mimI* mutant strain in comparison to the wild-type parent bacteria. However previous studies by our research group have shown that the *mimI* mutant strain did not display much distinction between proportions of organ colonization as opposed to wild-type when inoculated following ingestion (Root 2012). Experiments described here represent the *in vivo* effect on virulence of three novel mutants (*mimI, mimD* and *mimH)* and a well-defined avirulent mutant (*ΔRD1*) through oral infection route and then compared to results obtained following IP injections.

3.3.2.1 *In vivo* Analysis of *M. marinum mimI* Mutant Through Ingestion

This competition study aimed to evaluate the ability of *mimI* to colonize the fish organ when infected through oral route rather that an IP route. In this experiment, a group of ten seven-month old fish were inoculated with four meals of infected mosquito larvae (carrying both the wild-type and the *mimI* mutant) simulating infections given by IP injections with mixed cultures as described above and previously (Mutoji 2011). For each meal, mature mosquito larvae were allowed to graze for 24 hours on equal amounts of two different strains of *M. marinum*, diluted in PBS to an $O.D._{600}$ of 0.6. Fish were fed four meals over an interval of a week with five infected mosquito larvae per meal. An average colony count was generated for each meal for individual strains. Fish received the wild-type strain in concentrations of

$1.1x10^7$ cfu/meal I, $1.5x10^8$ cfu/meal II, $4.5x10^5$ cfu/meal III, and $1.5x10^7$ cfu/meal IV, for a total infective dose with the wild-type strain of $4.2x10^7$cfu. The mutant strain was delivered at concentration of $1.5x10^6$ cfu/meal I, $3.0x10^6$ cfu/meal II, $3.5x10^5$ cfu/meal III, and $1.6x10^6$ cfu/meal IV, resulting a total infective dose of $6.5x10^6$ cfu. The input ratio (mutant/wild-type) was calculated as 0.2 to 1, with an advantage to the wild-type strain. Fish mortality was monitored for six weeks after which the surviving animals were sacrificed. The liver and kidney were dissected from the five remaining fish and following homogenization were plated for colonies; both strains of bacteria were then scored on plates (Table 3.12). Comparative box plots of output colonization per unit input (in log scale) of mutant and wild-type for both liver and kidney are shown in Figure 3.26, which clearly shows that the median for colonization of wild-type is substantially higher than the *mimI* mutant for both liver and kidney. Competition indices were calculated for each organ, log transformed and plotted in (Figure 3.27) and since the CIs are all less than one, the data is in favor of the mutant strain being significantly less virulent. Statistical analysis was performed on the log of output colonization per unit input values for kidney and liver to determine if on an average the difference between mutant and wild-type were less than zero. Paired t-tests applied on the data showed that the average difference between colonization of mutant and wild-type are significantly less than zero with p-value 0.015 for livers and 0.457 for kidneys, indicating the wild-type strain is more infectious than the mutant strain. The data from this coinfection study through oral route followed the same trend as the results obtained from the IP injections using *mimI* mutant and wild-type strain. These results obtained from both oral and IP-infection experiments, it was evident that the extent of colonization by the mutant strain

was significantly less than the wild-type, indicating that the route of inoculation has no effect on the avirulence of the *mimI* mutant.

Fish #	Organ	*mimI* Mutant output cfu/organ	Wild-type output cfu/organ	Output Ratio (Mutant:Wild-type)	CI
1	LIVER	8.0×10^{4}	1.82×10^{6}	4.4×10^{-2}	2.2×10^{-1}
	KIDNEY	< 10	1.5×10^{5}	$< 6.8 \times 10^{-5}$	$<3.4 \times 10^{-4}$
2	LIVER	< 10	1.0×10^{5}	$< 1.0 \times 10^{-4}$	$<5.0 \times 10^{-4}$
	KIDNEY	8.0×10^{3}	2.0×10^{4}	4.0×10^{-1}	2.0
3	LIVER	< 10	1.6×10^{6}	$<6.4 \times 10^{-6}$	$<3.2 \times 10^{-5}$
	KIDNEY	< 10	9.4×10^{5}	$< 1.06 \times 10^{-5}$	$<5.3 \times 10^{-5}$
4	LIVER	4.60×10^{4}	1.5×10^{6}	3.01×10^{-2}	1.505×10^{-1}
	KIDNEY	3.0×10^{4}	2.2×10^{5}	1.25×10^{-1}	6.25×10^{-1}
5	LIVER	< 10	5.2×10^{5}	$< 1.91 \times 10^{-5}$	$<9.55 \times 10^{-5}$
	KIDNEY	< 10	1.0×10^{4}	$<7.14 \times 10^{-4}$	$<3.57 \times 10^{-3}$

Table 3.12 **Bacterial loads of co-infection experiment using *M. marinum* wild-type and *mimI* mutant**. Expressed here are the bacterial load in liver and kidney recovered from five fish co-infected (through ingestion) by *mimI* mutant (expressing no fluorescence) strain and wild-type *M. marinum* (expressing Hyg^{R} *rfp*) in a competition study. The input Ratio of mutant/wild-type was 0.2:1; accordingly, the output Ratio and CI values for liver and kidney of each individual fish were calculated and shown here. The cfu count of the wild-type strain from the organs ranged from 10^{4} to 10^{6} whereas, colonies of the mutant strain were below the detection level even at lowest dilutions in six out of ten organs, as such their values were considered to be less than ten.

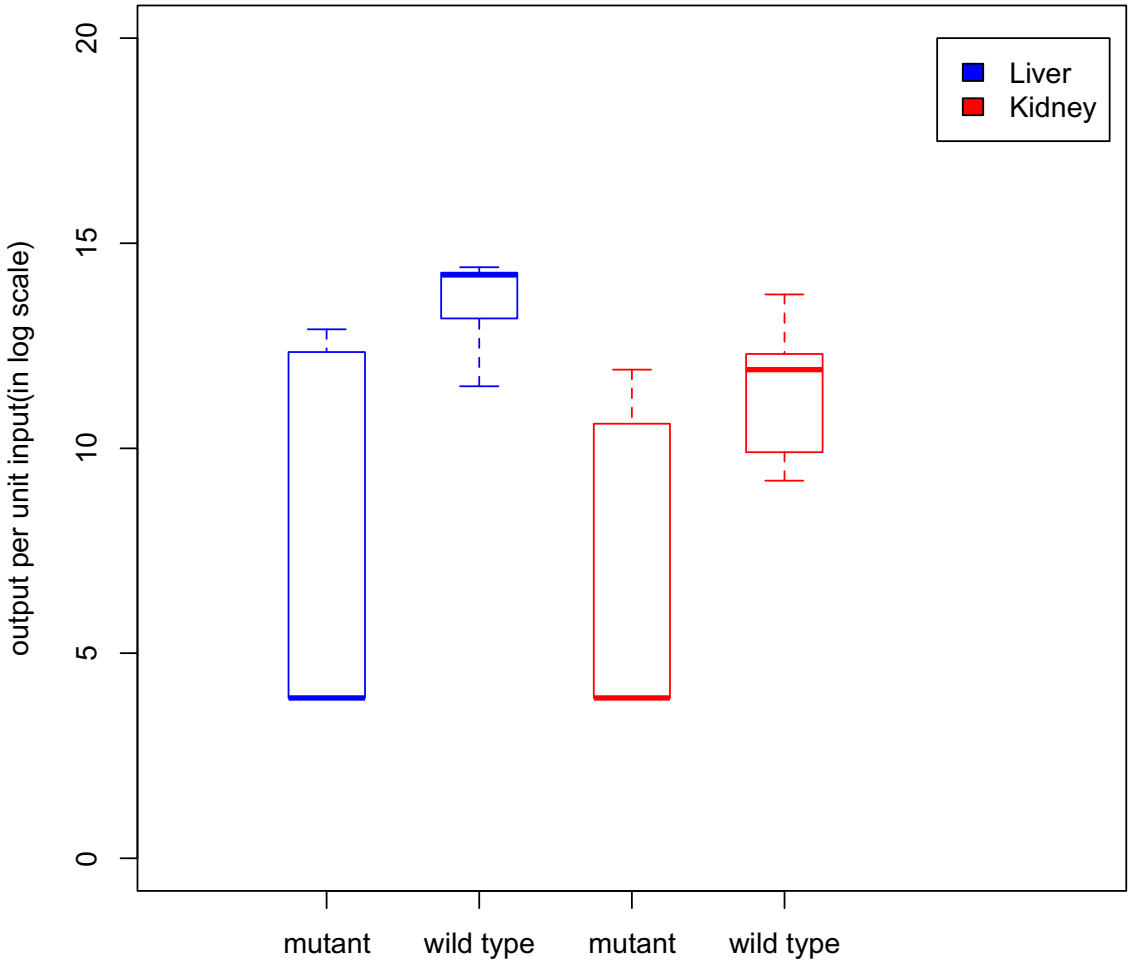

Figure 3.26 **The comparative box plot of output colonization per unit input (in log scale) of an oral co-infection experiment using *M. marinum* wild-type and *mimI* mutant**. Shown here are the minimum, first quartile, median (bar in bold), third quartile and the maximum. Log of output colonization per unit input is presented on the y-axis. In this experiment, for the mutant strain, no colonies were recovered from the organs at lowest dilution in six out of ten organs, as such their values were considered to be ten for the analysis. Through paired t-test for the above data, the p-values were determined to be 0.015 for liver and 0.457 for kidney.

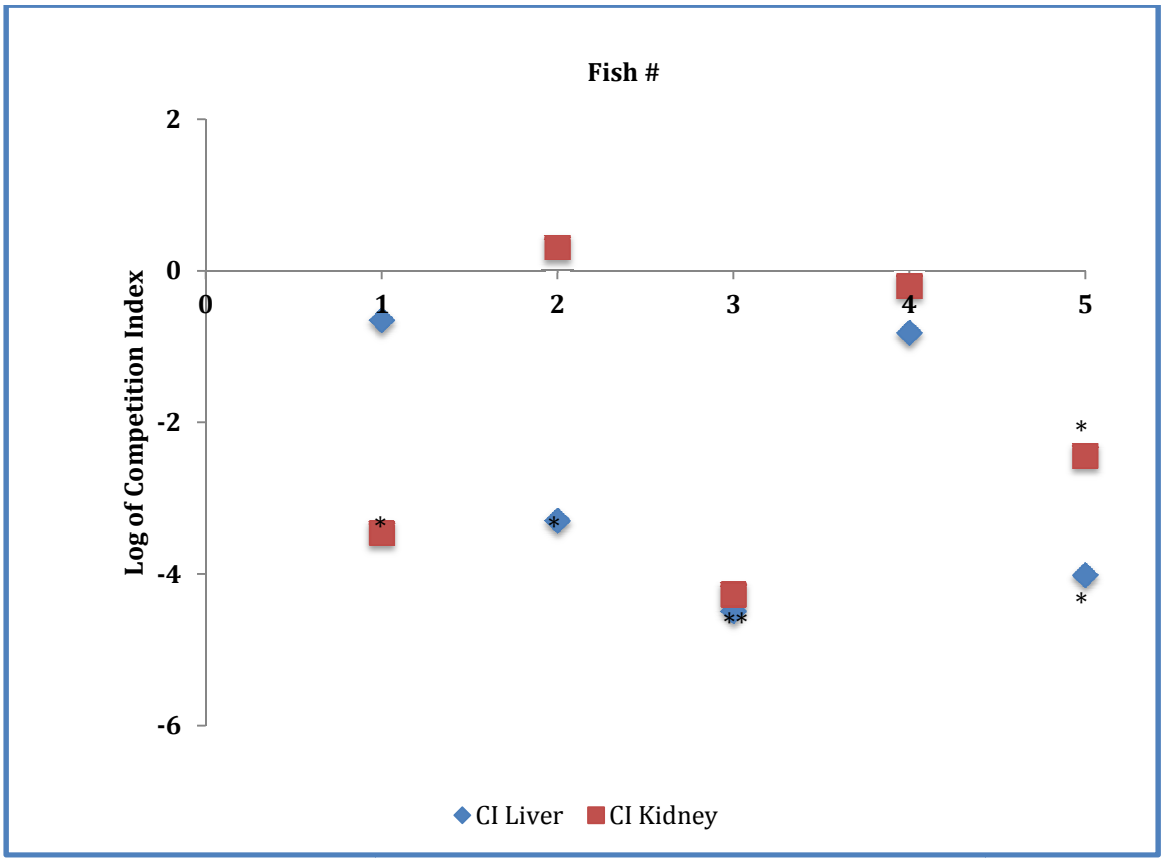

Figure 3.27 **Competition Index of individual organs in fish co-infected with *M. marinum* wild-type and *mimI* mutant.** Shown here are the log of CIs of liver and kidney of the five co-infected fish in the competition study using mutant and wild-type strain. Log of Competition Index is represented on y-axis, while and on x-axis is fish number from 1-5. CIs close to zero on log scale indicate equal colonization between the two strains. In almost all instances, the points are less than zero (in log scale) suggesting that the *mimI* mutant is deficient in establishing infections than the wild-type strain. * Indicates no colonies were recovered from the organs and the CIs were calculated using the mutant strain count to be less than ten.

3.3.2.2 *In vivo* Analysis of *M. marinum mimD* Mutant through Ingestion

This competition study aimed to investigate fitness of the *mimD* mutant strain in comparison to the wild-type parent bacteria when inoculated in equal ratio through oral route into fish. Ten seven-month old fish were inoculated with four meals of infected mosquito larvae (carrying mutant and wild-type strains) as was employed for study of *mimI*. Fish were fed four meals over an interval of a week with five infected mosquito larvae per meal. An average colony count was generated for each meal for individual strains. Fish received the wild-type strain in concentrations of $3.7x10^7$ cfu/meal I, $1.3x10^7$ cfu/meal II, $1.0x10^5$ cfu/meal III, and $5.6x10^6$ cfu/meal IV, for a total infective dose with the wild-type strain of $5.6x10^7$ cfu. The mutant strain was delivered at doses of $4.4x10^6$ cfu/meal I, $1.6x10^6$ cfu/meal II, $1.0x10^5$ cfu/meal III, and $7.2x10^5$ cfu/meal IV, for an accumulative infective dose of the mutant strain was $6.8x10^6$ cfu. The input ratio (mutant/wild-type) therefore, was calculated to be 0.1 to 1, with an advantage to the wild-type strain. Fish mortality was monitored for six weeks after which the surviving animals were sacrificed. The livers and kidneys were dissected from the surviving eight fish and plated for colonies and both strains of bacteria were scored on permissive plates (Table 3.13). Comparative box plots of output colonization per unit input of mutant and wild-type for both liver and kidney are shown in Figure 3.28; and it is clearly seen that the median of colonization for the wild-type strain is much greater than the *mimD* mutant in both organs. Competition indices were calculated for each organ, log transformed and plotted in (Figure 3.29). In almost all the cases for both organs, although the CI values are less than one, indicating that the wild-type strain is more infectious, supporting the idea that wild-type strain is more virulent. Statistical analysis was performed on the log of output colonization per unit input values for kidney and liver to determine if on

an average the difference between mutant and wild-type were less than zero. Paired t-tests applied on the data showed that the average difference between colonization of mutant and wild-type are significantly less than zero with p-value 0.0082 for livers and 0.01175 for kidneys, further bolstering the idea that wild-type strain was more infectious. By comparing the outcomes of *mimD* coinfection along with wild-type strain when introduced through different routes (oral and IP injection) into medaka, similar effects were seen. By both routes of infection, the *mimD* mutant conferred a modest defect in virulence when compared to wild-type.

Fish #	Organ	*mimD* Mutant cfu/organ	Wild-type output cfu/organ	Output Ratio (Mutant:Wild-type)	CI
1	LIVER	8.00×10^{1}	2.68×10^{3}	2.99×10^{-2}	2.99×10^{-1}
	KIDNEY	<10	8.40×10^{3}	$<1.19\times 10^{-3}$	$<1.19\times 10^{-2}$
2	LIVER	4.00×10^{1}	1.56×10^{3}	2.56×10^{-2}	2.56×10^{-1}
	KIDNEY	<10	1.16×10^{3}	$<8.62\times 10^{-3}$	$<8.63\times 10^{-2}$
3	LIVER	<10	6.96×10^{3}	$<1.44\times 10^{-3}$	$<1.44\times 10^{-2}$
	KIDNEY	<10	5.20×10^{3}	$<1.92\times 10^{-3}$	$<1.92\times 10^{-2}$
4	LIVER	<10	4.24×10^{3}	$<2.36\times 10^{-3}$	$<2.36\times 10^{-2}$
	KIDNEY	8.00×10^{1}	1.20×10^{3}	6.67×10^{-2}	6.67×10^{-1}
5	LIVER	<10	4.00×10^{3}	$<2.50\times 10^{-3}$	$<2.50\times 10^{-2}$
	KIDNEY	<10	2.48×10^{3}	$<4.03\times 10^{-3}$	$<4.03\times 10^{-2}$
6	LIVER	<10	1.20×10^{2}	$<8.33\times 10^{-2}$	$<8.33\times 10^{-1}$
	KIDNEY	4.00×10^{1}	1.20×10^{2}	3.33×10^{-1}	3.33
7	LIVER	<10	5.20×10^{3}	$<1.92\times 10^{-3}$	$<1.92\times 10^{-2}$
	KIDNEY	<10	3.60×10^{2}	$<2.78\times 10^{-2}$	$<2.78\times 10^{-1}$
8	LIVER	4.00×10^{2}	1.60×10^{5}	2.50×10^{-3}	2.50×10^{-2}
	KIDNEY	4.00×10^{1}	1.16×10^{3}	3.45×10^{-2}	3.45×10^{-1}

Table 3.13 **Bacterial loads of co-infection experiment using *M. marinum* wild-type and *mimD* mutant**. Expressed here is the bacterial load in liver and kidney recovered from eight fish co-infected (through ingestion) by *mimD* mutant (expressing no fluorescence) strain and wild-type *M. marinum* (expressing Hyg^{R} *rfp*) in a competition study. The input Ratio of mutant/wild-type was 0.1:1; accordingly, the output Ratio and CI values for liver and kidney of each individual fish were calculated and shown here. The cfu count of the wild-type strain from the organs ranged from 10^{2} to 10^{5} whereas, colonies of the mutant strain were below the detection level even at lowest dilutions in ten of the dissected organs, as such their values were considered to be less than ten.

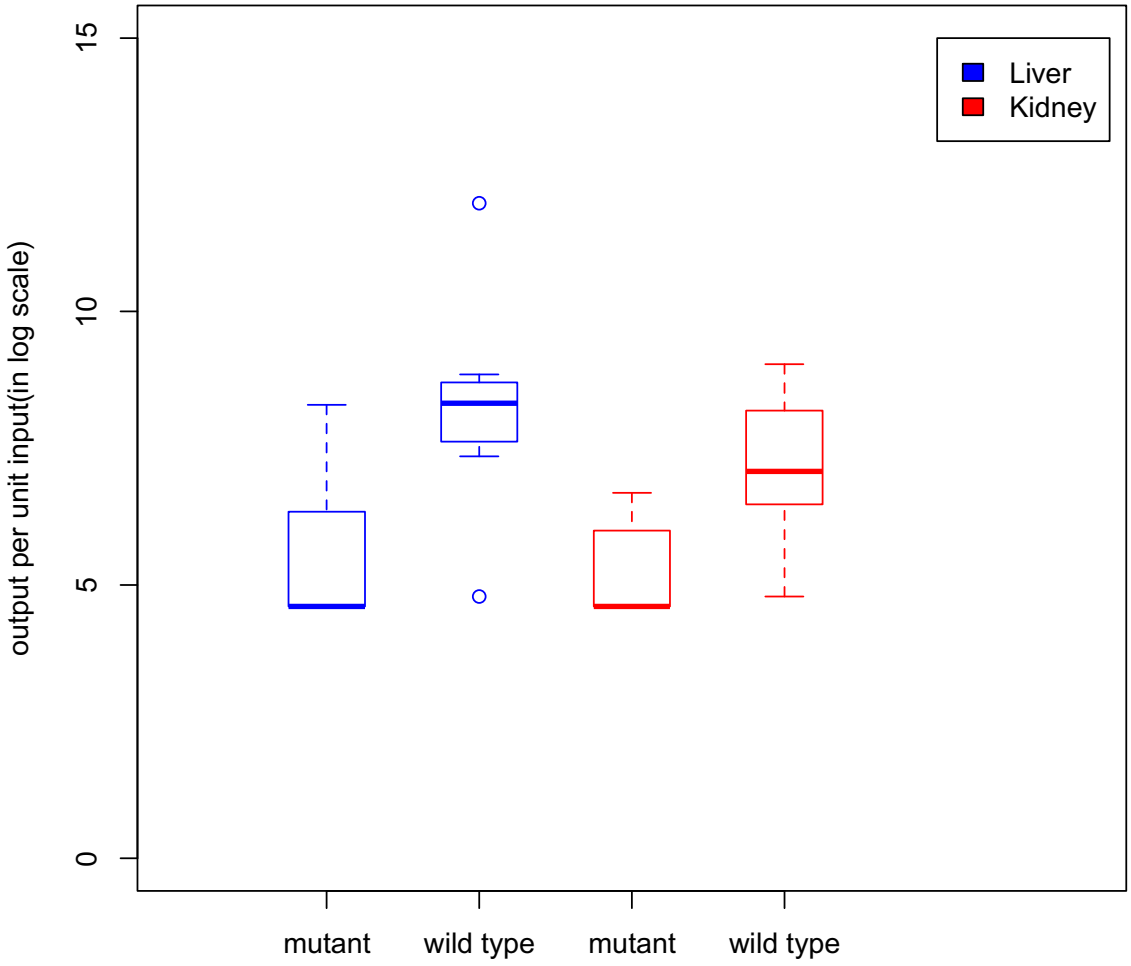

Figure 3.28 **The comparative box plot of output colonization per unit input (in log scale) of co-infection experiment using *M. marinum* wild-type and *mimD* mutant**. Shown here are the minimum, first quartile, median (bar in bold), third quartile and the maximum. The outliers (if present) are denoted by a dot. Log of output colonization per unit input is presented on the y-axis. In this experiment, for the mutant strain, no colonies were recovered from the organs at lowest dilution in ten out of sixteen organs, as such their values were considered to be ten for the analysis. Through paired t-test for the above data, the p-values were determined to be 0.0082 for liver and 0.01175 for kidney.

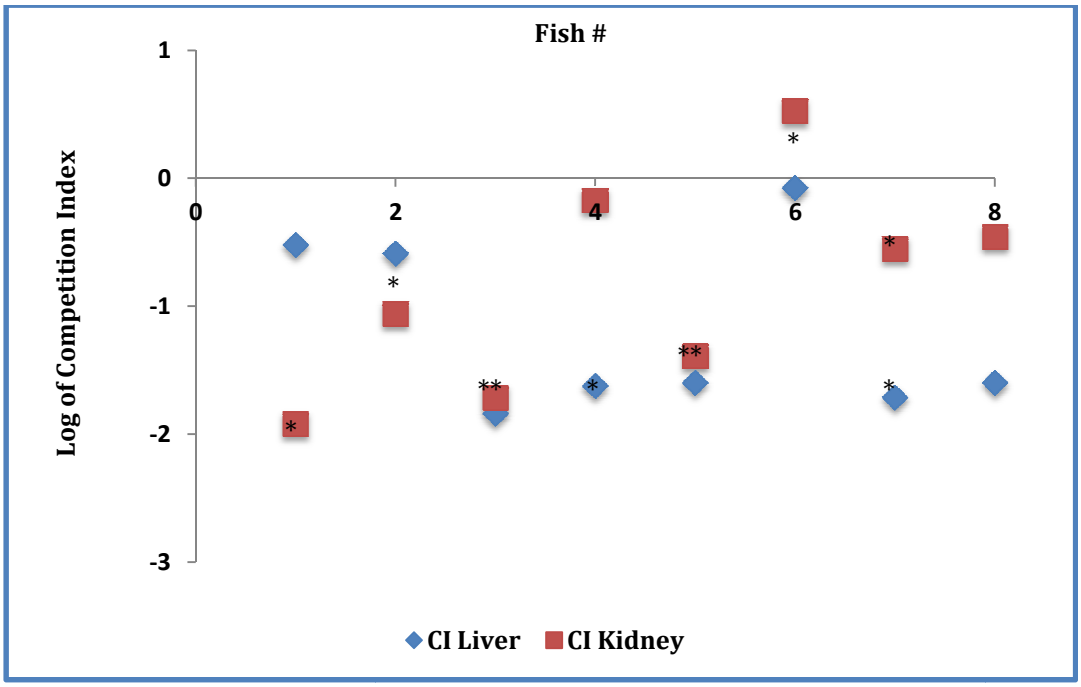

Figure 3.29 **Competition Index of individual organs in fish co-infected with *M. marinum* wild-type and *mimD* mutant.** Shown here are the log of CIs of liver and kidney of the eight co-infected fish in the competition study using mutant and wild-type strain. Log of Competition Index is represented on y-axis, while and on x-axis is fish number from 1-8. CIs close to zero on log scale indicate equal colonization between the two strains. In a rare instance, the point is greater than zero (in log scale) and in most; they are less than zero, suggesting that the *mimD* mutant has a reduced fitness compared to the wild-type strain in colonizing target organs for a particular fish. * Indicates no colonies were recovered from the organs and the CIs were calculated using the mutant strain count to be less than ten.

3.3.2.3 *In vivo* Analysis of *M. marinum mimH* Mutant through Ingestion

Ability of *mimH* to colonize the fish organ when infected through oral route was also evaluated using competition study. Ten seven-month old fish were inoculated with four meals of dually infected mosquito larvae (carrying both wild-type and *mimH* mutant strains) as described above. Fish were fed four meals over an interval of a week with five infected mosquito larvae per meal. An average colony count was determined for each meal for both strains. Fish received the wild-type strain in concentrations of $4.9x10^6$ cfu/meal I, $5.9 x10^6$ cfu/meal II, $5.0x10^5$ cfu/meal III, and $6.3x10^6$ cfu/meal IV, for a total infective dose with the wild-type strain of $1.7x10^7$ cfu. The mutant strain was delivered at concentrations of $7.0x10^5$ cfu/meal I, $1.1x10^6$ cfu/meal II, $3.5x10^5$ cfu/meal III, and $9.0x10^5$ cfu/meal IV, for a total infective dose with the mutant strain of $3.0x10^6$ cfu. The input ratio (mutant/wild-type) was calculated as 0.2 to 1, with an advantage to the wild-type strain. Fish mortality was monitored for six weeks after which the surviving animals were sacrificed. The livers and kidneys were dissected and homogenized from all the ten fish and plated on permissive plates, allowing detection of both differentially marked strains (Table 3.14). Comparative box plots of output colonization per unit input (in log scale) of mutant and wild-type for both liver and kidney are shown in Figure 3.30. It is evident from this plot that the *mimH* strain was seemingly more infectious than the wild-type strain in both liver and kidney; the median for colonization by the mutant strain was higher than the wild-type. Competition indices were calculated for each organ, log transformed and plotted in (Figure 3.31). Here the Log CI values for both the organs are more than zero in most cases suggesting fitness in favor of the *mimH* mutant strain as well. Statistical analysis was performed on the log of output colonization per unit input values for kidneys and livers to determine if on an average the

difference between mutant and wild-type were less than zero. Paired t-tests applied on the data comparing the average difference between colonization of mutant and wild-type yielded p-value of 0.9946 for liver and 0.994 for kidney (both p-values are greater than 0.05). These analyses suggest little or no significant difference between the colonization patterns of the wild-type and mutant strain in the infected organs and that the mutant strain is as infectious as the wild-type. These results by oral infection are in contrast to the data generated from IP infections of fish by the *mimH* mutant; in which case, *mimH* mutant was seen to be less virulent in mounting an infection compared to the wild-type (compare Figures 3.24 and 3.25). The CI values (ranging from 10^{-1} to 10^{4}), box plots (indicating that the median of colonization is much greater in wild-type strain) and p-value (0.0089 for livers and 0.00039 for kidneys) determined from the experiment further supported the idea that *mimH* is less infectious. As such, it is evident that the virulence of *mimH* mutant, (which was identified as defective in cell binding in *in vitro* studies) is influenced by the route adapted to inoculate the host. Surprisingly the *mimH* mutants were less infectious when introduced through oral feedings compared to IP injections. These data suggest that the *mimH* defect in macrophages binding is revealed in IP injections, but not by oral infections. We postulate that loss of the MimH protein does not block the crossing of the gut epithelia and its subsequent interactions with mucosal-associated phagocytes.

Fish #	Organ	*mimH* Mutant cfu/organ	Wild-type cfu/organ	Output Ratio (Mutant:Wild-type)	CI
1	LIVER	<10	1.20×10^{2}	8.33×10^{-2}	4.17×10^{-1}
	KIDNEY	2.80×10^{2}	3.72×10^{3}	7.53×10^{-2}	3.77×10^{-1}
2	LIVER	2.60×10^{4}	2.24×10^{4}	1.16	5.80
	KIDNEY	9.20×10^{2}	1.60×10^{2}	5.75	2.88×10^{1}
3	LIVER	8.00×10^{2}	4.00×10^{2}	2.00	1.00×10^{1}
	KIDNEY	1.60×10^{2}	3.60×10^{2}	4.44×10^{-1}	2.22
4	LIVER	8.00×10^{1}	8.00×10^{1}	1.00	5.00
	KIDNEY	1.20×10^{2}	1.20×10^{2}	1.00	5.00
5	LIVER	4.00×10^{1}	8.00×10^{1}	5.00×10^{-1}	2.50
	KIDNEY	2.40×10^{2}	6.00×10^{2}	4.00×10^{-1}	2.00
6	LIVER	3.60×10^{2}	3.60×10^{2}	1.00	5.00
	KIDNEY	1.80×10^{3}	4.76×10^{3}	3.78×10^{-1}	1.89
7	LIVER	5.44×10^{3}	7.24×10^{3}	7.51×10^{-1}	3.76
	KIDNEY	3.54×10^{4}	3.60×10^{2}	9.82×10^{1}	4.91×10^{2}
8	LIVER	1.60×10^{2}	2.80×10^{2}	5.71×10^{-1}	2.86
	KIDNEY	3.04×10^{3}	1.08×10^{3}	2.81	1.41×10^{1}
9	LIVER	4.00×10^{1}	2.00×10^{2}	2.00×10^{-1}	1.00
	KIDNEY	2.80×10^{2}	4.00×10^{1}	7.00	3.50×10^{1}
10	LIVER	4.00×10^{2}	1.80×10^{4}	2.22×10^{-2}	1.11×10^{-2}
	KIDNEY	3.20×10^{2}	3.60×10^{2}	8.89×10^{-1}	4.44

Table 3.14 **Bacterial loads of co-infection experiment using *M. marinum* wild-type and *mimH* mutant**. Expressed here is the bacterial load in liver and kidney recovered from ten fish co-infected by *mimH* mutant (expressing no fluorescence) strain and wild-type *M. marinum* (expressing Hyg^{R} *rfp*) in a competition study. The input Ratio of mutant/wild-type was 0.2:1; accordingly, the output Ratio and CI values for liver and kidney of each individual fish were calculated and shown here. The cfu count of the wild-type strain from the organs ranged from 10^{1} to 10^{4} and, colonies of the mutant strain also ranged from 10^{1} to 10^{4}, indicating colonization for both were comparable.

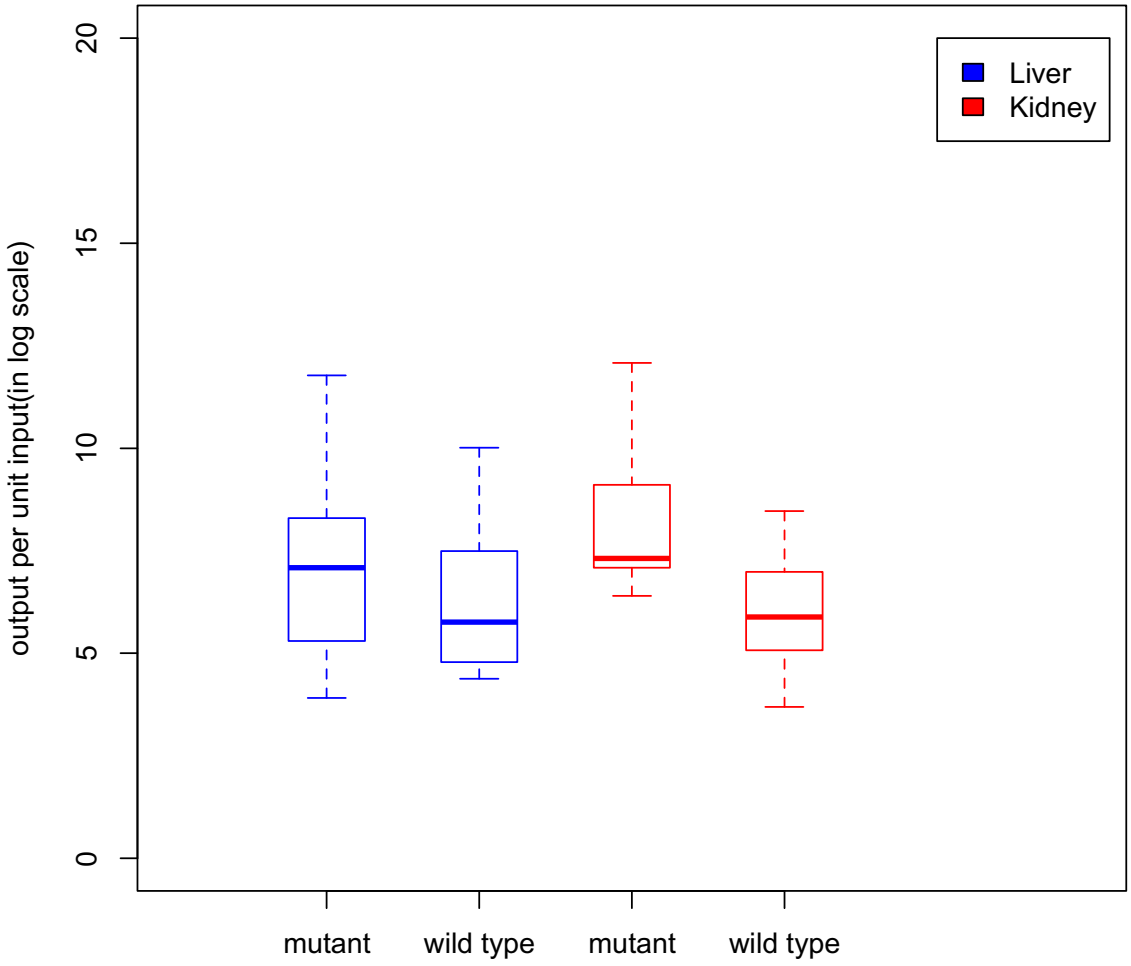

Figure 3.30 **The comparative box plot of output colonization per unit input (in log scale) of co-infection experiment using *M. marinum* wild-type and *mimH* mutant**. Shown here are the minimum, first quartile, median (bar in bold), third quartile and the maximum. Log of output colonization per unit input is presented on the y-axis. Through paired t-test for the above data, the p-values were determined to be 0.9946 for liver and 0.994 for kidney.

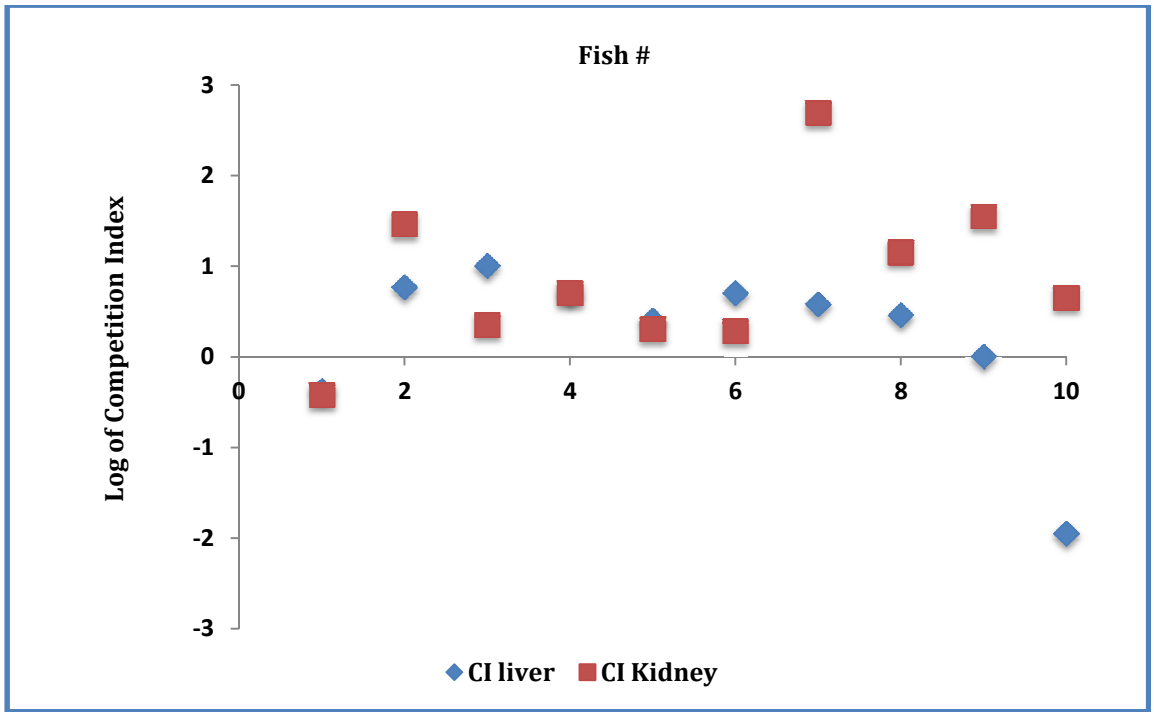

Figure 3.31 **Competition Index of individual organs in fish co-infected with *M. marinum* wild-type and *mimH* mutant.** Shown here are the log of CIs of liver and kidney of the ten co-infected fish in the competition study using mutant and wild-type strain. Log of Competition Index is represented on y-axis, while and on x-axis is fish number from 1-10. CIs close to zero on log scale indicate equal colonization between the two strains. Here, the points are distributed around zero (in log scale) suggesting that colonization for both strains appear to be similar, possibly *mimH* was slightly more efficient in establishing infections.

3.3.2.4 *In vivo* Analysis of *M. marinum* Δ*RD1* Mutant through Ingestion

The *ΔRD1* mutant engineered in *M. marinum* has been shown to be substantially attenuated in zebrafish experimental infections. The *RD1* chromosomal interval encodes a specialized secretion system for effector proteins ESAT-6 and CFP-10 that are well known virulence factors (Volkman et al. 2004). Here, we aimed to investigate the effect of this deletion mutant in a competition study in chronic medaka model when infected through oral route. Ten, seven-month old fish were inoculated with four meals of infected mosquito larvae (carrying both the *RD1* mutant and the wild-type) as employed above for other mutants. Fish were fed four meals over an interval of a week with five infected mosquito larvae per meal. An average colony count was calculated for each meal for individual strains. Fish received the wild-type strain in concentrations of $7.1x10^6$ cfu/meal I, $4.0x10^6$ cfu/meal II, $1.5x10^5$ cfu/meal III, and $5.6x10^6$ cfu/meal IV, for a total infective dose with the wild-type strain of $1.6x10^7$ cfu. The mutant strain was delivered at titres of $1.6x10^7$ cfu/meal I, $1.1x10^7$ cfu/meal II, $4.5x10^5$ cfu/meal III, and $1.0x10^7$ cfu/meal IV, for a total infective dose with the mutant strain of $3.9x10^7$ cfu. The input ratio (mutant/wild-type) was determined to be 2.3 to 1, with an advantage to the mutant strain. Fish mortality was monitored for six weeks after which the surviving animals were sacrificed. The livers and kidneys were dissected from the ten fish, then homogenized and plated for colonies for both strains of bacteria (Table 3.15). Comparative box plots of output colonization per unit input (in log scale) of mutant and wild-type for both liver and kidney are shown in Figure 3.32. Log of competition indices were calculated from the numbers of recovered bacteria in each organ as previously shown in Figure 3.33. These data indicates that the wild-type strain is substantially more infectious. Statistical analysis was performed on the log of output colonization per unit input values for

kidney and liver to determine if on an average the difference between mutant and wild-type were less than zero. Paired t-tests applied on the data showed that the average difference between colonization of mutant and wild-type are significantly less than zero with p-values less than 0.0015 for liver and 0.0021 for kidney, further supporting the conclusion that the mutant strain is much less infectious than the wild-type strain. Interestingly, although the CI values for the *ΔRD1* mutant are all below unity (Figure 3.33) as expected for this avirulent controls; however most CI values (15/20) are more than 10^{-2} by this oral route. We note that the CI values for other avirulent controls (for example, *iipA* and *Mh3868*) delivered by IP injections were far lower than observed here (Figures 3.15 and 3.17).

Fish #	Organ	ΔRD1 Mutant output cfu/organ	Wild-type output cfu/organ	Output Ratio (Mutant: Wild-type)	CI
1	LIVER	2.80×10^{3}	6.00×10^{3}	4.67×10^{-1}	2.03×10^{-1}
	KIDNEY	<10	1.08×10^{3}	$<9.26\times 10^{-3}$	$<4.03\times 10^{-3}$
2	LIVER	<10	3.92×10^{3}	$<2.55\times 10^{-3}$	$<1.11\times 10^{-3}$
	KIDNEY	<10	4.20×10^{3}	$<2.38\times 10^{-3}$	$<1.03\times 10^{-3}$
3	LIVER	<10	1.28×10^{6}	$<7.81\times 10^{-6}$	$<3.40\times 10^{-5}$
	KIDNEY	<10	1.92×10^{6}	$<5.21\times 10^{-6}$	$<2.27\times 10^{-6}$
4	LIVER	1.20×10^{2}	8.40×10^{2}	1.43×10^{-1}	6.22×10^{-2}
	KIDNEY	4.00×10^{1}	8.40×10^{2}	4.76E-02	2.07×10^{-2}
5	LIVER	8.00×10^{1}	4.80×10^{2}	1.67×10^{-1}	7.26×10^{-2}
	KIDNEY	5.00×10^{2}	1.70×10^{3}	2.94×10^{-1}	1.28E-01
6	LIVER	2.60×10^{2}	1.80×10^{3}	1.44×10^{-1}	6.26×10^{-2}
	KIDNEY	3.40×10^{2}	3.94×10^{3}	8.63E-02	3.75×10^{-2}
7	LIVER	6.80×10^{3}	6.48×10^{4}	1.05×10^{-1}	4.57×10^{-2}
	KIDNEY	3.60×10^{3}	1.08×10^{4}	3.33×10^{-1}	1.45×10^{-1}
8	LIVER	3.20×10^{3}	9.20×10^{3}	3.48×10^{-1}	1.51×10^{-1}
	KIDNEY	2.80×10^{3}	7.84×10^{4}	3.57E-02	1.55×10^{-2}
9	LIVER	8.00×10^{2}	8.80×10^{3}	9.09E-02	3.95×10^{-2}
	KIDNEY	2.52×10^{3}	8.40×10^{3}	3.00×10^{-1}	1.30×10^{-1}
10	LIVER	<10	3.92×10^{4}	2.55×10^{-4}	$<1.11\times 10^{-4}$
	KIDNEY	1.20×10^{2}	8.40×10^{2}	1.43×10^{-1}	6.22×10^{-2}

Table 3.15 **Bacterial loads of co-infection experiment using *M. marinum* wild-type and *ΔRD1* mutant**. Expressed here is the bacterial load in liver and kidney recovered from ten fish co-infected by ΔRD1 mutant (expressing no fluorescence) strain and wild-type *M. marinum* (expressing Hyg^{R} *rfp*) in a competition study. The input Ratio of mutant/wild-type was 2.3:1; accordingly, the output Ratio and CI values for liver and kidney of each individual fish were calculated and shown here. The cfu count of the wild-type strain from the organs ranged from 10^{2} to 10^{6} whereas, colonies of the mutant strain ranged from 10^{1} to 10^{3}, and in some cases they were below the detection level even at lowest dilutions, as such their values were considered to be less than ten.

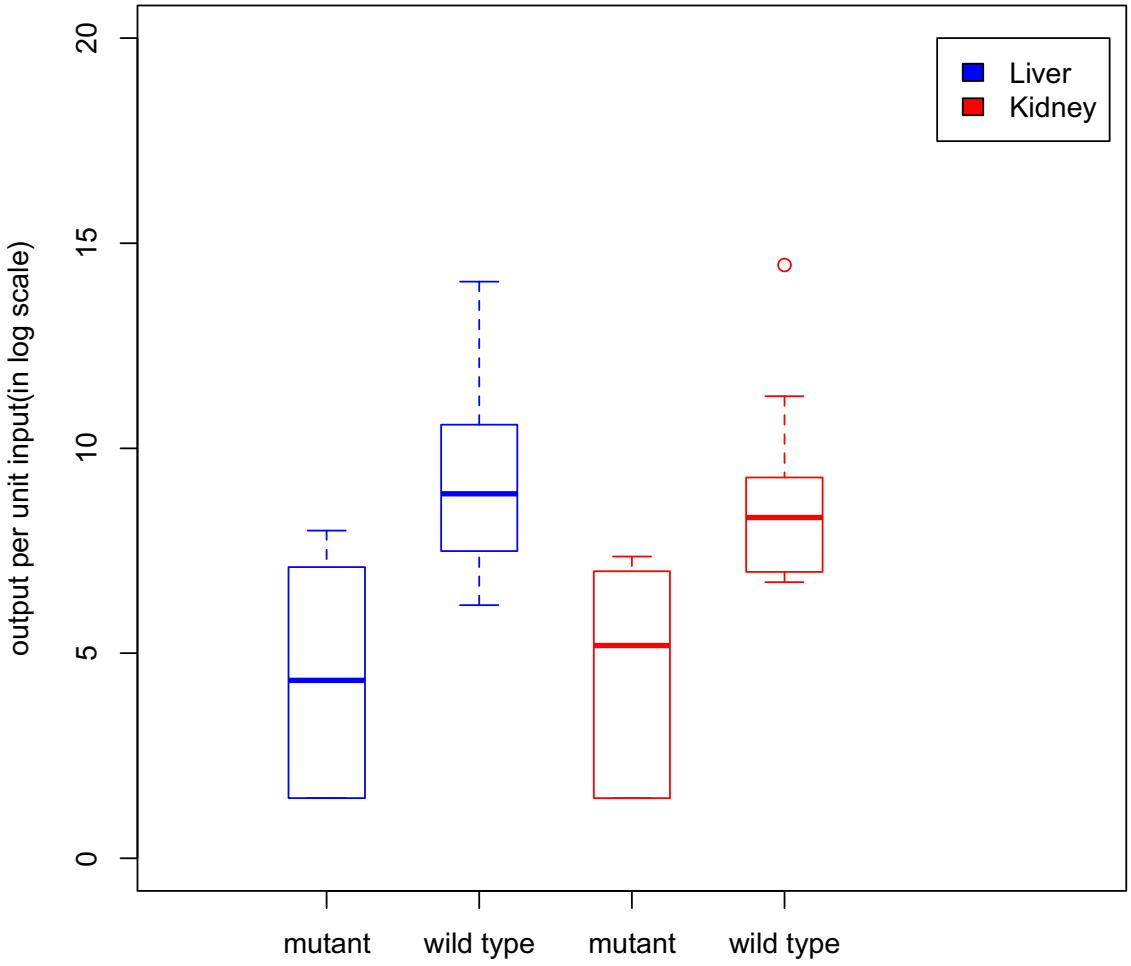

Figure 3.32 **The comparative box plot of output colonization per unit input (in log scale) of co-infection experiment using *M. marinum* wild-type and *ΔRD1* mutant**. Shown here are the minimum, first quartile, median (bar in bold), third quartile and the maximum. The outliers (if present) are denoted by a dot. Log of output colonization per unit input is presented on the y-axis. In this experiment, for the mutant strain, no colonies were recovered from six out of twenty organs at lowest dilution, as such their values were considered to be ten for the analysis. Through paired t-test for the above data, the p-values were determined to be 0.0015 for liver and 0.0021 for kidney.

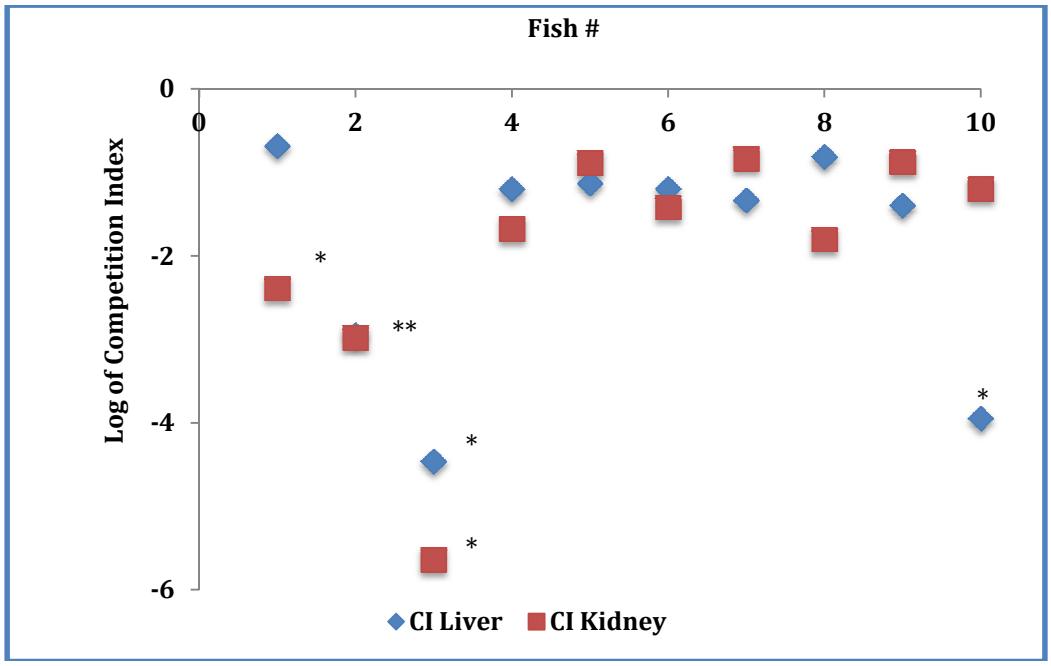

Figure 3.33 **Competition Index of individual organs in fish co-infected with *M. marinum* wild-type and *ΔRD1* mutant.** Shown here are the log of CIs of liver and kidney of the ten co-infected fish in the competition study using mutant and wild-type strain. Log of Competition Index is represented on y-axis, while and on x-axis is fish number from 1-10. CIs close to zero on log scale indicate equal colonization between the two strains. In all instances, the points are below zero (in log scale) suggesting that the *ΔRD1* mutant is deficient in establishing infections compared to the wild-type strain. * Indicates no *ΔRD1* mutant colonies were recovered from the organs and the CIs were calculated using the mutant strain count to be less than ten.

CHAPTER FOUR: Discussion

The global burden of TB (caused by *M.tuberculosis*) is enormous, with an approximately two billion people infected worldwide and is being exacerbated by factors like confluence of HIV epidemic and the emergence of multidrug resistant TB. TB is a socioeconomic burden for many countries, mostly targeting the poor and vulnerable populations. At present, the technologies available for diagnosis and prevention of TB are old and often prove to be inadequate. Treatment of TB is fairly successful against susceptible strains but is complicated due to prolonged and complex antibiotics regimen which are hard for many patients to comply with. Difficulties in treating TB is due in part by a small subpopulation of slowly growing bacteria, called 'persisters' who are refractory to months of antibiotic treatment. To date we lack a complete understanding about their physiological state or anatomical location of persisters within the host. Persisters exhibit a lack of sensitivity to drug perhaps in response to some altered physiological state, although they are genetically drug sensitive and hence the duration of therapy is extended to kill all of this persistent subpopulation. Using *M. tuberculosis* to study TB is a challenge as it has a slow generation time and requires BSL-3 containment. Also, *M. tuberculosis* is primarily a human pathogen, so studying TB in non-human hosts has its drawbacks. As such other closely related mycobacteria and surrogate model systems utilizing their natural hosts have been considered, *M. marinum* being one of them.

Mycobacteriosis in fish is most commonly caused by *M. marinum*, it is a major challenge for wild fish stocks, aquaculture and aquarium trade. According to recent studies, it infects more than 160 different species of fish, including some economically and recreationally significant species (Chinabut 1999; Jacobs et al. 2009). Even though there is a current scenario of

epizootic crisis, not much has been documented about its prevention and cure. Since many of the fish infections are chronic, the animals do not manifest symptoms of mycobacteriosis, such incidences go unnoticed. However, when individuals in a colony present active disease, the entire colony is typically called. Although there is mention of antibiotic treatment of aquatic animals by mixing the drugs with fish food or delivering directly into the water, unfortunately lack of employment standards and documented effective drug regimen is not available. Indeed very little peer-reviewed scientific literature is available that focuses on controlled drug delivery or its effectiveness for animals in aquatic setting.

Our lab has developed an experimental infection model for TB using medaka as the host for *M. marinum*, where both acute and chronic infections could be induced in a dose dependent manner. My intention was to treat the chronically infected fish by following several end points like monitoring survival of the fish and kinetics of reduction of bacterial burden in the target organs, to be able to establish an effective treatment regimen and finally target to study the physiological condition as well as location of the persisters. Attempts made by our research group to deliver antibiotics to the infected fish through oral gavage (by directly placing the antibiotic solution into the gut of the fish using a tiny hose through it mouth) was impractical and stressful for the animal; and by feeding the fish with food laced within drugs were unsuccessful (Broussard 2007; Mutoji et al. 2008; unpublished data). Moving onward, I wished to explore alternate drug delivery approaches to ensure a controlled and effective treatment regimen, hence considered approaches involving drug delivery vehicles such as microparticles and gelatin matrices.

Microparticles are FDA approved biodegradable polymers, made of polyanhydrides and has been promising for delivery of drugs, vaccine, protein and DNA (Ulery et al. 2009). These

polyanhydrides, copolymers of sebacic anhydride (SA) and 1,6-bis- (p-carboxyphenoxy) hexane (CPH) anhydride are composed of hydrophobic monomers connected by hydro-labile anhydride bonds, allowing its faster or controlled degradation and release of drugs thus, making it suitable for localized drug delivery. They are being used in clinical trails (Phase IV - post-marketing surveillance) for treatment of gliomas (brain cancer) as localized drug delivery agents (Jain et al. 2008). In mice models, polyanhydride microsphere encapsulated tetanus toxoid have successfully induced both primary and secondary immune response by its slow release and providing a prolong exposure to the toxoid (Kipper et al 2005). These and many more similar studies led us explore the potential use of microparticle polyanhydride to deliver antibiotics for the treatment of infected fish. For trial studies, FITC-dextran (a green fluorescent dye, florescein isothiocyanate) loaded microparticles were injected into the intraperitonial cavity of see-through medaka in order to study the distribution, interaction or kinetics of microparticles inside the fish. Initially minutes after injection, the microparticles were seen to be distributed throughout the intraperitonial cavity. We monitored the fish for three weeks post-injection or until the fish died, documenting the distribution of microparticles through fluorescent microscopy every week. These particles accumulated in the in their liver, were apparently toxic for the animal leading to their death (Figures 3.1 and 3.2). Therefore, unlike in the rodent models where microparticles have been used successfully for drug and vaccine delivery, in our fish system they were not neutral. Our results contributed to the awareness that the existing polymers are toxic to fish and alteration in their formulation would be required to render them more neutral for the fish system. Next, we attempted to orally deliver antibiotics embedded in gelatin matrix to minimize leaching of the drug in the surrounding water during administration. Gelatin has long been

used in the food and pharmaceutical industries as a gelling agent; it was my intent with the to use its gelling properties to 'hold' the drug inside its matrix for fish to consume and to minimize drug loss.

The antibiotic chosen and used for treatment of infected fish was frontline anti-TB antibiotic rifampin which is also effective against *M. marinum*, and acts by inhibiting bacterial transcription by binding strongly to the mycobacterial RNA polymerase forming a stable complex (Wherli 1983; Aubry et al. 2000). An additional benefit of considering rifampin as the antibiotic of choice is their intense orange colors that allowed its colorimetric quantification in aqueous solution and monitor the drug when needed.

I developed a recipe for treating the chronically infected fish with antibiotic rifampin incorporated into 13% gelatin along with other components like fish food and fish oil to make it palatable for the fish. The solidified beads were called "Jell-O shots" and used to feed infected medaka in order to treat them and different end-points like comparing infection burden in target organs and survival of the fish were monitored in the study. Fish injected with same dose of bacteria were divided into three groups. The first group that received benefit from rifampin (2 μg/day) in Jell-O shots starting day one post injection showed minimum mortality with 90 %survival even after five weeks. The second group fish that also received rifampin (2 μg/day) treatment, but starting day 14 post injection showed 50 %survival after five weeks, where as, the third group that did not get any treatment of antibiotics yielded 100 %mortality in five weeks (Figure 3.5). Therefore we concluded that administration of rifampin did have a beneficial effect on the survival of the infected fish, as decrease in mortality was evident among the rifampin treated fish compared to the ones that did not receive any treatment. Interestingly, the bacterial burdens from the infected fish in all

the three groups were surprisingly comparable. One possible explanation is that these fish carried a similar proportion of latent as actively growing bacteria and rifampin killed the growing bacteria and thus spared these animals from developing active disease.

Natural environments like soil and aquatic systems are ubiquitously inhabited by free-living protozoa, which consume large number of bacteria and offer intracellular niche to some species of pathogenic bacteria including mycobacteria. These protists offer a niche for mycobacterial survival, replication, distribution and most importantly protection against adversity (Barker et al. 1994; Adékambi et al. 2006; Tenant 2006). The intra-protozoal bacterial growth induces phenotypical changes in physiological status, survival and infectivity profile compared to that of strains grown *in vitro*. *M. avium* was shown to gain entry and survive successfully within its environmental host amoebas by inhibiting lysosomal fusion. These protozoan hosts also play a role in the selection of virulence traits, for example, *M. avium* once uptaken by *amoeba,* upregulates a number of genes and many of these genes are similar to the ones upregulated upon phagocytosis by macrophage (Barker et al. 1994; Greub et al. 2004; Harriff et al. 2009). Intra-amoebae grown *M. avium* displayed an enhanced invasion and intracellular replication in macrophage as well as increased virulence in and mouse infection models compared to bacteria grown in broth, possibly due to alteration in the expression of genes involved in these process (Cirrillo et al. 1997). *Dictyostelium discoideum,* a free-living unicellular soil amoebae have been shown to host many intracellular pathogens including *M. marinum,* and an *M. marinum* mutant attenuated for growth within macrophages was shown to be defective for growth within the amoeba in a comparable manner as well (Solomon et al. 2003).

In addition to amoeba, other small aquatic invertibrates such as mosquito larva are also known to feed on environmental mycobacteria; consequently, large quantities of algae, plankton and bacteria, like *M. marinum* and *M. ulcerans* accumulate in the gut of mosquito larvae. Mosquito larvae were implicated to play a role as primary and secondary consumers in natural route of human infection with *M. ulcerans* (Wallace et al. 2010). Similarly, previous studies in our lab also postulated that ingested *M. marinum* carried in mosquito larvae might serve as a natural vector for mycobacteriosis in fish as the fish naturally predate on mosquito larvae (Mutoji 2011; Ackleh et al. 2014). This larvae-vector notion was extensively investigated previously in our lab, using larvae from the yellow fever mosquito (*Aedes aegypti*) and medaka-*M. marinum* infection model. Mosquito larvae were shown to consume significant quantities of *M. marinum* from either biofilms or planktonic bacteria, essentially filling their entire gut with these bacteria overnight ($>10^4$ bacteria per larvae). When these *M. marinum*-laced larvae were fed to the fish, many of them presented "classic" fish mycobacteriosis in a dose dependent manner, with significant colonization of the host target organs and the appearance of granulomatous lesions carrying acid-fast rods (Mutoji 2011; Ackleh et al. 2014). Similar results were seen with *M. marinum* retrieved from infected tissues, when fish ingested tissues from other experimentally infected fish; most of them became infected by *M. marinum* and their organs were heavily colonized and some individuals developed acute mycobacteriosis and died (Mutoji 2011). In contrast, when fish fed with *M. marinum* that was grown in culture, then delivered orally in Jell-O shots rarely produced infections (Mutoji 2011). These observations reiterated the findings in the literature in other mycobacterial pathogens and led us to believe that passage through caustic environments such as mosquito larval gut or possibly phagocytic cell of the gut hemolymph

resulted in the induction of infectious potential of *M. marinum.* This activation of virulence is believed to result from the induction of a metabolic state primed for infection, where specific virulence gene sets are induced by the caustic environments within phagosomes and phagolysosome of professional phagocytes (Tenant et al. 2006; Harriff et al. 2008). Our lab has proposed that the caustic environments within the larval digestive tracts also serve to induce *M. marinum* virulence*,* probably into a similar activated metabolic state when residing in macrophages. Interestingly, similar level of enhanced virulence was observed when *M. marinum* was exposed to fluid obtained from mascerated larvae called 'mosquito larvae extracts' (MLE) prior to infection and orally fed to the fish. Because the gut is a prominent organ of larvae (approximately a half of the larval volume), we reasoned that gastric juices were a large component of MLE. The use of MLE to activate bacteria allowed for a larval-free system and more controlled experiments. Although, previous experiments in our lab (by Mutoji 2011; Root 2012) showed that fish inoculated orally with *M. marinum* incubated in MLE became infected at a much higher frequency than the fish inoculated with bacteria only exposed to PBS. But the extent of this increased virulence or the quantification of bacterial activation was not very well quantified. Also in question was if the MLE preconditioned bacteria were more infectious only by an oral route, or perhaps these bacteria were generally more infectious, by other routes as well. In order to address these issues, I designed an experiment using two differentially marked strains of wild-type *M. marinum* (one strain, expressing no fluorescence and the other expressing Kan^R *rfp*) in a competition infection study. The study was conducted in two ways, in order to eliminate potential strain bias, using two groups of IP injected fish and two groups of orally infected fish, where in one group, the *rfp*-marked strain was incubated in MLE and the other, the non-fluorescent strain was

incubated, mixed in equal ratios with the non treated strain and used to IP inject fish. Interestingly, the level of colonization of the *M. marinum* strain incubated with MLE was always seen to be higher in the fish organs, ranging up to almost 500 times in some cases, strongly suggesting that pre-conditioned bacteria are more infectious (Figures 3.6-3.9; Tables 3.4 and 3.5). We conclude that bacteria becomes activated for virulence following incubation with MLE and mount a more successful infection in the animals as compared to bacteria grown in culture. These results support the idea that preconditioning in MLE served to activate bacteria under caustic conditions. These results also indicate general increase in virulence of *M. marinum* in MLE is a phenotypic change that occurs regardless of the route of infection (for example, oral or IP).

Although properties of mosquito larvae extracts are largely unknown, but within mosquito larvae, larval infections by bacteria are known to act as a stress that elicits cellular and other innate responses along with some stress- responsive molecules like heat shock proteins and ubiquitin-63. Phagocytes are considered to be extremely important in mosquito immune response against invading pathogens, mosquito larvae have professional phagocytic hemocytes, such as granulocytes, quite similar to the macrophages and neutrophils found in higher animals (Hillyer et al. 2002; Castillo et al. 2006; Strand 2008). Immune response-challenged hemocytes up-regulate production of caustic anti-microbial peptides like defensins, cecropins, and lysozyme; that have broad spectrum activity against Gram-positive microbes. In addition, another hemocyte-mediated immune response, melanin biosynthesis, involves cytotoxic enzymes like prophenoloxidase and phenylalanine hydroxylase. In summary, there would appear to be numerous potential germicidal effector proteins in hemolymph of *Aedes aegypti*, potentially enough to induce stress response and hence,

virulence factors of *M. marinum*, comparable to when the bacteria become activated inside of the hostile environment of fish or human macrophages. The multitude of potential components present in mosquito larvae extracts have the capability to change the behavior of *M. marinum*, creating a more virulent phenotype, which has been observed in these experiments.

Mycobacteria principally grow within the phagocytic vacuoles of vertebrate macrophages during animal infections. Intra-phagosomal environment exposes the pathogenic mycobacteria to a drop in pH along with a variety of other stressful conditions like reactive oxygen and nitrogen species, a change in nutrient availability (Cook et al. 2009). *M. tuberculosis* also encounters acidic phagolysosomal content of activated macrophages that are released in inflamed lesions (Tan et al. 2010). Mycobacteria can sense the pH of their environment and exhibit intracellular pH homeostasis over a large range of external pH values in order for enzymes and proteins to function normally (Rao et al. 2001). Exposure to an acidic external pH was shown to cause differential expression of a large number of genes in *M. tuberculosis* (Fisher et al. 2002; Kim et al. 2008). An acid sensitive *M. tuberculosis* mutant was also attenuated for growth in human macrophages, suggesting that the bacteria's response to acidic conditions is important for virulence in the host cells (Piddington et al. 2000). Studies have shown that *M. avium* survives the extreme acidic condition of the mammalian gastrointestinal tract naturally and this increased acid resistance could be due to pre-adaptation in similar conditions in their environmental niche (Bodmer et al. 2000). However, mosquito larvae gut harbors an alkaline pH (as great as pH 10) (Dadd 1975; Boudko et al. 2001) and larval gut extracts are presumably basic in nature.

Equipped with these insights, I wanted to assess if prior exposure to either higher or lower pH conditions would activate virulence of the *M. marinum* in a similar manner as mosquito larvae extracts in fish infections. In other words, I was curious to discover if the alteration of pH alone is the key factor in intact larvae or MLE that is responsible for activating the virulence and increasing the frequency of infection by preconditioning the bacteria for encountering the phagolysosome of macrophages in the Japanese medaka. In these studies, competition experiments were employed, using differentially marked strains of bacteria that were pre-incubated in either low (pH 5) or high (pH 9) pH prior to infecting medaka though IP injection. The data obtained from these experiments surprisingly indicated a small decline in virulence for bacteria preincubated in pH 9 (Figures 3.10 and 3.12) and pH 5 (Figures 3.11 and 3.13). The colonization level of pre-treated (in acidic or basic pH) bacteria were slightly less than the un-treated ones. We suggest that there was no enhanced virulence due to exposures in higher or lower pH; instead these exposures likely reduced fitness of the bacteria in mounting infections. Hence, the pH factor alone of the mosquito larvae gut or MLE is apparently not playing this role in inducing the bacterial virulence like we anticipated.

A major emphasis of this dissertation was to investigate the roles of different *M. marinum* mutants in establishing infection. We again exploited our chronic infection model using medaka and *M. marinum* (Broussard et al. 2007). The chronically-infected medaka are indistinguishable from the uninfected fish, typically not presenting any external signs of disease; but progressive granuloma formation in the organs such as liver and kidney can be observed, as well as bacteria could be retrieved from plating of dissected and homogenized organs (Broussard et al. 2007; Mutoji 2011). In experiments described here, I tried to explore the effect of both established as well as less characterized mutants on virulence in medaka by

studying different end-points like survival of the fish and the level of bacterial colonization in target organs following IP injection. An important aspect of any competition studies described here for mutant analysis is that, individual fish were inoculated through IP injection with essentially equal doses of both wild-type and mutant strains being investigated, then monitored for the duration of the experiment and finally sacrificed to obtain colony counts in organs for both strains to score a CI (Competition Index) ratio. The data obtained from each competition study were analyzed statistically through box plots and paired t-test (the bacterial count for both the strains were expressed as colonization of output per unit input) to further strengthen the conclusions. The well-known mutant strains were first employed to establish a baseline allowing comparison of their relative fitness with novel mutants**.** Moreover, most of these better-characterized mutants have been studied using the acute *M. marinum*–zebrafish model previously. Unlike zebrafish, the chronic medaka model produce latent TB infections as seen in human TB and allows for monitoring the colonization of organs for a longer period of time. The mutant genes considered here are highly conserved and are functionally interchangeable between *M. marinum* and *M. tuberculosis* so the outcome of the studies focuses on their role in *M. tuberculosis* virulence and allows insight into chronic human tuberculosis pathogenesis (Gao et al. 2004; El –Etr et al. 2004; Gao et al. 2006; Mehta et al. 2006).

Mutant analysis indicates that the *iipA* gene product of *M. marinum* is required for both invasion and intracellular survival in macrophages; invasion and growth in macrophages are key virulence properties for pathogenic mycobacteria (Gao et al. 2006). Zebrafish infection with *iipA* mutant was highly attenuated as judged by not a single mortality during a period of 16 weeks as well as very poor colonization of organs. In contrast infection with the wild-type

strain showed 100% mortality within 3 to 5 weeks. Both defects of the *iipA* strain, macrophage infection and virulence to zebra fish, could be completely complemented by *M. tuberculosis* homolog Rv1477 (Gao et al. 2006). Although, structural or functional elucidation of *iipA* has not been achieved, but it has a C-terminal NLPC_p60 domain that is conserved through a variety of bacterial lineages and resemblances with murein hydrolases, that cleave peptide linkages within peptidoglycan (Gao et al. 2006). In addition, this mutant is also exhibits decreased cording, and decreased resistance to antibiotics and to lysozyme; all of which are hypothesized to be due to lack of this peptidoglycanase activity, one of the factors required for virulence (Gao et al. 2006).

In the competition experiment I performed infections through IP injections using both wild-type and *iipA* mutant strains in medaka, which showed that the mutant was significantly (nearly 40,000 fold less for liver and 100,000 fold less for kidney by comparing the median in the box plot) less infectious than the wild-type strain (Figures 3.14 and 3.15). Also the mutant strain could be detected from any of the organs even at the lowest dilutions, indicated that the mutants had been cleared; where as the wild-type strain was detected in most animals (Table 3.6). These results are consistent with the findings in the zebrafish model, but using medaka eliminated the complications of the host succumbing. Through a competition approach, we were able to see the difference in colonization level of the two strains in the same animal. Thus, we conclude that *iipA* mutant is also attenuated for chronic infection in medaka. In other words, we provide evidence that *iipA* gene; previously shown to be essential for *M. marinum* invasion and intracellular persistence in macrophages and acute infections in zebrafish but is also integral for chronic infections in medaka.

The insertion mutant (*Mh3868*::*Kan*) of *M. marinum* has a disruption in the gene homologous to *Rv3868* of *M. tuberculosis* that is in the extended RD1 region (*Rv3871– Rv3879c*), a documented virulence gene cluster, absent from the genome of the less virulent BCG vaccine strain of *M. bovis* (Gao et al. 2004). The *Mh3868::Kan* mutant was isolated based on its diminished *in vitro* haemolytic activity, a characteristic of pathogenic mycobacteria that is associated with virulence in *M. tuberculosis* as well as in *M. marinum.* The *Mh3868* mutant was also shown to be incompetent in intracellular release of important mycobacterial excreted virulence factors such as, ESAT-6 and CFP-10 (Gao et al. 2004). Recently *Mh3868* encoded protein has been shown to be an ATPase with a co-factor-induced "open-close" movement and probably interact with other factors of ESAT-6 secretion system to provide energy for the export of the ESAT-6 and CFP-10 virulence factors, but does not have a known general chaperone-like function as predicted before (Luthra et al. 2008). Compared to wild-type *M. marinum*, *Mh3868* mutant was also extremely defective in cytolysis, cytotoxicity, spreading in macrophage and epithelial cell monolayers *in vitro* as well as virulence *in vivo*. Zebrafish infection by the *Mh3868* mutant with the same dose as wild-type strain resulted in longer survival with granulomas containing fewer mycobacteria. Disruptions in the *Mh3868* or some of the surrounding genes in the extended *RD1* gene cluster have also showed similar deficiencies that could be complemented by *M. tuberculosis* homologues (Gao et al. 2004).

In the competition experiment using *Mh3868* and wild-type strain in medaka showed that this mutant is greatly attenuated for infection in terms of colonization of the organs, as has been observed in the zebrafish and adult frog model (Figures 3.16, 3.17 and Table 3.7). The CI values obtained from the liver and kidney of IP-infected fish were highly in favor of the wild-

type strain and statistical analysis also supported the fact that the *Mh3868* mutant was significantly less infectious for both kidney and liver as compared to the wild-type strain. Therefore, we suggest that secretion of functional virulence factors ESAT-6 and CFP-10 are extremely essential in medaka infection as well. Over the years, similar results have been observed in all cases of mycobacterial infection; for example, in mice model, *M. tuberculosis esat*-6 and *cfp*-10 mutants were shown to be highly attenuated for virulence (Hsu et al. 2003). Although the exact role of ESAT-6 and CFP-10 in mycobacterial virulence at the molecular and cellular level has not yet been elucidated but more recently its been known that ESAT-6 induces MMP9 secretion in epithelial cells adjacent to sites of infection and there by signals enhanced apoptosis of infected macrophages, recruiting new macrophages at the site of nascent granuloma to aid in its expansion and dissemination of the pathogen (Volkman et al. 2010). Moreover, we also documented that the bacterial count of the *Mh3868* mutant strain could be detected from only four organs as opposed to wild-type strain detected from all twenty (Table 3.7).

The *melF* (Mycobacterial Enhanced Infection Locus *F*) mutant of *M. marinum* is less well characterized, but was shown to be defective in its ability to infect both fish and murine macrophages in *in vitro* studies. This defect was shown to be complemented by the homolog (*Rv1936*) from *M. tuberculosis*, thus confirming the genes are functional orthologs (El –Etr et al. 2004). It was an interesting fact that the *melF* locus was present only in *M. marinum* and *M. tuberculosis* complex and absent in many other mycobacteria, indicating its significance in pathogenesis. MelF resembles with other bacterial proteins with known biochemical functions (oxidoreductases) related to fatty acid or polyketide biosynthesis, but little is

known about its exact structure and role in virulence (El –Etr et al. 2004). However, *in vivo* effects of *melF* had not been studied previously.

M. marinum–medaka infection with *melF* mutant and wild-type strains by IP-injections here have clearly documented the important role of *melF* in pathogenesis *in vivo*. The extents of organ colonization are significantly in favor of the wild-type strain as shown by CI ratio and by statistical analysis (Figures 3.18, 3.19 and Table 3.8).

We have also investigated the role of three additional novel macrophage infection mutants (mim) following IP-injections; *mimI*, *mimD* and *mimH* of *M. marinum* that were previously shown to be defective in *in vitro* studies using murine macrophages, but their role in virulence had not been tested in any of the animal model (Mehta et al. 2006). Of these mutants, *mimH* showed diminished cell association or binding ability *in vitro*, but once the bacteria was taken up was taken up (in low numbers compared to the wild-type), it survived inside the macrophage to the level comparable to the wild-type. On the other hand, *mimD* was able to bind to macrophages in the same way as the wild-type but in contrast, its ability to survive inside the macrophage was significantly less. Both attachment to the macrophage and survival inside was substantially compromised for *mimI* mutant. *M. tuberculosis* homologue of *mimI*, *Rv1502* (with an average of more than 70% amino acid similarity) successfully complemented the defect indicating conserved structure and function between both pathogens. These mutants did not appear to grow any differently from the wild-type in laboratory media suggesting that these mutant defects are specific for growth in association with macrophages.

Mycobacteria needs to infect, survive and replicate within macrophages which is an important aspect of the disease pathogenesis, but we do not have absolute or comprehensive knowledge of the molecular mechanisms or genes involved in the mycobacterial interactions with macrophages. This is also evident from the fact that the *mim* mutants carry mutations in genes that have not been previously described. In the research presented here, we show evidence of *in vivo* effects of these three *mim* mutants for the first time.

Of the eight surviving fish coinfected by IPs with equal doses of the *mimI* mutant and the wild-type strain we saw a substantial difference in the colonization level ranging from a hundred to a million times between the two, implying *mimI* mutant is severely attenuated for infection in the fish (Figures 3.20, 3.21 and Table 3.9). Only four out of sixteen organs were culture positive for *mimI* mutant where as all sixteen of the dissected organs had high burdens of the wild-type strain. The reduced fitness of *mimI* mutant was also statistically significant. The *in vivo* avirulence of *mimI* is expected as the loss of *mimI* function is associated with reduced attachment to and survival inside the macrophage. These results show that survival and replication inside the host macrophages is also important for pathogenesis in vivo that involves multiple factors including *mimI*.

The *mimD* mutant that was shown to be defective in its ability to survive inside murine macrophages in *in-vitro* studies, reduced virulence was observed in medaka infections, but not as severe as *mimI*. Data received from seven coinfected fish by IP-injection, showed that the wild-type strain was around ten to hundred fold more infectious than the mutant, and *mimD* could not be detected in the organs of only one fish (Figures 3.22, 3.23 and Table 3.10). We suggest that over all, *mimD* mutant is only mildly avirulent in medaka infection, which was somewhat surprising since survival inside the macrophages is important for

virulence. It is possible that the mutant detected in the organs were mostly surviving in extracellular niche but the question about their dissemination to different organs may have been retained as macrophage play an important role in the transport of mycobacteria to other anatomical locations.

Bacterial loads obtained from the seven surviving co-infected fish with *M. marinum* wild-type and *mimH* mutant revealed that the wild-type strain was always present in all the infected organs examined, whereas, colonies of the mutant strain were below the detection level in eleven out of fourteen dissected organs. The magnitude of competition indices ranged up to ten thousand times between the two indicating that the *mimH* is significantly less virulent which was further supported by statistical analysis (Figures 3.24, 3.25 and Table 3.11). This was expected as *mimH* showed diminished cell association or binding ability in *in vitro* studies.

Advancing further, we wanted to test the fitness of these *mim* mutants by introducing them into the fish through a different more natural portal, an oral route of infection, and compare the results described above using IP injection. We wished to test if these mutants would also confer similar defect in mounting an infection if they did not have the advantage of being invasively introduced into the fish intraperitoneal cavity where immune system cells reside. Although IP injection has always been a well controlled and successful method for infection in medaka and other vertebrates, it's also very invasive for the animal and is not a natural route. Studies involving transmission of mycobacteriosis in our lab revealed a natural mode of infection includes the oral route (Mutoji 2011). A well investigated oral route for fish infection with two different strains involved incubating mosquito larvae in equal mixtures of two bacterial strains and then feed five infected larvae as a single meal to medaka. Four such

larval feedings, stretched out in a week time, were given to each fish to establish chronic infections. As mentioned in the previous sections, passage of bacteria through mosquito larvae gut greatly enhanced *M. marinum* virulence.

Coinfection through oral route with *mimI* mutant and the wild-type strain showed that the wild-type strain was much better suited at colonizing the organs than the mutant strain and these results were judged to be statistically significant. For the wild-type strain, all the ten organs examined were culture positive, but no mutant bacteria were detected by colony counts on the plates for six of these organs (6/10). The extent of colonization of the wild-type strain was always at least ten to hundred thousand folds greater than the mutant (Figures 3.26, 3.27 and Table 3.12). The outcome of oral infections is quite comparable to the result obtained from experiments using IP infections, where the disparity of colonization between the wild-type strain and the mutant was also around ten to hundred thousand folds in favor of the wild-type. On average, the CI data for liver and kidney in the IP infection showed that wild-type bacteria predominated over the mutant as observed in oral infection and the extent of reduced fitness were comparable (Figures 3.20, 3.21, 3.26, 3.27; Table 3.10 and 3.12). These results are in contrast to previous preliminary studies where the *mimI* mutant was judged to be as competent as the wild-type strain in oral infection (Root 2012). Of the eight organs that were culture positive for *M. marinum*, four organs (kidney) showed significantly higher colonization for the wild-type strain and four (liver) exhibited more colonies of the mutant strain (Root 2012).

The *mimD* mutant was seen to be less avirulent in the oral coinfection (than *mimI*). Only five out of sixteen infected organs were culture-positive for the mutant and the wild-type strain outnumbered the mutant strain in all the sixteen infected organs dissected from eight fish but

interestingly, the magnitude of difference is only ten to hundred folds, but judged to be statistically significant (Figures 3.28, 3.29 and Table 3.13). These results very closely mimicked the results obtained from IP infections, the CI values indicate that the wild-type bacteria were also ten to hundred folds better suited to mount infections in all but two out of fourteen organs. In two of these, the wild-type were hundred thousand times more infectious and the mutants were undetected. On an average CI of liver and kidney were also very comparable in both the routes of infections (Figures 3.22, 3.23, 3.28, 3.29; Table 3.10 and 3.13).

Interestingly, the *mimH* mutant was not avirulent in medaka infection through an oral route. The level of colonization of the two strains was comparable following ingest of infected larvae. Of the twenty infected organs obtained from ten fish, eleven organs showed higher colonization for the wild-type strain and nine exhibited more colonies of the mutant strain (Figures 3.30, 3.31 and Table 3.14). On an average, the mutant showed better colonization for both the target organs. Statistical analysis also suggested no significant difference between the colonization patterns of the wild-type and mutant strain and that the *mimH* mutant strain was as infectious as the wild-type. These observations were in contrast to data obtained from IP infection (Figures 3.24, 3.25 and Table 3.11), where the wild-type strain was up to ten thousand times more infectious than the mutant.

In conclusion, we present here results comparing the effects on virulence of the three novel *mim* mutants of *M. marinum*; *mimI*, *mimD* and *mimH* using medaka model by two different routes. We compared their relative virulence by either IP or oral routes of infection. The *mimI* mutant was the most attenuated mutant of the three, followed by *mimD*. Depending on the mutant strain of *M. marinum* used in these competition studies, the similarities between

outcomes of IP injection and oral infections varied. In case of both *mimI* and *mimD* there was no clear difference observed for oral or IP routes of infection, since the average CIs for the infected organs were comparable. However for *mimH* this was not the case, in IP infected fish, wild-type *M. marinum* showed higher colonization than the mutant bacteria in all the organs, in contrast in orally infected fish, both wild-type and mutant strains were present, but the *mimH* mutant in greater abundance.

It is possible that the two modes of infection are different enough to result in non-synonymous colonization due to immune responses located within the gastro-intestinal tract and the peritoneal cavity. Clearly, the bacteria in orally infected fish must cross the gut epithelia to colonize the target organs. The mucosal surfaces of gut have GI associated lymphoid tissue (GALT). Little is known of fish immune systems and even less is known of the GALT system of the digestive tract in teleost fish. In general, M (microfold) cells of GALT samples and takes up pathogens from the lumen, then passes it to the closely associated macrophages, which then process the antigens and elicit the production of CTLs (cytotoxic T cells) and antibodies (IgA) by the B cells. IgAs are transported from basal surfaces to the apical region and released in the lumen. In other studied pathogens crossing the epithelia is achieved by using the GALT system as a portal. We hypothesisze that perhaps *M. marinum* in oral infection also exploits the GALT system to gain entry across the gut epithelia and; passage though the M cell makes *mimH* mutant overcome its loss of *mimH* function and become more infectious. Additionally, IP injected bacteria were not at all activated before inoculation. Perhaps ingestion by live mosquito larvae could influence the pattern by which each strain of bacteria infects the organs of the host.

Finally we made efforts to shed some light into the poorly characterized *mim* genes (especially *mimI*, since it conferred the greatest attenuation) by in-silico analyses in hopes of gaining insights into their function. The *mimI* sequence of *M. marinum* is 909 bp long, with a Locus tag of MMAR_2318. Unfortunately, blast analysis of the gene did not identify any obvious established homolog, structurally nor functionally, at either nucleotide or amino acid level, which hindered predictions of *mimI* structure or function. The protein structure derived from the predicted amino acid sequence of *mimI*, revealed a few putative secretion signals and some repeats that are common to almost all sugar-binding homologs. Although the primary MimI protein has some internal repeats in its sequence, none of these repeats corresponded to other known motifs. The *M. tuberculosis* homolog of *mimI* is *Rv1502*, also codes for a hypothetical protein, which has been annotated as a possible glycosylase. The known secretion signals in mycobacteria are absent in MimI protein, but a 5-bladed beta-propeller domain was predicted for MimI amino acid sequence that consists of five 4-stranded beta-sheet motifs belonging to arabinase superfamily. These motifs in some better-characterized proteins are sugar binding protein. The structure and function of both *mimH* and *mimD* also could not be readily predicated through in-silico analysis of these predicted proteins since well-characterized homologues were not available.

Through studies described here, we provide valuable resource towards characterizing new genes and thus, proteins important to pathogenesis. It is understood that there are virulence mechanisms that are unique to mycobacteria due to presence of these genes, which have no obvious homologs outside of mycobacteria like that of the Mims. The molecular mechanisms of mycobacterial pathogenicity are still not elucidated entirely so the information obtained

from such physiological study of mutants are critical to attain complete understanding of *M. tuberculosis* genome for developing new antitubercular drugs and diagnostic tools.

References

Ackleh, A. S., K. L. Sutton, K. N. Mutoji, A. Mallick, and D. G. Ennis. 2014. A structured model for the transmission dynamics of *Mycobacterium Marinum* between aquatic animals. J. Biol. Syst. **22:**29-60.

Adams, K. N., K. Takaki, L. E. Connolly, H. Wiedenhoft, K. Winglee, O. Humbert, P. H. Edelstein, C. L. Cosma, and L. Ramakrishnan. 2011. Drug tolerance in replicating mycobacteria mediated by a macrophage-induced efflux mechanism. Cell. **145:**39-53.

Adékambi, T., S. Ben Salah, M. Khlif, D. Raoult, and M. Drancourt. 2006. Survival of environmental mycobacteria in *Acanthamoeba polyphaga*. Appl. Environ. Microbiol. **72:**5974-5981.

Alderman, D. J., and T.S. Hastings. 1998. Antibiotic Use in Aquaculture: Development of Resistance - Potential for Consumer Health Risks. Int. J. of Food Sci. Tech. **33:**139-155.

Almeida Da Silva, P. E., and J. C. Palomino. 2011. Molecular basis and mechanisms of drug resistance in *Mycobacterium tuberculosis*: classical and new drugs. J. Antimicrob. Chemother. **66:**1417-1430.

Andersen, P., and T. M. Doherty. 2005. The success and failure of BCG - implications for a novel tuberculosis vaccine. Nat. Rev. Microbiol. **3:**656-662.

Aubry, A., V. Jarlier, S. Escolano, C. Truffot-Pernot, and E. Cambau. 2000. Antibiotic susceptibility pattern of *Mycobacterium marinum*. Antimicrob. Agents. Chemother. **44:**3133-3136.

Bardouniotis, E., H. Ceri, and M. E. Olson. 2003. Biofilm formation and biocide susceptibility testing of *Mycobacterium fortuitum* and *Mycobacterium marinum*. Curr. Microbiol. **46:**28-32.

Barker, J., and M. R. Brown. 1994. Trojan horses of the microbial world: protozoa and the survival of bacterial pathogens in the environment. Microbiology. **140:**1253-1259.

Bartholomay, L. C., W. L. Cho, T. A. Rocheleau, J. P. Boyle, E. T. Beck, J. F. Fuchs, P. Liss, M. Rusch, K. M. Butler, R. C. Wu, S. P. Lin, H. Y. Kuo, I. Y. Tsao, C. Y. Huang, T. T. Liu, K. J. Hsiao, S. F. Tsai, U. C. Yang, A. J. Nappi, N. T. Perna, C. C. Chen, and B. M. Christensen. 2004. Description of the transcriptomes of immune response-activated hemocytes from the mosquito vectors *Aedes aegypti* and *Armigeres subalbatus*. Infect. Immun. **72:**4114-4126.

Benbrook, B. M. 2002. Antibiotic Drug Use in U.S. Aquaculture. The Northwest Science and Environmental Policy Center Sandpoint, Idaho.

Biron, D. G., P. Agnew, L. Marché, L. Renault, C. Sidobre, and Y. Michalakis. 2005. Proteome of *Aedes aegypti* larvae in response to infection by the intracellular parasite *Vavraia culicis*. Int. J. Parasitol. **35:**1385-1397.

Bodmer, T., E. Miltner, and L. E. Bermudez. 2000. *Mycobacterium avium* resists exposure to the acidic conditions of the stomach. FEMS Microbiol. Lett. **182:**45-49.

Bolin, C. A., D. L. Whipple, K. V. Khanna, J. M. Risdahl, P. K. Peterson, and T. W. Molitor. 1997. Infection of swine with *Mycobacterium bovis* as a model of human tuberculosis. J. Infect. Dis. **176:**1559-1566.

Boudko, D. Y., L. L. Moroz, P. J. Linser, J. R. Trimarchi, P. J. Smith, and W. R. Harvey. 2001. In situ analysis of pH gradients in mosquito larvae using non-invasive, self-referencing, pH-sensitive microelectrodes. J. Exp. Biol. **204:**691-699.

Bouley, D. M., N. Ghori, K. L. Mercer, S. Falkow, and L. Ramakrishnan. 2001. Dynamic nature of host-pathogen interactions in *Mycobacterium marinum* granulomas. Infect. Immun. **69:**7820-7831.

Brosch, R., S. V. Gordon, M. Marmiesse, P. Brodin, C. Buchrieser, K. Eiglmeier, T. Garnier, C. Gutierrez, G. Hewinson, K. Kremer, L. M. Parsons, A. S. Pym, S. Samper, D. van Soolingen, and S. T. Cole. 2002. A new evolutionary scenario for the *Mycobacterium tuberculosis* complex. Proc. Natl. Acad. Sci. USA **99:**3684-3689.

Broussard, G. W. 2007. Development and application of medaka and *Mycobacterium marinum* as an infection model for human tuberculosis. Ph. D. Dissertation, University of Louisiana at Lafayette, Lafayette, LA.

Broussard, G. W., and D. G. Ennis. 2007. *Mycobacterium marinum* produces long-term chronic infections in medaka: a new animal model for studying human tuberculosis. Comp. Biochem. Physiol. C. Toxicol. Pharmacol. **145:**45-54.

Cabello, F. C., H. P. Godfrey, A. Tomova, L. Ivanova, H. Dölz, A. Millanao, and A. H. Buschmann. 2013. Antimicrobial use in aquaculture re-examined: its relevance to antimicrobial resistance and to animal and human health. Environ. Microbiol. **15:**1917-1942.

Castillo, J. C., A. E. Robertson, and M. R. Strand. 2006. Characterization of hemocytes from the mosquitoes *Anopheles gambiae* and *Aedes aegypti*. Insect Biochem. Mol. Biol. **36:**891-903.

Centers for Disease Control and Prevention (CDC). 2006. Emergence of Mycobacterium tuberculosis with extensive resistance to second-line drugs--worldwide, 2000-2004. MMWR. Morb. Mortal. Wkly. Rep. **55:**301-305.

Chemtob, D., and J. Merrick. 2010. Preventing and treating tuberculosis and HIV/AIDS: A worldwide public health challenge. International Public Health Journal. **2:**265-267.

Chinabut, S. 1999. Mycobacteriosis and nocardiosis. Fish diseases and disorders: Viral, Bacterial and Fungal Infections. **3:**319-340. CAB International, Wellington.

Cirillo, J. D., S. Falkow, L. S. Tompkins, and L. E. Bermudez. 1997. Interaction of Mycobacterium avium with environmental amoebae enhances virulence. Infect. Immun. **65:**3759-3767.

Clark, H. F., and C. C. Shepard. 1963. Effect of environmental temperatures on infection with *Mycobacterium marinum* (balnei) of mice and a number of poikilothermic species. J. Bacteriol. **86:**1057-1069.

Cole, S. T. 2002. Comparative and functional genomics of the *Mycobacterium tuberculosis* complex. Microbiology **148:**2919-2928.

Collins, C. H., J. M. Grange, and M. D. Yates. 1984. Mycobacteria in water. J. Appl. Bacteriol. **57:**193-211.

Comas, I., M. Coscolla, T. Luo, S. Borrell, K. E. Holt, M. Kato-Maeda, J. Parkhill, B. Malla, S. Berg, G. Thwaites, D. Yeboah-Manu, G. Bothamley, J. Mei, L. Wei, S. Bentley, S. R. Harris, S. Niemann, R. Diel, A. Aseffa, Q. Gao, D. Young, and S. Gagneux. 2013. Out-of-Africa migration and Neolithic coexpansion of *Mycobacterium tuberculosis* with modern humans. Nat. Genet. **45:**1176-1182.

Converse, P. J., A. M. Dannenberg Jr., J. E. Estep, K. Sugisaki, Y. Abe, B. H. Schofield, and M. L. Pitt. 1996. Cavitary tuberculosis produced in rabbits by aerosolized virulent tubercle bacilli. Infect. Immun. **64:**4776-4787.

Corena, M., T. J. Seron, H. K. Lehman, J. D. Ochrietor, A. Kohn, C. Tu, and P. J. Linser. 2002. Carbonic anhydrase in the midgut of larval *Aedes aegypti*: cloning, localization and inhibition. J. Exp. Biol. **205:**591-602.

Cousins, D. V. 2001. *Mycobacterium bovis* infection and control in domestic livestock. Rev. Sci. Tech. **20:**71-85.

Dadd, R. H. 1975. Alkalinity within the midgut of mosquito larvae with alkaline-active digestive enzymes. J. Insect Physiol. **21:**1847-1853.

Daniel, T. M. 2006. The history of tuberculosis. Respir. Med. **100:**1862-1870.

Daniels, M. 1949. Tuberculosis in Europe During and After the Second World War.-II. Br. Med. J. **2:**1135-1140.

Dannenberg, A. M. 1994. Rabbit model of tuberculosis. In B. R. Bloom (ed.), Tuberculosis: pathogenesis, protection, and control. ASM Press: 149-156.

Davis, J. M., and L. Ramakrishnan. 2009. The role of the granuloma in expansion and dissemination of early tuberculous infection. Cell. **136:**37-49.

Deretic, V., S. Singh, S. Master, J. Harris, E. Roberts, G. Kyei, A. Davis, S. de Haro, J. Naylor, H. H. Lee, and I. Vergne. 2006. *Mycobacterium tuberculosis* inhibition of phagolysosome biogenesis and autophagy as a host defence mechanism. Cell. Microbiol. **8:**719-727.

Drolet, G. J. 1945. World War I and Tuberculosis. A Statistical Summary and Review. Am. J. Public Health Nation's Health. **35:**689-697.

Floss, H. G., and T. W. Yu. 2005. Rifamycin-mode of action, resistance, and biosynthesis. Chem. Rev. **105:**621-632.

Gagneux, S., K. DeRiemer, T. Van, M. Kato-Maeda, B. C. de Jong, S. Narayanan, M. Nicol, S. Niemann, K. Kremer, M. C. Gutierrez, M. Hilty, P. C. Hopewell, and P. M. Small. 2006. Variable host-pathogen compatibility in *Mycobacterium tuberculosis*. Proc. Natl. Acad. Sci. USA **103:**2869-2873.

Gao, L. Y., M. Pak, R. Kish, K. Kajihara, and E. J. Brown. 2006. A mycobacterial operon essential for virulence in vivo and invasion and intracellular persistence in macrophages. Infect. Immun. **74:**1557-1567.

Garnier, T., K. Eiglmeier, J. C. Camus, N. Medina, H. Mansoor, M. Pryor, S. Duthoy, S. Grondin, C. Lacroix, C. Monsempe, S. Simon, B. Harris, R. Atkin, J. Doggett, R. Mayes, L. Keating, P. R. Wheeler, J. Parkhill, B. G. Barrell, S. T. Cole, S. V. Gordon, and R. G. Hewinson. 2003. The complete genome sequence of *Mycobacterium bovis*. Proc. Natl. Acad. Sci. USA **100:**7877-7882.

Goude, R., A. G. Amin, D. Chatterjee, and T. Parish. 2009. The arabinosyltransferase EmbC is inhibited by ethambutol in *Mycobacterium tuberculosis*. Antimicrob. Agents. Chemother. **53:**4138-4146.

Greub, G., and D. Raoult. 2004. Microorganisms resistant to free-living amoebae. Clin. Microbiol. Rev. **17:**413-433.

Gusmão, D. S., A. V. Santos, D. C. Marini, S. Russo Ede, A. M. Peixoto, M. Bacci Júnior, M. A. Berbert-Molina, and F. J. Lemos. 2007. First isolation of microorganisms from the gut diverticulum of *Aedes aegypti* (Diptera: Culicidae): new perspectives for an insect-bacteria association. Mem. Inst. Oswaldo Cruz. **102:**919-924.

Gutierrez, M. C., S. Brisse, R. Brosch, M. Fabre, B. Omaïs, M. Marmiesse, P. Supply, and V. Vincent. Ancient origin and gene mosaicism of the progenitor of *Mycobacterium tuberculosis*. PLoS Pathog. **1:**55-61.

Hagedorn, M., and T. Soldati. 2007. Flotillin and RacH modulate the intracellular immunity of Dictyostelium to *Mycobacterium marinum* infection. Cell. Microbiol. **9:**2716-2733.

Harries, A. D., C. Dye. 2006. Tuberculosis. Ann. Trop. Med. Parasitol. **100:**415-431.

Harriff, M., and L. E. Bermudez. 2009. Environmental amoebae and mycobacterial pathogenesis. Methods Mol. Biol. **465:**433-442.

Hayman, J. 1984. *Mycobacterium ulcerans*: an infection from Jurassic time? Lancet **2:**1015-1016.

Hillyer, J. F., and B. M. Christensen. 2002. Characterization of hemocytes from the yellow fever mosquito, *Aedes aegypti*. Histochem. Cell Biol. **117:**431-440.

Hsu, T., S. M. Hingley-Wilson, B. Chen, M. Chen, A. Z. Dai, P. M. Morin, C. B. Marks, J. Padiyar, C. Goulding, M. Gingery, D. Eisenberg, R. G. Russell, S. C. Derrick, F. M. Collins, S. L. Morris, C. H. King, and W. R. Jacobs Jr. 2003. The primary mechanism of attenuation of bacillus Calmette-Guerin is a loss of secreted lytic function required for invasion of lung interstitial tissue. Proc. Natl. Acad. Sci. USA. **100:**12420-12425.

Imaeda, T. 1985. Deoxyribonucleic acid relatedness among selected strains of *Mycobacterium tuberculosis*, *Mycobacterium bovis*, *Mycobacterium bovis* BCG, *Mycobacterium microti*, and *Mycobacterium africanum*. Int. J. Syst. Bacteriol. **35:**147–150.

Jain S. K., G. Lamichhane, S. Nimmagadda, M. G. Pomper, and W. R. Bishai. 2008. Antibiotic Treatment of Tuberculosis: Old Problems, New Solutions. Microbe. **3:**285-292.

Jain, A., and R. Mondal. 2008. Extensively drug-resistant tuberculosis: current challenges and threats. FEMS Immunol. Med. Microbiol. **53:**145-150.

Jain, J. P., D. Chitkara, and N. Kumar. 2008. Polyanhydrides as localized drug delivery carrier: an update. Expert. Opin. Drug. Deliv. **5:**889-907.

Kaattari, I. M., M. W. Rhodes, S. L. Kaattari, and E. B. Shotts. 2006. The evolutionary story of *Mycobacterium tuberculosis* clade members detected in fish. J. Fish Dis. **29:**509-520.

Kipper, M. J., J. H. Wilson, M. J. Wannemuehler, and B. Narasimhan. 2006. Single dose vaccine based on biodegradable polyanhydride microspheres can modulate immune response mechanism. J. Biomed. Mater. Res. A. **76:**798-810.

Koeck, J. L., M. Fabre, F. Simon, M. Daffé, E. Garnotel, A. B. Matan, P. Gérôme, J. J. Bernatas, Y. Buisson, and C. Pourcel. 2011. Clinical characteristics of the smooth tubercle bacilli *'Mycobacterium canettii*' infection suggest the existence of an environmental reservoir. Clin. Microbiol. Infect. **17:**1013-1019.

Laurenzi, M., A. Ginsberg, and M. Spigelman. 2007. Challenges associated with current and future TB treatment. Infect. Disord. Drug. Targets. **7:**105-119.

Leoni, E., P. Legnani, M. T. Mucci, and R. Pirani. 1999. Prevalence of mycobacteria in a swimming pool environment. J. Appl. Microbiol. **87:**683-688.

Lewis, K. N., R. Liao, K. M. Guinn, M. J. Hickey, S. Smith, M. A. Behr, and D. R. Sherman. 2003. Deletion of RD1 from *Mycobacterium tuberculosis* mimics bacille Calmette-Guérin attenuation. J. Infect. Dis. **187:**117-123.

LoBue, P. A., D. A. Enarson, and C. O. Thoen. 2010. Tuberculosis in humans and animals: an overview. Int. J. Tuberc. Lung. Dis. **14:**1075-1078.

Luthra, A., A. Mahmood, A. Arora, and R. Ramachandran. 2008. Characterization of Rv3868, an essential hypothetical protein of the ESX-1 secretion system in *Mycobacterium tuberculosis*. J. Biol. Chem. **283:**36532-36541.

McMurray, D. N.1994. Guinea pig model of tuberculosis. In B. R. Bloom (ed.), Tuberculosis: pathogenesis, protection, and control. ASM Press: 135-148.

Mehta, P. K., A. K. Pandey, S. Subbian, S. H. El-Etr, S. L. Cirillo, M. M. Samrakandi, and J. D. Cirillo. 2006. Identification of *Mycobacterium marinum* macrophage infection mutants. Microb. Pathog. **40:**139-151.

Merritt, R. W., E. D. Walker, P. L. Small, J. R. Wallace, P. D. Johnson, M. E. Benbow, and D. A. Boakye. 2010. Ecology and transmission of Buruli ulcer disease: a systematic review. PLoS Negl. Trop. Dis. **4:**e911.

Mostowy, S., J. Inwald, S. Gordon, C. Martin, R. Warren, K. Kremer, D. Cousins, and M. A. Behr. 2005. Revisiting the evolution of *Mycobacterium bovis*. J. Bacteriol. **187:**6386-6395.

Mukherjee, J. S., M. L. Rich, A. R. Socci, J. K. Joseph, F. A. Virú, S. S. Shin, J. J. Furin, M. C. Becerra, D. J. Barry, J. Y. Kim, J. Bayona, P. Farmer, M. C. Smith Fawzi, and K. J. Seung. 2004. Programmes and principles in treatment of multidrug-resistant tuberculosis. Lancet **363:**474-481.

Mutoji, K. N. 2011. Investigation into mechanisms of mycobacterial transmission between fish. Ph. D. Dissertation, University of Louisiana at Lafayette, Lafayette, LA.

Nerlich, A. G., C. J. Haas, A. Zink, U. Szeimies, and H.G. Hagedorn. 1997. Molecular evidence for tuberculosis in an ancient Egyptian mummy. Lancet **350:**1404.

Ottenhoff, T. H., and S. H. Kaufmann. 2012. Vaccines against tuberculosis: where are we and where do we need to go? PLoS. Pathog. **8:**e1002607.

Ottinger, C. A., and J. M. Jacobs. 2006. USGS/NOAA Workshop on Mycobacteriosis in Striped Bass. Annapolis, MD.

Peterson T. S., J.A. Furguson, V. G. Watral, K. N. Mutoji, D. G. Ennis, M. L. Kent. 2013. *Paramecium caudatum* enhances transmission and infectivity of *Mycobacterium marinum* and *M. chelonae* in zebrafish *Danio rerio*. Dis Aquat Organ **106(3):**229-239**.**

Philips, J. A., and J. D. Ernst. 2012. Tuberculosis pathogenesis and immunity. Annu. Rev. Pathol. **7:**353-384.

Prouty, M. G., N. E. Correa, L. P. Barker, P. Jagadeeswaran, and K. E. Klose. 2003. Zebrafish-*Mycobacterium marinum* model for mycobacterial pathogenesis. FEMS Microbiol. Lett. **225:**177-182.

Ramakrishnan, L. 2004. Using *Mycobacterium marinum* and its hosts to study tuberculosis. Current Science **86:**82-92.

Ramakrishnan, L. 2012. Revisiting the role of the granuloma in tuberculosis. Nat. Rev. Immunol. **12:**352-366.

Ramakrishnan, L., R. H. Valdivia, J. H. McKerrow, and S. Falkow. 1997. *Mycobacterium marinum* causes both long-term subclinical infection and acute disease in the leopard frog (Rana pipiens). Infect. Immun. **65:**767-773.

Raviglione, M. C. 2007. The new Stop TB Strategy and the Global Plan to Stop TB, 2006-2015. Bull. World Health Organ. **85:**327.

Raviglione, M. C., and A. Pio. 2002. Evolution of WHO policies for tuberculosis control, 1948-2001. Lancet **359:**775-780.

Riley, L. W. 2013. Microbiology and pathogenesis of tuberculosis. UpToDate.

Root, K. M. 2012. Characterizing *Mycobacterium marinum* infections in *oryzias latipes*: Activation of virulence by using *Aedes aegypti* larval extracts. Master's Thesis, University of Louisiana at Lafayette, Lafayette, LA.

Rosenthal, I. M., R. Tasneen, C. A. Peloquin, M. Zhang, D. Almeida, K. E. Mdluli, P. C. Karakousis, J. H. Grosset, and E. L. Nuermberger. 2012. Dose-ranging comparison of rifampin and rifapentine in two pathologically distinct murine models of tuberculosis. Antimicrob. Agents. Chemother. **56:**4331-4340.

Russell, D. G. 2001. *Mycobacterium tuberculosis*: here today, and here tomorrow. Nat. Rev. Mol. Cell. Biol. **2:**569-577.

Salo, W. L., A. C. Aufderheide, J. Buikstra, and T. A. Holcomb. 1994. Identification of *Mycobacterium tuberculosis* DNA in a pre-Columbian Peruvian mummy. Proc. Natl. Acad. Sci. USA **91:**2091-2094.

Sarkar, S., and M. R. Suresh. 2011. An overview of tuberculosis chemotherapy - a literature review. J. Pharm. Pharm. Sci. **14:**148-161.

Smith, N. H., T. Crawshaw, J. Parry, and R. J. Birtles. 2009. *Mycobacterium microti*: More diverse than previously thought. J. Clin. Microbiol. **47:**2551-2559.

Solomon, J. M., G. S. Leung, and R. R. Isberg. 2003. Intracellular replication of *Mycobacterium marinum* within Dictyostelium discoideum: efficient replication in the absence of host coronin. Infect. Immun. **71:**3578-3586.

Solomon, J. M., G. S. Leung, and R. R. Isberg. 2003. Intracellular replication of *Mycobacterium marinum* within *Dictyostelium discoideum*: efficient replication in the absence of host coronin. Infect. Immun. **71:**3578-3586.

Stewart, G. R., J. Patel, B. D. Robertson, A. Rae, and D. B. Young. 2005. Mycobacterial mutants with defective control of phagosomal acidification. PLoS Pathog. **1:**269-278.

Stinear, T. P., T. Seemann, P. F. Harrison, G. A. Jenkin, J. K. Davies, P. D. Johnson, Z. Abdellah, C. Arrowsmith, T. Chillingworth, C. Churcher, K. Clarke, A. Cronin, P. Davis, I. Goodhead, N. Holroyd, K. Jagels, A. Lord, S. Moule, K. Mungall, H. Norbertczak, M. A. Quail, E. Rabbinowitsch, D. Walker, B. White, S. Whitehead, P. L. Small, R. Brosch, L. Ramakrishnan, M. A. Fischbach, J. Parkhill, and S. T. Cole. 2008. Insights from the complete genome sequence of *Mycobacterium marinum* on the evolution of *Mycobacterium tuberculosis*. Genome Res. **18:**729-741.

Strand, M. R. 2008. The insect cellular immune response. Insect Sci. **15:**1-14**.**

Swaim, L. E., L. E. Connolly, H. E. Volkman, O. Humbert, D. E. Born, and L. Ramakrishnan. 2006. *Mycobacterium marinum* infection of adult zebrafish causes caseating granulomatous tuberculosis and is moderated by adaptive immunity. Infect. Immun. **74:**6108-6117.

Takayama, K., and J. O. Kilburn. 1989. Inhibition of synthesis of arabinogalactan by ethambutol in *Mycobacterium smegmatis*. Antimicrob. Agents. Chemother. **33:**1493-1499.

Talaat, A. M., R. Reimschuessel, S. S. Wasserman, and M. Trucksis. 1998. Goldfish, Carassius auratus, a novel animal model for the study of *Mycobacterium marinum* pathogenesis. Infect. Immun. **66:**2938-2942.

Tenant, R., and L. E. Bermudez. 2006. *Mycobacterium avium* genes upregulated upon infection of *Acanthamoeba castellanii* demonstrate a common response to the intracellular environment. Curr. Microbiol. **52:**128-133.

Timmins, G. S., and V. Deretic. 2006. Mechanisms of action of isoniazid. Mol. Microbiol. **62:** 1220-1227.

Tobin, D. M., and L. Ramakrishnan. 2008. Comparative pathogenesis of *Mycobacterium marinum* and *Mycobacterium tuberculosis*. Cell. Microbiol. **10:**1027-1039.

Ulery, B. D., Y. Phanse, A. Sinha, M. J. Wannemuehler, B. Narasimhan, and B. H. Bellaire. 2009. Polymer chemistry influences monocytic uptake of polyanhydride nanospheres. Pharm. Res. **26:**683-690.

Vergne, I., J. Chua, H. H. Lee, M. Lucas, J. Belisle, and V. Deretic. 2005. Mechanism of phagolysosome biogenesis block by viable *Mycobacterium tuberculosis*. Proc. Natl. Acad. Sci. USA **102:**4033-4038.

Volkman, H. E., H. Clay, D. Beery, J. C. Chang, D. R. Sherman, and L. Ramakrishnan. 2004. Tuberculous granuloma formation is enhanced by a mycobacterium virulence determinant. PLoS Biol. **2:**1946-1956.

Volkman, H. E., T. C. Pozos, J. Zheng, J. M. Davis, J. F. Rawls, and L. Ramakrishnan. 2010. Tuberculous granuloma induction via interaction of a bacterial secreted protein with host epithelium. Science. **327:**466-469.

Wallace, J. R., M. C. Gordon, L. Hartsell, L. Mosi, M. E. Benbow, R. W. Merritt, and P. L. Small PL. 2010. Interaction of *Mycobacterium ulcerans* with mosquito species: implications for transmission and trophic relationships. Appl. Environ. Microbiol. **76:**6215-6222.

Wehrli, W. 1983. Rifampin: mechanisms of action and resistance. Rev. Infect. Dis. **5:**S407-411.

Wehrli, W., and M. Staehelin. 1971. Actions of the rifamycins. Bacteriol. Rev. **35:**290-309.

WHO (2013). Global Tuberculosis Report 2012. Geneva, Switzerland: World Health Organisation.

Wirth, T., F. Hildebrand, C. Allix-Béguec, F. Wölbeling, T. Kubica, K. Kremer, D. van Soolingen, S. Rüsch-Gerdes, C. Locht, S. Brisse, A. Meyer, P. Supply, and S. Niemann. 2008. Origin, spread and demography of the *Mycobacterium tuberculosis* complex. PLoS Pathog. **4:**1-10.

Wittbrodt, J., A. Shima, and M. Schartl. 2002. Medaka - a model organism from the far East. Nat. Rev. Genet. **3:**53-64.

Zhang, M., S. Y. Li, I. M. Rosenthal, D. V. Almeida, Z. Ahmad, P. J. Converse, C. A. Peloquin, E. L. Nuermberger, and J .H. Grosset. 2011. Treatment of tuberculosis with rifamycin-containing regimens in immune-deficient mice. Am. J. Respir. Crit. Care. Med. **183:**1254-1261.

Zhang, Y., M. M. Wade, A. Scorpio, H. Zhang, and Z. Sun. 2003. Mode of action of pyrazinamide: disruption of *Mycobacterium tuberculosis* membrane transport and energetics by pyrazinoic acid. J. Antimicrob. Chemother. **52:**790-795.

Zimmerman, M. R. 1979. Pulmonary and osseous tuberculosis in an Egyptian mummy. Bull. N. Y. Acad. Med. **55:**604-608

Mallick, Amrita. Bachelor of Science, Bangalore University, India, Spring 2002;
Master of Science, Bangalore University, India, Spring 2004;
Doctor of Philosophy, University of Louisiana at Lafayette, Summer 2014
Major: Biology
Title of Dissertation: *In Vivo* Characterization of *Mycobacterium marinum* Virulence Genes with Unknown Functions and Larval Activation of Mycobacterial Virulence in the Medaka Infection Model
Thesis Director: Dr. Don G. Ennis
Pages in Thesis: 196; Words in Abstract: 342

ABSTRACT

Human infection by *Mycobacterium tuberculosis* is endemic, with approximately 2 billion infected people worldwide. Because of the slow doubling time of *M. tuberculosis* and the risk of infection to researchers, other mycobacterial species like *Mycobacterium marinum* have been employed as a surrogate pathogen. *M. marinum* has a sequenced genome and is closely related to the *M. tuberculosis* complex. It has been shown to confer human TB-like chronic infection and pathology in some fish, such as the Japanese medaka (Oryzias latipes). Medaka also has a sequenced genome and has served as a laboratory fish model for toxicology, genotoxicity, etc. We have shown that the Medaka-*M. marinum* can model TB-like chronic infections and disease presentation. We have developed an approach of infection by utilizing larvae of *Aedes aegypti* (yellow fever mosquito) as vessels for the delivery of the bacteria to medaka. The passage of *M. marinum* through the caustic environment of the gastrointestinal tract of Mosquito larvae has been shown to increase the virulence of the bacteria when compared to using bacteria from culture. In addition, bacteria incubated in extracts of the macerated tissues of the mosquito larvae have also shown to activate bacteria comparable to the passage of *M. marinum* through the gastrointestinal tract of live mosquito larvae.

We have used Medaka-*M. marinum* model to study the fitness of mutants carrying defects in established virulence genes as well as novel mutant strains when compared to the wild-type

reference strain when inoculated to the same animal. In this approach, the survival of the infected fish and colonization of the host organs were monitored as end points and bacteria were introduced through IP injections as well as an oral route of infection. Randomly isolated by Transposon mutagenesis, *mimI* mutant of *M. marinum* was previously shown in *in vitro* studies to be impaired in attachment and growth inside a macrophage was also shown to be severely defective in colonization *in vivo* when compared to the wild-type. Although the role played by *mimI* is not known, the in-silico and molecular characterization of its product is in progress.

BIOGRAPHICAL SKETCH

Amrita Mallick was born Amrita Sarkar on December 24, 1981, in Kolkata, India to her parents, Asok and Shikha Sarkar. Amrita has one older sister, Arita Roy. She graduated high school in 1999 from Central School Cossipore, Kolkata, India. She earned her Bachelor of Science in Microbiology, Chemistry and Zoology in 2002 as well as a Master of Science in Biotechnology in 2004 from the Bangalore University in Bangalore, India. She married her husband, Dr. Avishek Mallick, on May13, 2007. During her pursuit of her PhD, she had a daughter, Anvi Mallick, who was born on January21, 2013. Amrita earned her PhD in Biology in summer 2014 from the University of Louisiana at Lafayette.